FEDERAL UNIVERSITY OF SANTA CATARINA
SCHOOL OF TECHNOLOGY
DEPARTMENT OF SANITARY AND ENVIRONMENTAL ENGINEERING

Maycon Machado Fontana

# Evaluation of global-scale precipitation products using the DHI Global Hydrological Model

Florianópolis
2021

Maycon Machado Fontana

# Evaluation of global-scale precipitation products using the DHI Global Hydrological Model

Undergraduate thesis report presented to the Sanitary and Environmental Engineering course at the Federal University of Santa Catarina as a partial requirement to obtain the Bachelor`s Degree in Sanitary and Environmental Engineering.
Supervisor: Prof. Davide Franco, PhD
Co-Supervisor: Henrik Madsen, PhD

Florianópolis
2021

Study identification sheet

Fontana, Maycon
Evaluation of global-scale precipitation products using the DHI Global Hydrological Model / Maycon Fontana ; orientador, Davide Franco, coorientador, Henrik Madsen, 2021.
100 p.

Trabalho de Conclusão de Curso (graduação) - Universidade Federal de Santa Catarina, Centro Tecnológico, Graduação em Engenharia Sanitária e Ambiental, Florianópolis, 2021.

Inclui referências.

1. Engenharia Sanitária e Ambiental. 2. NAM. 3. Global Hydrological Models. 4. Precipitation datasets. 5. Observed discharge. I. Franco, Davide . II. Madsen, Henrik. III. Universidade Federal de Santa Catarina. Graduação em Engenharia Sanitária e Ambiental. IV. Título.

Maycon Machado Fontana

**Evaluation of global-scale precipitation products using the DHI Global Hydrological Model**

This graduation work was considered adequate for obtaining the title of Sanitary and Environment Engineer, and approved in its final version by the course of Sanitary and Environmental Engineering.

Florianópolis, Wednesday 12th May 2021.

Documento assinado digitalmente
Maria Elisa Magri
Data: 19/05/2021 16:32:59-0300
CPF: 044.011.369-50
Verifique as assinaturas em https://v.ufsc.br

Prof. Maria Elisa Magri, PhD
Course coordinator
Federal University of Santa Catarina

Documento assinado digitalmente
Davide Franco
Data: 19/05/2021 16:03:17-0300
CPF: 003.932.009-06
Verifique as assinaturas em https://v.ufsc.br

Prof.ª Davide Franco, PhD
Supervisor
Federal University of Santa Catarina

Henrik Madsen, PhD
Co-Supervisor
DHI A/S

**Examiners:**

Prof Patrícia, PhD
Federal University of Santa Catarina

Alejandro E. Lasarte, MSc
DHI A/S

This study is dedicated to my grandmothers: Emília and Maria

## ACKNOWLEDGEMENTS

Firstly, I would like to say thank you to my parents for all the support along with my life, also for my younger sister, who has been a great friend. Additionally, to my grandparents and family.

Thanks to my university colleagues who I have spent the daily routine with for the last years – especially to my sweet friend Isadora Mendel.

Also, to my Professor and thesis supervisor Davide Franco, who has inspired me to work with hydraulics since the first subject on the topic.

Finally, thank you to DHI for open the possibility to develop this study – especially to Henrik Madsen, Peter Godiksen, and Alejandro Lasarte.

“Water is the driving force of all nature.”

Leonardo da Vinci

## RESUMO

Simulações de vazões de rios em escala global através de modelos hidrológicos estão sujeitas a diversos tipos de incertezas. Dessa forma, os dados de entrada de precipitação são os principais causadores de variabilidade nos resultados simulados. Por esse motivo, esse estudo focou em analisar a habilidade individual de produtos de precipitação em reproduzir as vazões de rios simuladas através do Modelo Hidrológico Global da DHI no território Brasileiro. Assim, o trabalho comparou os resultados de vazões simulados com os hidrogramas observados em todas as regiões hidrográficas Brasileiras. Os seguintes quatro produtos de precipitação em escala global foram analisados como forçantes do modelo: Climate Hazards Group InfraRed Precipitation with Station data (CHIRPS), Global Precipitation Measurement (GPM) - Final and Late versions, e ERA5 reanalysis. Além disso, uma grade de precipitação observada foi utilizada. O estudo investigou a disponibilidade de dados de vazões de rios no no território Brasileiro. Por conseguinte, analisamos as séries temporais de vazão simuladas pelo Modelo Hidrológico Global da DHI forçado pelos diferentes produtos de precipitação. A capacidade do modelo hidrológico em reproduzir os fluxos nos rios, o quais funcionam como variáveis independentes do modelo para validação, determina a acurácia dos produtos de precipitação como forçantes do modelo. Nesse sentido, os coeficientes de eficiência do modelo incluem a avaliação do balanço hídrico: Erro Médio (ME) e Erro Médio Relativo (MRE), e também, o coeficiente de eficiência Kling-Gupa (KGE), e seus componentes: correlação linear (r), variabilidade do erro (Alfa), e o viés (Beta). O Modelo Hidrológico Global da DHI é uma versão distribuída do modelo chuva-vazão NAM, também chamado de RDII em Inglês (*Rainfall Dependent Inflow and Infiltration model*). Adicionalmente, o método *Kinematic* descreve o roteamento nos rios. Resultaods preliminares do modelo em países como Estados Unidos da América (EUA) e França foram classificados como razoáveis quando forçados com os produtos de precipitação CHIRPS e GPM. Os resultados do estudo mostraram que em termos de balanço hídrico (ME e MRE) e KGE, a grade observada é uma referência suficiente para avaliar os produtos globais de precipitação. Além disso, ERA5 apresentou resultados não esperados, uma vez que mostrou os melhores resultados simulados entre os produtos de precipitação ($ME_{Q50\%}$=95.02 mm e $MRE_{Q50\%}$=23.66 %). Contudo, ERA5 apresentou o menor KGE calculado entre as simulações, à medida que apontou baixos coeficientes de correlação. Entre os produtos com dados de satélite/corrigidos com observações (CHIRPS e GPM Final), CHIRPS mostrou os melhores resultados ($ME_{Q50\%}$ = 153.86 mm e $MRE_{Q50\%}$ = 40.16 %). De forma geral, o GPM Final apresenta melhora relevante quando corrigido pelas observações (GPM Late). Finalmente, em relação às regiões hidrográficas Brasileiras, os produtos de precipitação mostraram acurácias diferentes - CHIRPS performou melhor que o GPM Final nas regiões do sul (subtropical). Enquanto o GPM Final apresentou os melhores resultados ($MRE_{Q50\%}$ = 19.86 %) na bacia Amazônica (floresta tropical).



**Palavras-chave**: NAM. Modelos hidrológicos globais. Grades de precipitação. Vazão observada.

## ABSTRACT

Rivers discharge simulations on a global-scale by hydrological models are subject to several types of uncertainties. Thus, precipitation data inputs are the main cause of simulated results variability. For this reason, this study aimed to evaluate the ability of individual global-scale precipitation datasets to reproduce river discharges simulated by the DHI Global Hydrological Model in the Brazilian territory. In this regard, we compared the discharge model results against observed hydrographs from all the Brazilian Hydro-Regions. The following four global precipitation datasets were analyzed as simulation forcings: Climate Hazards Group InfraRed Precipitation with Station data (CHIRPS), Global Precipitation Measurement (GPM) - Final and Late versions, and ERA5 reanalysis. Additionally, an observed precipitation grid was analyzed. The study investigated the availability of observed river discharge data in the Brazilian territory. Therefore, we evaluated the simulated discharge time-series from the DHI Global Hydrological Model forced by the different precipitation products. The hydrological model capacity to reproduce the in-situ rivers-flows, which act as a model-independent validation variable, determined the accuracy of the simulation-input precipitation datasets. In this sense, the model efficiency coefficients included the water balance assessment: Mean Error (ME) and Mean Relative Error (MRE), also, the Kling-Gupta efficiency coefficient (KGE), and its components: linear correlation (r), variability error (Alpha), and the bias (Beta). The DHI Global Hydrological Model is a grid-based version of the NAM rainfall-runoff model, also named RDII in English standing for Rainfall Dependent Inflow and Infiltration model. Additionally, the Kinematic method describes the river routing. Previous results of the model in countries as the United State of America (USA) and France were classed as good when forced by CHIRPS and GPM precipitation datasets. The study results showed that in terms of water balance (ME and MRE) and KGE, the observed grid is an enough reference to evaluate the global precipitation datasets. Also, ERA5 presented not expected results, since it provides the best-simulated values among the precipitation products ($ME_{Q50\%}$=95.02 mm and $MRE_{Q50\%}$=23.66 %). However, ERA5 showed the lowest calculated KGE, since it gives low linear correlation coefficients. Among the satellite/observation-corrected datasets (CHIRPS and GPM Final), CHIRPS showed the best results ($ME_{Q50\%}$ = 153.86 mm and $MRE_{Q50\%}$ = 40.16 %). In general, GPM Final shows a relevant improvement after the observation corrections (GPM Late). Finally, over the Brazilian Hydro-Regions, the precipitation products showed different accuracy - CHIRPS performs much better than GPM Final in the southern regions (subtropical). While GPM Final presents the best results ($MRE_{Q50\%}$ = 19.86 %) in the Amazon Basin (tropical rainforest).



**Keywords:** NAM. Global Hydrological Models. Precipitation datasets. Observed discharge.

## LIST OF FIGURES

## LIST OF TABLES

## LIST OF ABBREVIATIONS AND ACRONYMS

| | |
|---|---|
| ANA | Brazilian Water Agency |
| CHG | Climate Hazards Group |
| CHPclim | Climate Hazards group Precipitation climatology |
| CHIRP | Climate Hazards group Infrared Precipitation |
| CHIRPS | Climate Hazards Infrared Precipitation with Stations |
| CPRM | Geological Survey of Brazil |
| COHIDRO | Water Resources and Irrigation Development Company of Sergipe State |
| DAEE-SP | Water and Energy Department of the São Paulo State |
| EPAGRI | Agricultural Research and Rural Extension Company of Santa Catarina |
| ECMWF | European Centre for Medium-Range Weather Forecasts |
| FAO | Organization of the United Stations |
| GHCN | Global Historical Climate Network |
| GPM | Global Precipitation Measurement |
| IGAM | Water Management Institute of Minas Gerais |
| IAP | Paraná Water Institute |
| IFS | Integrated Forecasted System |
| INMET | National Meteorological Institute |
| IR | Microwave-calibrated infrared |
| JAXA | Japan Aerospace Exploration Agency |
| KGE | Kling-Gupta efficiency |
| MAE | Mean Absolute Error |
| MARE | Mean Absolute Relative Error |
| NASA | National Aeronautics and Space Administration |
| ORE | Environmental Research Observatory |
| TRMM | Tropical Rainfall Measuring Mission |
| UFC | Federal University of Ceará |
| UFSC | Federal University of Santa Catarina |

**TABLE OF CONTENTS**

# 1 INTRODUCTION

Modeling water flows and water storage variations on a global scale according to a temporal and spatial approach is essential to deal with water resources (DÖLL *et al.*, 2016). The models that aim to represent global hydrological phenomena, which include the main and associated process, have a similar structure over several stand-alone hydrological models and hydrological components of the general circulation models (GCMs). Global hydrological models (GHMs) simulate the hydrologic dynamics of continental-scale river basins at the land surface. As most of the hydrological models, GHMs represent mainly the rainfall-runoff processes and river flows ( SIMON; NIGEL, 2010; MOTOVILOV *et al.*, 1999)

Hydrological simulations require accurate and representative climatological variables (e.g. temperature, precipitation, evaporation) as forcing, and their representation in space and time is necessary (BEVEN, 2011; KIRCHNER, 2009; WATSON *et al.*, 1996). Additionally, the spatial resolution of the available input data often determines the GHMs discretization, having model-specif effects on the simulation results. In this way, the modeling approach is becoming more complex and resolute since high-resolution global datasets have been made available for the last decades (SOOD SMAKHTIN, 2015; DÖLL *et al.*, 2008, LAMMERS *et al.*, 2008).

The uncertainties in hydrological simulation mainly can be separated in model uncertainty (structure, parameters, and forcings) and observation uncertainty (SOOD & SMAKHTIN, 2015). Accurate precipitation data is essential in hydrological modeling since rainfall is the major driving force of basin runoff generation (CHO *et al.*, 2009). Nevertheless, the spatial variability of precipitation input is related to the major source of uncertainty in hydrological modeling. The relation is notable in large and small catchments (SCHILLING & FUCHS, 1986; KREJCI & SCHILLING, 1989; BONACCI, 1989). In this sense, the precipitation uncertainty is linked to (i) magnitude, (ii) temporal distribution, and (iii) spatial distribution of the rainfall (MASKEY; GUINOT; PRICE, 2004).

In situ precipitation measurements can present large spatial-temporal variability (BOHNENSTENGEL; SCHLÜNZEN; BEYRICH, 2011). Traditionally, gauge measurements have been used as actual precipitation in hydrological models (MUSIE; SEN; SRIVASTAVA, 2019; ZHU *et al.*, 2015). In this sense, rain gauge punctual observations are interpolated to regular grids, representing the precipitation at basins or sub-basins locations (BELETE *et al.*, 2020; OREGGIONI WEIBERLEN; BÁEZ BENÍTEZ, 2018). In places with low gauge density

as mountainous regions or remote areas such as the Amazon basin, interpolated observation might represent a rough estimation. Additionally, in tropical regions precipitation has a convective origin with high spatial variation during the day (COLLISCHONN; COLLISCHONN; TUCCI, 2008). Also, rain stations are vulnerable to errors from meteorological phenomena as wind effects and evaporation (STRANGEWAYS, 2004).

As a result of this limited gauge representativeness, several gridded precipitation datasets have been developed for large-scale hydrological modeling during the last decades, these products differ in terms of data sources: radar, gauge, satellite, numerical weather model, or combinations thereof (BECK *et al.*, 2017). Among the different options of sources, precipitation radar measurements might present errors associated with rain-intensity relationships, range effects, clutter, etc (JAMESON; KOSTINSKI, 2002). For the last decades, a global effort has been taking to develop satellite-based precipitation retrieval algorithms. More recently, satellite-based precipitation products have emerged, providing uninterrupted precipitation time series with quasi-global coverage (BEHRANGI *et al.*, 2011). In this way, the satellite systems present a range of variety in respect to sensor technology, temporal sampling, and measurement variables (HUFFMAN *et al.*, 2007; SAPIANO; ARKIN, 2009).

In this regard, many studies focused to evaluate the different precipitation products to understand their accuracy. For this purpose, data is compared to field observations or gauge-adjusted radar fields in terms of spatio-temporal patterns. While others evaluate the performance of precipitation datasets assessing simulated river discharge from hydrological modeling forced by the specific rainfall data (BECK *et al.*, 2017). The advantage of evaluating remote sensing rainfall estimates by running hydrological models is to directly identify the rainfall impact over simulated river discharge (COLLISCHONN; COLLISCHONN; TUCCI, 2008). Additionally, there are not too many studies that have focused on catchment modeling over the entire Brazilian territory. Altough, Siqueira *et al.* (2018), and David (2020) had recently made great progress on the topic.

With this in view, this study aims to evaluate the ability of individual global-scale precipitation datasets to reproduce river discharges simulated by the DHI Global Hydrological Model in the Brazilian territory.

## 1.1 OBJECTIVES

### 1.1.1 General objective

Evaluate the ability of individual global-scale precipitation datasets to reproduce river discharges simulated by the DHI Global Hydrological Model in the Brazilian territory.

### 1.1.2 Specific objectives

- Investigate the availability of river discharge data in the Brazilian territory.
- Establish a database of precipitation products with the following datasets: Observed grid, Climate Hazards Group InfraRed Precipitation with Station data (CHIRPS), Global Precipitation Measurement (GPM) - Final and Late versions, and ERA5 reanalysis.
- Compare the different global precipitation datasets according to a spatial and temporal approach.
- Evaluate the simulated discharge time-series from the DHI Global Hydrological Model forced by the different precipitation products.

# 2 LITERATURE REVIEW

This section describes the theoretical background of this study. It is mainly focused on a review of the utilized hydrological model. Section 2.1 covers the basics topics about the NAM model, while Section 2.2 presents the DHI Global Hydrological Model and the distributed version of the NAM model.

## 2.1 NAM RAINFALL-RUNOFF MODEL

NAM stands for the Danish abbreviation of "Nedbør-Afstrømnings-Model", which means Precipitation-Runoff-Model or RDII in English - Rainfall Dependent Inflow and Infiltration model (DHI, 2017). The model was proposed by Nielsen & Hansen (1973), the work presented the model as an engine to simulate the rainfall-runoff process of rural watersheds. Firstly, the model was tested in three different Danish watersheds, providing promissory results. Since its first application, the model has been applied worldwide to simulate the rainfall-runoff phenomena in many hydrological conditions. The NAM model is characterized as a deterministic, lumped, conceptual model with moderate input data requirements (DHI, 2017). However, as described in Section 2.2, the DHI Global Hydrological Model utilizes a physically based distributed NAM version.

### 2.1.1 Model forcings

*2.1.1.1Meteorological data*

2.1.1.1.1Precipitation

Precipitation is the principal input for catchments water balance, the phenomena determine the water quantity and quality. The spatial and temporal distribution of precipitation drives the available water in space and time. The rainfall intensity controls the amount and peak of runoff during a storm event. The seasonality during the year determines the need for irrigation in an agricultural system. However, its measurement is difficult and small errors will affect the entire water balance on the catchment scale (DAVIE; QUINN, 2019).

With this in view, the precipitation forces the NAM model. Additionally, for the validation process, the time resolution of the rainfall time series should follow the time resolution of the discharge measurements (DHI, 2017).

2.1.1.1.2Evapotranspiration

Evaporation is the only loss away from the surface in the water balance equation, it has an important influence on the catchment water quantity. In this sense, the loss of water from the soil through direct evaporation and plant's transpiration impact the amount of water flowing into the rivers during a storm event. Also, it partially determines the amount of water available to infiltrate into groundwater. However, the impact of evapotranspiration on the water balance is not as great as for precipitation, but it presents a significant role in the spatial and temporal runoff process (DAVIE; QUINN, 2019).

In this sense, the evapotranspiration forces the NAM model. The evapotranspiration specified as a model forcing is the potential evapotranspiration. For a daily time step simulation, monthly values of potential evapotranspiration are usually sufficient. Thus, only minor improvements might be obtained by utilizing daily data (DHI, 2017).

*2.1.1.2Hydrological data*

2.1.1.2.1Discharge

Ruoff is the term utilized to describe the water dynamic movement to the streams after it has reached the ground as precipitation. When the water flows into the rivers in a channelized form, hydrology science refers to it as streamflow or riverflow - expressed as discharge (DAVIE; QUINN, 2019).

Observed discharge data at the catchment outlet are utilized for comparison with the simulated discharge. The time step discharge value is the average discharge since the last input data (DHI, 2017).

### 2.1.2 Model structure

The NAM model is based on physical structures and equations combined with semi-empirical ones - a conceptual model. Figure 1 shows the model structure. The structure aims to imitate the land phase of the hydrological cycle. This structure allows representing the physical process by simulating the rainfall-runoff through continuously accounting for the water content in four different and interrelated storages. The storages are:

- Snow storage
- Surface storage
- Lower or root zone storage
- Ground storage

Figure 1 - Model Structure.

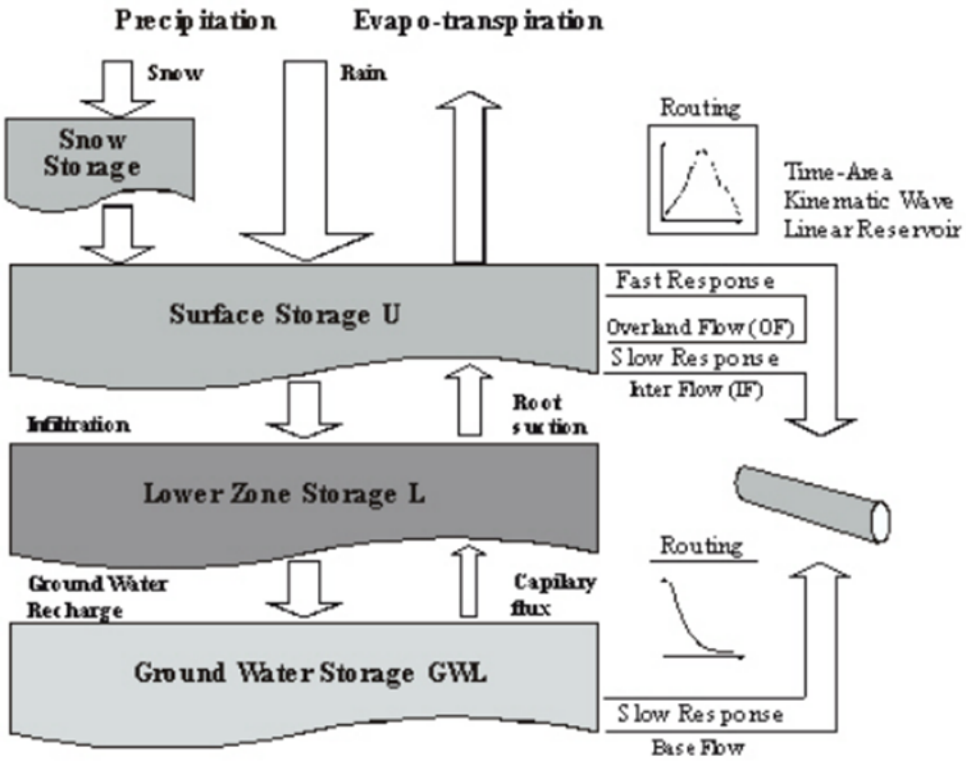


Source: DHI, 2021.

The meteorological inputs force the NAM model. The produced outputs are runoff (overland flow, interflow, and baseflow), evapotranspiration, soil moisture content, groundwater recharge, and groundwater levels (DHI, 2017).

### 2.1.3 Basic modeling components and parameters

This section summarizes the NAM basic modelling components and the main model parameters. Besides, the section focus on the components and parameters that are cited along with the study as background for the methodology presentation and results sections. More information is fully described in the main model reference: DHI (2021). Figure 2 shows the model conceptualization of the physical processes represented by NAM.

Figure 2 - Model Components.

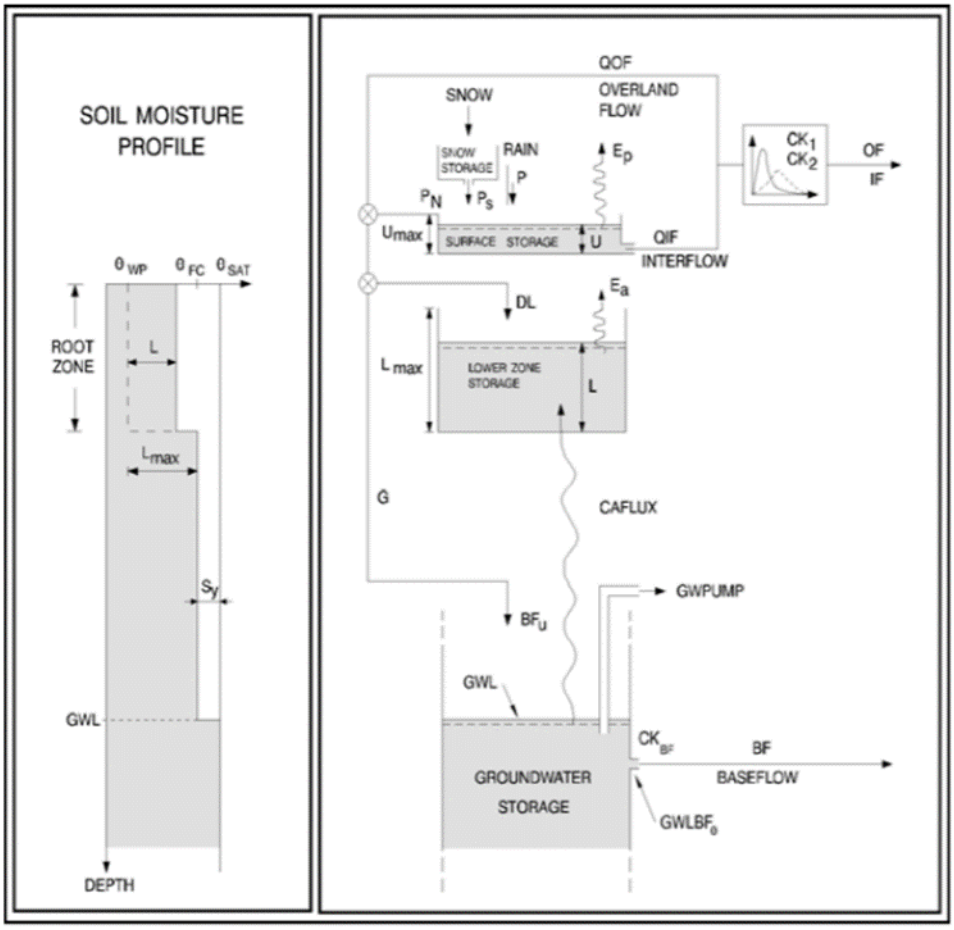


Source: DHI (2021).

*Surface storage*

The surface storage represents the moisture intercepted on the vegetation, water trapped in depressions and in the uppermost, and cultivate ground part. $U_{max}$ [mm] introduces the maximum amount of water in the model storage. Common values for $U_{max}$ stand from 10 to 20 mm. Dynamically, the storage will generate $P_N$ (net excess rainfall) when $U \geq U_{max}$. It is consumed by evaporation and horizontal leakage (interflow) (DHI, 2021).

*Lower zone or root zone storage*

The lower zone or root zone storage stands for the soil layer above the surface. $L_{max}$ defines the maximum water quantity in the compartment, which acts as the maximum potential soil moisture for vegetation transpiration. Thus, in terms of water balance, the root zone plays an important role. Additionally, besides other simplifications, $L_{max}$ represents the average root depths of the individual vegetation types. The reference value is 100 mm (DHI, 2021).

*Evapotranspiration*

Initially, the evapotranspiration demand meets the potential rate from the surface storage. When $U < E_p$, the remaining fraction is linearly consumed by root activity from the lower storage according to the soil moisture content ratio $L/L_{max}$ (DHI,2021). The following (1 explains the process.

$$E_a = (E_p - U)\frac{L}{L_{max}} \qquad (1)$$

Where,

$E_a$ = Actual Evapotranspiration [mm]

$E_p$ = Potential Evapotranspiration [mm]

$U$ = Surface water content [mm]

$L$ = Root zone water content [mm]

$L_{max}$ = Root zone maximum water content [mm]

## 2.2 DHI GLOBAL HYDROLOGICAL MODEL

### 2.2.1 General information

The DHI Global Hydrological Model is an operational data service providing access to reliable and frequently update hydrological model results all over the world using an increasing number of global datasets. The ongoing project goals to create automatic modelling workflows, which produces hydrological data to provide boundary conditions for local models, or even for direct data usage (DHI, 2021).

The model grid runs in a global tiles scheme, covering all the longitudes (-180˚ to 180˚), and latitudes from -60˚ to 60˚ - the model mesh will be extended to global coverage in

the future. There are 251 tiles with a resolution of 10˚x10˚ (432 tiles would cover the entire globe). Then, each tile comports 10,000 models, providing a resolution equals to 0.1˚x0.1˚ (approximately 11 km). There is also a sub-grid resolution, which is mainly applied to mountain areas. The sub-grid defines the different elevation zones in these regions, this downscaling allows expressing the variation in temperature or other parameters related to the elevation. In this regard, regions as the Andes or the Himalayas present further discretization for each grid cell. With this in view, the hydrological model corresponds to a distributed version of the classical DHI rainfall-runoff NAM model (DHI, 2021).

Thus, the parameter estimation process can be divided into two different approaches: (i) regionalization, in which the parameters are calibrated according to discharge gauge observations in the catchments. Subsequently, the parameters are extrapolated to ungauged catchments. However, it is sensitive to the model forcings and observation uncertainties - the biases on the observations and model forcings are transferred to parameters estimation. Also on a global scale, there is a limited network of streamflows observations. (ii) physical-based, in which the parameters are estimated from observed physical quantities. This approach easily allows combining available gridded datasets to the hydrological model grid. Also, it provides reasonable parameters in ungauged areas. Nevertheless, a merged procedure rises as a reasonable option, since the physical-based method would work as priori estimation, while the regionalization makes the local calibration possible. Thus, the model results, forcing global datasets, and physical observed quantities are evaluated through the discharge observations in the rivers (DHI, 2021).

Additionally, the Fast Kinematic method describes the river routing, using the discharge estimations from the rainfall-runoff model as the primary input. The river routing happens according to three levels: (i) On the grid through the NAM routing (ii) Routing from the grid to the basin outlets through the Kinematic routing (iii) Routing between the basins through the Kinematic routing.

### 2.2.2 Basins delineation and real basin area

The basins are described by the database HydroBASINS (LEHNER; GRILL, 2013), which is a series of polygon layers that represent watershed boundaries and sub-basins at a global scale. The used algorithm provides the up and downstream connectivity between the basins. In this sense, to evaluate the simulated discharges against the observations, the model

corrected the simulated flow by the real basin area - provided in the station's catalog. (2 is used for the discharge correction.

$$Q_{final} = \frac{A_{basin}}{A_{model}} Q_{sim} \qquad (2)$$

Where,

$Q_{final}$ = Corrected discharge [$m^3/s$]

$Q_{sim}$ = Simulated discharge [$m^3/s$]

$A_{basin}$ = Real basin area [$km^2$]

$A_{model}$ = Model basin area [$km^2$]

# 3 METHODOLOGY

## 3.1 METHODOLOGY SCHEME

Figure 3 shows the study methodology scheme. In this sense, five precipitation datasets were evaluated. The rainfall products correspond to four different types of data sources: observations-only (Observed Grid), satellite/observation-corrected products (CHIRPS and GPM Final), satellite-only (GPM Late), and reanalysis (ERA5).

Therefore, each one of the precipitation products forced a specific DHI Global Hydrological Model simulation over the model area (Section 3.5) - according to the simulation specifications (Section 3.8). Thus, the agreement between the simulated and observed discharge indicates the performance of the precipitation products to estimate the stream flows through the rainfall-runoff process.

Additionally, the model performance is evaluated at different geographical scales. The country scale compares the model results against the field observations from 769 discharge gauges in the Brazilian territory. While the region scale selected three Brazilian Hydro Regions - which presented the best results among the twelve existing ones (Section 3.2). The selected areas are Amazônica (#1), Atlântico Sul (#6), and Uruguai (#12). Finally, one basin for each region was analyzed. Thus, the model precipitation products were evaluated in well-calibrated basins. Also, the basins present different magnitude areas.

Figure 3 - Methodology scheme.

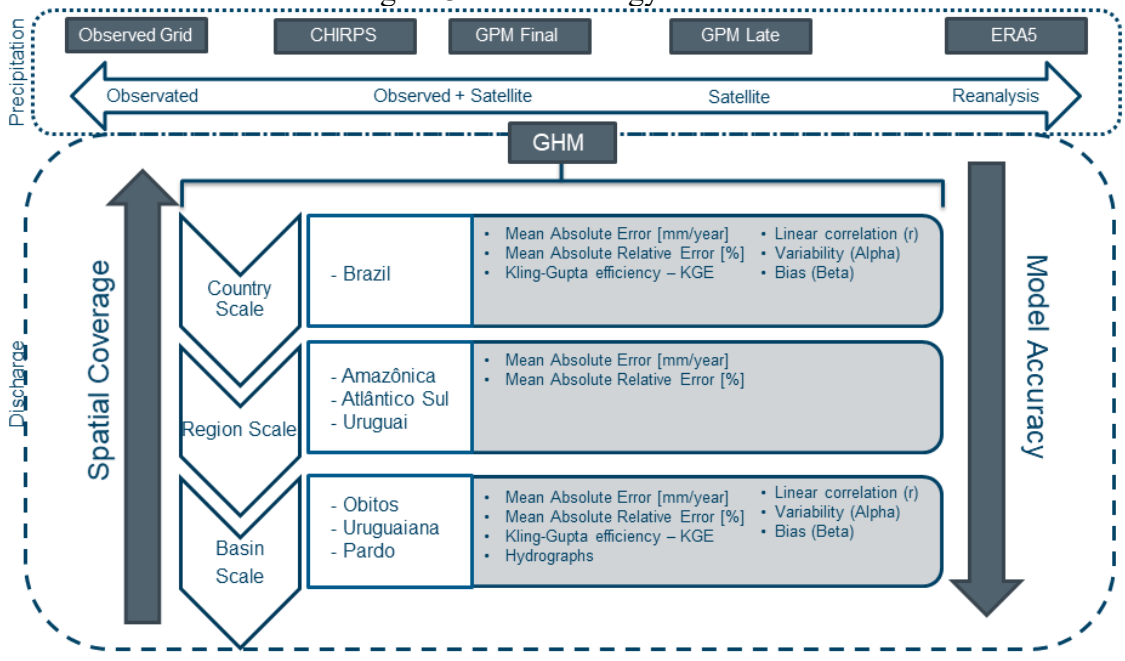

## 3.2 STUDY AREA

The model results were evaluated in the entire Brazilian territory. However, for a better understanding of the model accuracy over the different hydrological patterns, the study used the 12 Brazilian Hydro-Regions to cluster the model performance evaluation. The Brazilian Water Agency (ANA) groups the Brazilian Hydro-Regions according to their natural, social, and economic mutual characteristics, which region is described by a close basin, group of basins, or sub-hydro-regions (ANA, 2021a). The Brazilian Hydro Regions are:

- Amazônica (#1)
- Altântico Leste (#2)
- Altântico Nordeste Ocidental (#3)
- Altântico Nordeste Oriental (#4)
- Altântico Sudeste (#5)
- Altântico Sul (#6)
- Paraguay (#7)
- Paraná (#8)
- Paranaíba (#9)
- São Francisco (#10)
- Tocantins-Araguaia (#11)
- Uruguai (#12)

Figure 4 shows the Brazilian Hydro-Regions locations:

Figure 4- Brazilian Hydro-Regions

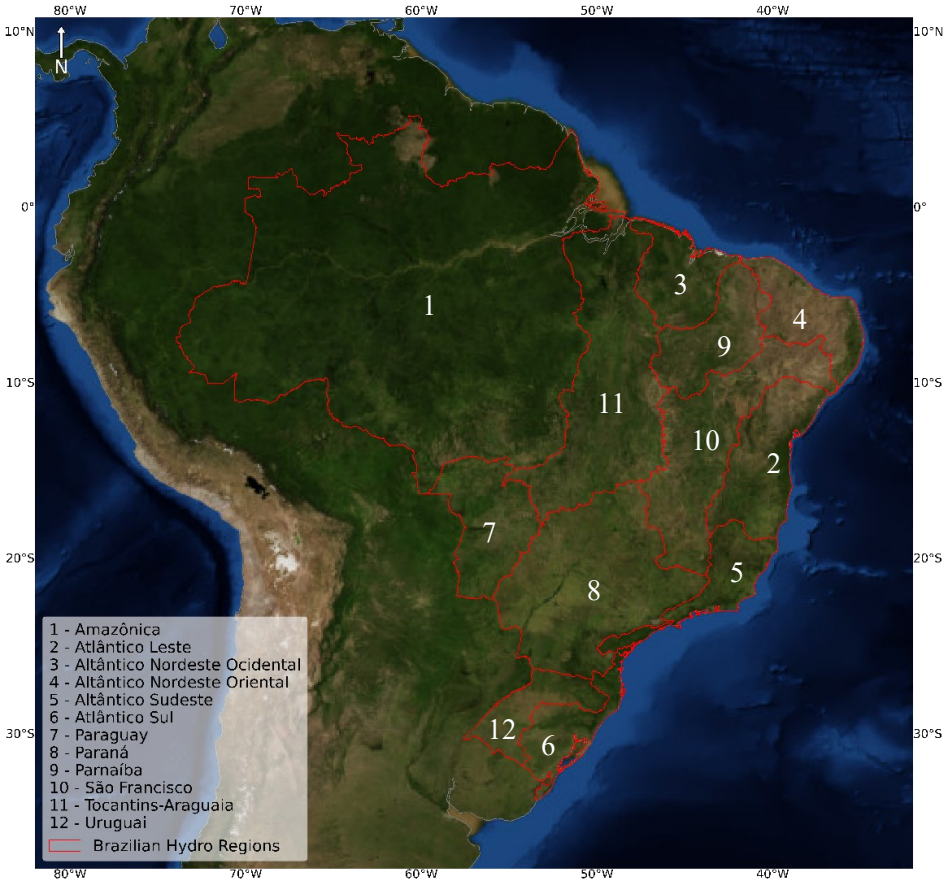


Source: Author.

## 3.3 MODEL AREA

The model area (12,890,685 km²) covers approximately 72% of the South American area (17,840,000 km²). The drainage area is mainly delimited by the Andes Mountains on the west, the Atlantic Ocean coast on the east, the Guiana Shield on the north, and the Argentinian Pampas region on the southern border. Figure 5 shows the model area and the major rivers.

Figure 5 - Model area.


Source: Author.

## 3.4 OBSERVED DISCHARGE

The model performance corresponds to the ability of the simulation results to reproduce the in-situ streamflow values. Therefore, this worked aimed to build a solid river discharge database. As a result, the final frame covers mainly the Brazilian territory, which was submitted to further data screening analysis.

### 3.4.1 Datasets

The study utilizes two different observed river discharge datasets: (1) Environmental Research Observatory (ORE) - Geodynamical, Hydrological, and Biogeochemical control of erosion/alteration and material transport in the Amazon River Basin/HYBAM (HYBAM, 2021). The organization is a partnership between the hydrological and meteorological agencies /services for some of the countries located in the Amazon Basin: Brazilian Water Agency/ANA (ANA, 2021a) in Brazil, National Meteorology and Hydrology Service/SENHAMI in Peru (SENAMHI-PE, 2021), and Bolivia (SENAMHI-BO, 2021), National Meteorology and Hydrology Institute/INAMHI in Ecuador (INAMHI, 2021), and the French Institute of Research for Development/IRD (IRD, 2021). Commonly called SO-HYBAM - how the study refers the database for the rest of the document.

The database's geographical coverage is the Amazon Basin. The time series are available on a daily time step. As a result, the database has been used as a streamflow observation reference by several researchers in the Amazon, which facilities information exchanging and comparison to the previous studies. Among the studies are (CHEN *et al.*, 2020; GUIMBERTEAU *et al.*, 2012; PAIVA *et al.*, 2013).

Additionally, (2) the Brazilian Water Agency/ANA (ANA, 2021b) observed discharge dataset has been gathered. The agency makes available the most complete hydrological dataset (water-level and discharge) on the country territory, hence it incorporates the database from several local Brazilian hydrological and meteorological agencies/services. The enrolled public organizations are the Geological Survey of Brazil/CPRM (CPRM, 2021), the Agricultural Research and Rural Extension Company of Santa Catarina/EPAGRI (EPAGRI, 2021), the Water and Energy Department of the São Paulo State/DAEE-SP (DAEE-SP, 2021), the Water Management Institute of Minas Gerais/IGAM (IGAM, 2021), the Paraná Water Institute/IAP (IAT, 2021), and the contracted companies as the Water Resources and Irrigation Development Company of Sergipe State/COHIDRO (COHIDRO, 2021), CONSTRUFAM (CONSTRUFAM, 2021), and the Federal University of Ceará/UFC (UFC, 2021). The rest of the document refers to the dataset only as ANA dataset.

The dataset is composed of discharge [$m^3/s$] time series on a daily resolution. There is a quality control code for each measurement, where "1" means a raw level for the observed flow, and "2" means that the agency has realized a further treatment on the measured value. The present study defines number "2" as the preference level when both codes are available.

Besides, only the station gauges with available rating curve data have been chosen for the quality control process, working as a first quality assessment. The ANA data covering the Amazon was not utilized, since the SO-HYBAM database is the reference over the region.

A total of 3,658 stations were computed from the two datasets. Among the discharge gauges, 210 stations (5.74%) correspond to the SO-HYBAM source, while 3,448 stations (94.26%) stand for the ANA dataset. Therefore, further data screening analysis considered the entire created frame. Figure 6 shows the station's spatial distribution.

Figure 6 - Preliminary stations locations.

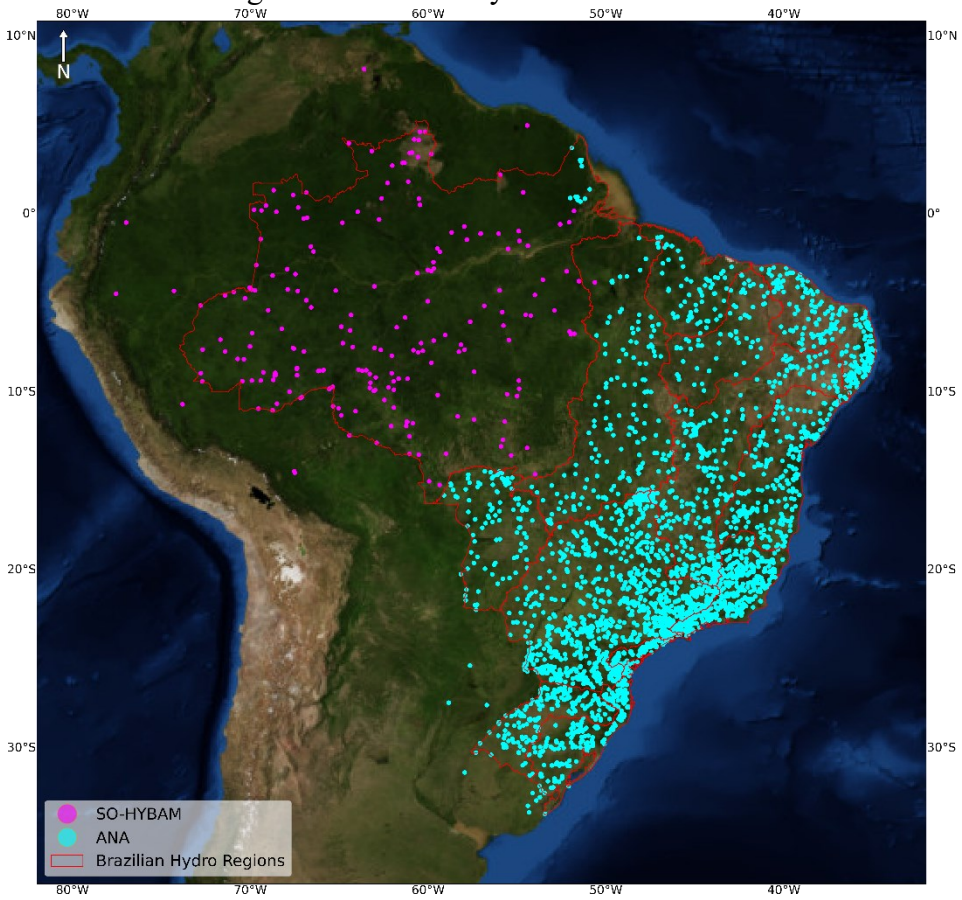


Source: Author.

### 3.4.2 Data Screening

The data screening procedure focused on the studying period, completeness, and data quality. Additionally, this study focuses on the period from the year 2000 to the near present. Firstly, the database was filtered by two conditions: (1) Time series longer than 15 years after the year 2000 (2) time series with less than 10% of missing data. Secondly, a visual inspection

of the plots for the daily discharge time series, yearly maximum discharge, yearly minimum discharge, and flow duration curve. Thus, some of the stations were removed from the database due to unexpected values (i.e. too many outliers or a clear step in the time series). Figure 7 shows an example of the plots for the most downstream station in the Amazon Basin (Obidos - 17050001).

Figure 7 - Discharge Gauge Statistics - Obidos - 17050001.

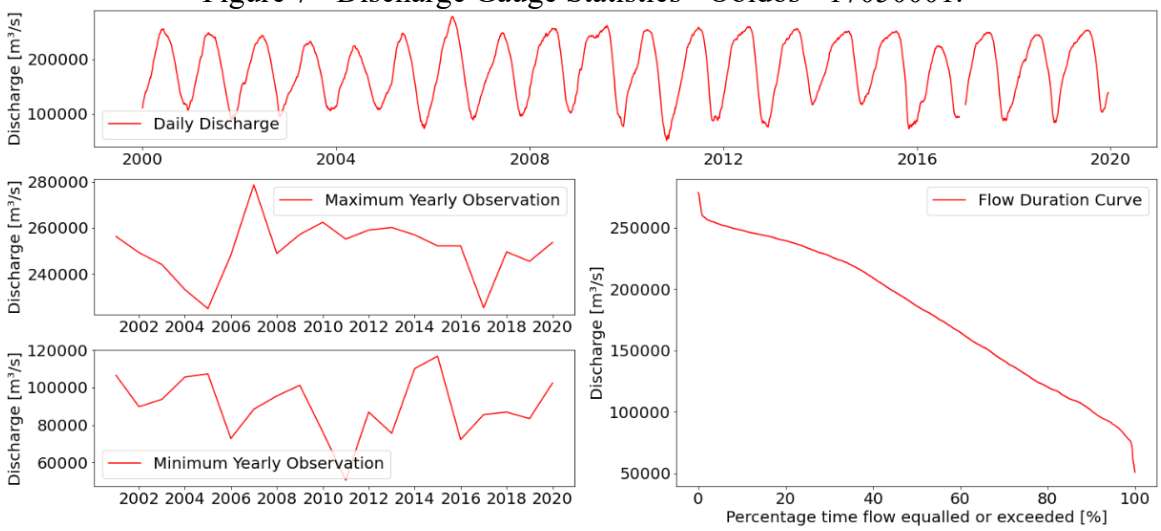


Source: Author.

Also, the last quality control was developed through the methodology presented by Cole, Johnston and Robinson (2003), which recommends the visualization of the yearly flow duration curves. Some of the stations were removed due to the visual variance among the different yearly flow duration curves, or an unexpected shape. Finally, the gauges were filtered by three additional conditions: (1) minimal drainage area of 500 km2, and (2) maximal difference of |10%| between the catchment model area and the metadata catchment area, and (3) only discharge stations located in the Brazilian territory. As a result, there are 769 stations in the treated frame, 50 stations (6.5 %) from the SO-HYBAM source, and 717 stations (93.50 %) from the ANA database. Although a visual data quality assessment was realized, uncertainties about the observation may be present. Figure 8 shows the discharge station's spatial distribution after the treatment.

Figure 8 - Treated stations locations.


Source: Author.

## 3.5 PRECIPITATION DATASETS

The following section describes each studied precipitation dataset: Observed, CHIRPS, GPM Final, GPM Late, and ERA5. In this regard, all the grids were interpolated to a 0.1° resolution over the model area when necessary. Table 1 shows the main information about the datasets.

Table 1 - Precipitation Datasets Details

| **Short name** | **Data source(s)** | **Full name** | **Spatial resolution** | **Spatial coverage** | **Temporal resolution** | **Temporal Coverage** | **Ref.** |
|---|---|---|---|---|---|---|---|
| Observed grid | G | Daily grided meteorological variables in Brazil | 0.25° | Brazilian territory | Daily | Jan/1980 to Dec/2015 | 1 |
| CHIRPS | S, G | Climate Hazards Infrared Precipitation with Stations | 0.05° | -50° to 50° | Daily | Jan/1981 to near-present | 2 |
| GPM Late | S | Global Precipitation Measurement - IMERG Late Run | 0.1° | -60° to 60° [1] | Daily | Jun/2000 to near-present | 3 |

| | | | | | | | |
|---|---|---|---|---|---|---|---|
| GPM Final | S, G | Global Precipitation Measurement - IMERG Final Run | 0.1° | -60° to 60° [1] | Daily | Jun/2000 to near-present | 3 |
| ERA5 | R | European Centre for Medium-range Weather Forecasts ReAnalysis | ~0.28° | -90° to 90° | Hourly | Jan/1979 to near-present | 4 |

*Where, [1] - 90° to 90° for not-full coverage; G - Gauge data; S - Satellite; R - Reanalysis.
Source: 1- Xavier, King and Scanlon (2017); 2 - Funk *et al.*( 2015); 3 - NASA (2021); 4 - ECMWF (2021).

### 3.5.1 Observed

Xavier, King, and Scalon (2016) developed a gridded dataset for meteorological variables in Brazil. The dataset contains precipitation and reference ET (ETo) based on the most comprehensive meteorological station data available for Brazil. The database spatial resolution is 0.25° (~28 km) for daily and monthly temporal resolution (1980 to 2013). In this sense, Xavier, King, and Scalon (2017) took an update on the previous product. The latest version made use of 9,259 rainfall gauges instead of 3,630 in the preliminary version. Additionally, the temporal coverage was extended by two years (1980-2015).

Most of the observed data were collected from the Brazilian Water Agency (ANA) and the National Meteorological Institute (INMET), combing 8,515 and 744 gauge stations respectively. The spatial distribution of the gauge stations presents a high variation across the Brazilian Hydro-Regions. The Parana Basin shows the highest spatial coverage over the national territory, while the Amazon Basin shows the lowest one. The dataset covers the entire Brazilian territory

The observed precipitation is measure on a daily base, accumulated over 24 hours. Interpolated methods over the grid were validated by comparing interpolated results with observations on meteorological stations. Thus, the associated value [mm/day] of each grid point represents the fixed representative amount of precipitation for the specific day on the entire cell. The dataset is considered an observation only-dataset.

### 3.5.2 CHIRPS

Funk *et al.* (2015) presented the Climate Hazards Infrared Precipitation with Stations (CHIRPS) precipitation dataset. The data covers the period from 1981 to the near-present (~40 years) on a daily, pentadal, and monthly time resolution. The database presents a spatial resolution equals to 0.05° on a quasi-global coverage, spanning from -50° to 50° (and all

longitudes). The Climate Hazards Center, University of California - Santa Barbara operationally maintains the dataset.

The CHIRPS building appropriates three different sources of precipitation data: 1) the Climate Hazards group Precipitation climatology (CHPclim), 2) the satellite-only Climate Hazards Group Infrared Precipitation (CHIRP), and 3) the station blending procedure that finally generates the CHIRPS.

The CHPclim represents monthly precipitation climatological data based on two sets of monthly historical long-term means. The two sets are a combination of 27,453 monthly stations from the Organization of the United Stations (FAO), and 20,591 stations from version two of the Global Historical Climate Network (GHCN). Additionally, besides the traditional physiographic indicators (elevation, latitude, and longitude) utilize in climatological products, the main algorithm also includes monthly statistics from five different satellite products. Secondly, the CHIRP products present the variation grid from the CHPclim mean. The methodology follows a local calibration with satellite precipitation estimations. The Climate Hazards Group (CHG) station archive built through the combination of several private and public data sources is used to set a global base of 47,390 observation stations.

Therefore, the CHIRPS algorithm combines the last datasets to calculate the final results. The interpolation algorithm approach is classified as a modified inverse distance weighting method. The blending procedure takes the radio between the five closest stations and the CHIRP product. Thus, the final CHIRPS version is a merging between the unadjusted and bias-adjusted CHIRP data.

### 3.5.3 GPM

The Global Precipitation Measurement (GPM) is a satellite mission headed by the National Aeronautics and Space Administration (NASA) and the Japan Aerospace Exploration Agency (JAXA). The mission aims to provide next-generation global observations of rain and snow, utilizing the previous successful mission: Tropical Rainfall Measuring Mission (TRMM). The GPM's satellite carries an advanced radar/radiometer system to measure the precipitation phenomena from space. Besides, the measurements serve as a reference for unifying observed rainfall from a combination of research and operational satellites. The GPM Core Observatory satellite launched in February/2014.

The algorithm approach intercalibrate, merge, and interpolate satellite microwaves precipitation estimates with microwave-calibrated infrared (IR) satellite estimates from the entire satellite network, precipitation gauge analyses, and potentially other precipitation estimators on a close time and space scale to GPM.

About the spatial resolution, the grid full coverage is provided from -60° to 60°, while the gap latitudes on the upper and under area (-90° to 90°) are understood as not a full coverage. The grid resolution is 0.1°. The daily time step stands from June/2000 to the near-present (~21 years) (NASA, 2021).

*3.5.3.1GPM Late Run and Final Run*

The algorithm system runs many times for each observation time. In this sense, the first estimation gives a quick result (IMERG Early Run), as soon as more data arrives, a better estimation is provided through the IMERG Late Run. The main difference between the two stages is that the Early Run only presents the possibility of forwarding propagation (applying extrapolation), while the Late Run provides both forward and backward propagation (applying interpolation).

The final step (IMERG Final Run) uses monthly gauge data to provide research-level products. The method combines the monthly gauges analysis from the Global Climatology Centre (GPCC) to the satellite data. The final results respect the adjustment of a fixed value for the month, but spatially varying. For research working applications, the Final Run version is always indicated, mainly when a fine time resolution is required (NASA, 2021).

### 3.5.4 ERA5

The European Centre for Medium-Range Weather Forecasts (ECMWF) built and maintained the ERA5 dataset. The grid is generated by a 4D-Var data assimilation and model forecasts of ECMWF's Integrated Forecasted System (IFS), combining different levels in the vertical. However, for the precipitation variable, the data extends over a 2D grid (surface or single level).

The dataset contains both: a high-resolution realization (reanalysis) and a reduced resolution ten-member ensemble (ensemble). The data is available at a sub-daily and monthly frequency, which consists of analyses and short (18 hours) forecasts. The present study considers the accumulated precipitation on a daily time-step. The database covers the period

from 1979 to the near-present (~42 years). The spatial grid covers the entire world from -90° to 90° on a ~0.28° grid resolution (ECMWF, 2021).

## 3.6 EVAPOTRANSPIRATION DATASETS

The following section describes each studied Evapotranspiration dataset: Observed (model forcing), TerraClimate (model forcing), and MODIS (only utilized in terms of comparison). In this regard, all the grids were interpolated to a 0.1° resolution over the model area when necessary. Table 2 shows the main information about the datasets.

Table 2 - Evapotranspiration dataset details.

| Short name | Full name | Spatial resolution | Spatial coverage | Temporal resolution | Temporal Coverage | Ref. |
|---|---|---|---|---|---|---|
| Observed grid | Daily grided meteorological variables in Brazil | 0.25° | Brazilian territory | Daily | Jan/1980 to Dec/2015 | 1 |
| TerraClimate | TerraClimate | ~0.04° | -90° to 90° | Monthly | Jan/1985 to to Dec/2019 | 2 |
| MODIS | MODIS Global Evapotranspiration Project | 500 m | -90° to 90° | 8 accumulated days | Jan/2000 to near-present | 3 |

Source: 1 - (XAVIER; KING; SCANLON, 2017) ; 2 - (ABATZOGLOU *et al.*, 2018); 3 - (NTSG, 2021) .

### 3.6.1 Observed

Section 3.5.1 describes the general specifications related to the dataset (XAVIER, KING and SCALON, 2016). Besides precipitation data, the dataset makes available estimated reference evapotranspiration (ETo). Also, the frame combines the necessary meteorological data used for the evapotranspiration estimation: maximum and minimum temperature ($T_{max}$ and $T_{min}$), solar radiation ($R_s$), wind speed at 2 m height ($u_2$), and relative humidity (RH). The meteorological data is collected from conventional and automatic weather stations of the National Meteorological Institute (INMET). The dataset methodology uses the Food and Agriculture Organization of the United Nations (FAO) Penman-Monteith method (ALLEN *et al.*, 1998). The equation estimates reference potential evapotranspiration for grass cover according to the following (3):

$$ET_O = \frac{0.408\,\Delta\,(R_n - G) + \gamma\,\frac{900}{T+273}\,u_2(e_s - e_a)}{\Delta + \gamma\,(1 + 0.34\,u_2)} \quad (3)$$

Where,

$ET_O$ = Reference Potential Evapotranspiration [mm/day]

$R_n$= Net Radiation [MJ/m2day]

$G$ = Soil heat flux density [MJ/m2day]

$T$ = Air temperature at 2 m [°C]

$u_2$= Wind speed at 2 m [m/s]

$e_s$= Saturation vapour pressure [kPa]

$e_a$= Actual vapour pressure [kPa]

$(e_s - e_a)$ = Saturation Vapour Pressure Deficit [kPa]

$\Delta$ = Slope vapour pressure curve [kPa/°C]

$\gamma$ = Psychrometric constant [kPa/°C]

### 3.6.2 TerraClimate

Abatzoglou *et al.* (2018) developed a high-spatial resolution dataset (~0.04°) for monthly climate/climatic water balance with global coverage from Jan/1985 to Dec/2019. The methodology uses climatically data from the WorldClim dataset and other sources to produce a primary monthly frame with Precipitation, Maximum and Minimum Temperature, Wind Speed, Vapor Pressure, and Solar Radiation. From the primary data, evapotranspiration (ETo) is calculated using the Equation (3). However, it reaffirms that the approach assumes a reference grass surface cover, which might provide biases where the vegetation presents different behavior compared to this assumption.

### 3.6.3 MODIS Evapotranspiration

MODIS Global Evapotranspiration Project (NTSG, 2021) estimates global terrestrial evapotranspiration using a combination of satellite remote data and global meteorological data. The dataset methodology to calculate potential evapotranspiration utilizes the Penman-Monteith approach Monteith (1965) through the following Equation (4):

$$\lambda ET = \frac{\Delta\,(R_n - G) + p_a c_p\,\frac{(e_s - e_a)}{r_a}}{\Delta + \gamma\,(1 + \frac{r_s}{r_a})} \quad (4)$$

Where,

$ET$ = Potential Evapotranspiration [mm]

$\lambda$ = Latent Heat [J/kg]

$R_n$= Net Radiation [MJ/m2day]

$G$ = Soil heat flux density [MJ/m2day]

$T$ = Air temperature at 2 m [°C]

$u_2$= Wind speed at 2 m [m/s]

$e_s$= Saturation vapour pressure [kPa]

$e_a$= Actual vapour pressure [kPa]

$(e_s - e_a)$ = Saturation Vapour Pressure Deficit [kPa]

$\Delta$ = Slope vapour pressure curve [kPa/°C]

$\gamma$ = Psychrometric constant [kPa/°C]

$r_s$ = Surface resistance [s/m]

$r_a$ = Aerodynamics resistance [s/m]

The main difference between the more generic approach from equation (3) to (4) is the term $\frac{r_s}{r_a}$, which describes the stomatal and aerodynamics resistance for the considered vegetation cover. The MODIS algorithm uses the LAI (Leaf Area Index) to estimate vegetation parameters.

## 3.7 MODEL EFFICIENCY COEFFICIENTS

The evaluation of the hydrological model's performance usually utilizes a comparison between observed and simulated river discharges at the catchment outlet. In this sense, the conclusion may be based on a simple visual inspection of the observed and simulated hydrograph. However, objective assessment requires a mathematical approach, which estimates the error between the simulated and observed discharge through efficiency coefficients (KRAUSE; BOYLE; BÄSE, 2005).

Firstly, the present study uses an adaptation of the Mean Relative Error (MRE) and the Mean Error (ME), computing the yearly average of both coefficients along the simulation years.

Finally, the Kling-Gupta efficiency (KGE) is calculated, the more complex coefficient allows comparison between different models and applications, besides a further comprehension of the model performance through its terms. The coefficients are described below.

### 3.7.1 Mean Error (ME) and Mean Relative Error (MRE)

As a first model evaluation, the Mean Error (ME, mm) and Mean Relative Error (MRE, %) are calculated in terms of depth runoff - a measurement of the water balance agreement between observed and simulated discharge. The chosen methodology adapts both coefficients to a yearly average over the simulation period. Besides, the depth runoff normalizes the discharge according to the gauge catchment area, as a result, the comparison between catchments with different areas is made possible. According to Unduche *et al.* (2018), the MRE calculates the error as a percentage of the observed values. In this sense, the coefficient presents a limitation that a small deviation in error can result in representative changes in MRE when dealing with small denominators. With regards to the limitation, the Mean Error (ME) is also computed, allowing a direct interpretation related to the precipitation phenomena on the catchment. The equations are shown below (the time step is only computed if there are valid values for simulated and observed discharges at the time step).

The simulated mean yearly depth runoff (5):

$$\bar{Q}_{sim} = \frac{1}{N} \sum_{ts=1}^{ts} Q_{sim,ts} \tag{5}$$

The observed mean yearly depth runoff (6):

$$\bar{Q}_{obs} = \frac{1}{N} \sum_{ts=1}^{ts} Q_{obs,ts} \tag{6}$$

Where,

$\bar{Q}_{sim}$ = simulated mean yearly depth runoff [mm]

$Q_{sim,ts}$ = simulated depth runoff at the time step [mm]

$\bar{Q}_{obs}$ = observed mean yearly depth runoff [mm]

$Q_{obs,ts}$ = observed depth runoff at the time step [mm]

N = number of simulated years

ts = time step

Therefore,

Mean error (ME, mm) is shown below ((7):

$$ME = \bar{Q}_{sim} - \bar{Q}_{obs} \quad (7)$$

Mean relative error (MRE, %) is shown below ((8):

$$MRE = \left[\frac{(\bar{Q}_{sim} - \bar{Q}_{obs})}{\bar{Q}_{obs}}\right] X\ 100 \quad (8)$$

### 3.7.2 Kling-Gupta Efficiency (KGE)

The Kling-Gupta efficiency (KGE) was developed from the Nash-Sutcliffe (NSE) coefficient, which has been widely used to calibrate and evaluate hydrological models for the last decades. The KGE approach decomposes the NSE into its constitutive components (correlation, variability bias and mean bias). The method utilization has been increasing for model calibration and evaluation, hence it facilitates the analysis of the relative importance of its different components. Therefore, KGE = 1 indicates a perfect match between simulations and observations(GUPTA *et al.*, 2009). The KGE equation is shown below (Eq. (9)).

$$KGE = 1 - \sqrt{(r-1)^2 + (\alpha-1)^2 + (\beta-1)^2}$$

$$KGE = 1 - \sqrt{(r-1)^2 + \left(\frac{\sigma_{sim}}{\sigma_{obs}} - 1\right)^2 + \left(\frac{\mu_{sim}}{\mu_{obs}} - 1\right)^2} \quad (9)$$

Where,

$KGE =$ Kling-Gupta efficiency (KGE)

$r =$ linear correlation between observations and simulations

$\alpha =$ a measure of the flow variability error

$\beta =$ a bias term

$\sigma_{sim} =$ standard deviation in simulations

$\sigma_{obs} =$ standard deviation in observations

$\mu_{sim} =$ simulation mean

$\mu_{obs} =$observation mean

This study sets the KGE threshold of 0.5 as a satisfactory model performance to evaluate the precipitation products. A reference combination of the KGE components would be:

$KGE \geq 0.5$

Where,

$r \geq 0.8$

$0.67 \leq \alpha \leq 1.33$

$0.67 \leq \beta \leq 1.33$

## 3.8 SIMULATION SPECIFICATIONS

Finally, Table 3 describes the general information about each simulation. In this sense, each running of the DHI Global Hydrological Model was forced by one of the five different studied precipitation datasets. Thus, the name of the specific precipitation forcing identifies the simulation. Also, the available period coverage of the precipitation product determines the simulation period.

Table 3 - Simulation Specifications.

| Simulation Name | Precipitation Dataset | Evapotranspiration Dataset | Start[1] | End[2] | Duration |
|---|---|---|---|---|---|
| Observed | Observed Grid[3] | Observed Grid[4] | 02/01/2000 | 01/01/2016 | 16 years |
| CHIRPS | CHIRPS | TerraClimate | 02/01/2000 | 01/01/2020 | 20 years |
| GPM Final | GPM Final | TerraClimate | 01/01/2001 | 01/01/2020 | 19 years |
| GPM Late | GPM Late | TerraClimate | 01/01/2001 | 01/01/2020 | 19 years |
| ERA5 | ERA5 | TerraClimate | 02/01/2000 | 01/01/2020 | 20 years |

*Where, 1,2 - dd/mm/yyyy, 3 - The Observed grid only covers the Brazilian Territory. Thus, the model area was filled by CHIRPS dataset; 4 - The Observed grid only covers the Brazilian Territory. Thus, the model area was filled by TerraClimate dataset.

The Appendix A shows the NAM parameters in the model area.

## 3.9 POST-PROCESSING PROGRAM

Each batch simulation (five precipitation datasets) generates a matrix with approximately 35 million values (365 days/year x 20 simulated years x 769 stations x (5 simulations + observed data).

Thus, a Python module named *ghm.py* was developed for the study. The Object-Oriented Programming (OOP) paradigm was utilized to guide the development. Besides, the Test-Driven development (TDD) approach was chosen for the coding process. Besides, the following data science, scientific, and GIS Python libraries compose the program: pandas, numpy, matplotlib, cartopy, and seaborn. Also, a specific library for hydrology studies was utilized (hydroeval). The program generates, in a matter of minutes, the final statistics, plots, ands maps.

# 4 RESULTS AND DISCUSSION

## 4.1 PRECIPITATION ANALYSIS

This section investigates the different model precipitation forcings: Observed Grid, CHIRPS, GPM Final, GPM Late, and ERA5. The mean yearly precipitation was calculated for the intersection period between the products (Jan/2001 to Jan/2016) for each model area pixel. The average values were grouped by the twelve Hydro-Regions (section 3.2). The regional yearly means indicate the expected model outputs in each model sub-area according to the rainfall dataset. Table 4 summarizes the results for the sixty possible combinations (12 Hyro-Regions x 5 precipitation products). While Figure 9 shows the precipitation spatial distribution over the Brazilian Territory.

The Hydro-Region Amazônica presents the highest mean yearly precipitation among the regions. The Observed grid gives the lowest value between the products. However, all the datasets provide close values, the GPM Late shows the highest bias (145.90 mm/year) when compared to the Observed grid, which represents only 6.5%. Figure 9 shows that the CHIRPS product utilizes an algorithm able to smooth the interpolation over this complex area. Additionally, some sharp peaks appear in the Observed grid, it might be a result of the lack of data in the area.

The GPM Final product tends to overestimate the precipitation in the entire Brazilian territory - Observed grid as the reference. Particularly, in the southern regions (Region Uruguai #12 and Atlântico Sul #6). The bias reaches positive values of approximately 15% (281.66 mm/year and 242 mm/year respectively).

Table 4 - Hydro-Regions: Mean Yearly Precipitation.

| **Hydro-Region** | **#** | **Observed [mm/year]** | **CHIRPS [mm/year]** | **GPM Final [mm/year]** | **GPM Late [mm/year]** | **ERA5 [mm/year]** |
|---|---|---|---|---|---|---|
| Amazônica | 1 | 2246.24 | 2302.10 | 2322.37 | 2392.14 | 2356.11 |
| Atlântico Leste | 2 | 879.75 | 871.49 | 812.58 | 741.15 | 803.98 |
| Atlântico Nordeste Ocidental | 3 | 1617.11 | 1610.69 | 1636.37 | 1680.48 | 1591.06 |
| Atlântico Nordeste Oriental | 4 | 828.89 | 823.55 | 860.50 | 730.81 | 704.40 |
| Atlântico Sudeste | 5 | 1411.46 | 1390.09 | 1487.41 | 1343.46 | 1436.43 |
| Atlântico Sul | 6 | 1673.80 | 1652.43 | 1818.53 | 1915.80 | 1641.91 |
| Paraguay | 7 | 1341.85 | 1336.80 | 1508.23 | 1727.00 | 1384.67 |
| Paraná | 8 | 1475.51 | 1470.53 | 1588.95 | 1705.99 | 1430.20 |
| Parnaíba | 9 | 990.71 | 991.55 | 1054.31 | 1140.04 | 992.58 |
| São Francisco | 10 | 896.77 | 913.47 | 987.07 | 1031.95 | 842.26 |
| Tocantins-Araguaia | 11 | 1769.49 | 1809.37 | 1842.79 | 1940.69 | 1703.83 |
| Uruguai | 12 | 1771.55 | 1760.75 | 1883.14 | 2053.22 | 1754.52 |
| Mean | - | 1408.59 | 1411.06 | 1483.52 | 1533.55 | 1386.82 |

Figure 9 - Map Mean Yearly Precipitation.

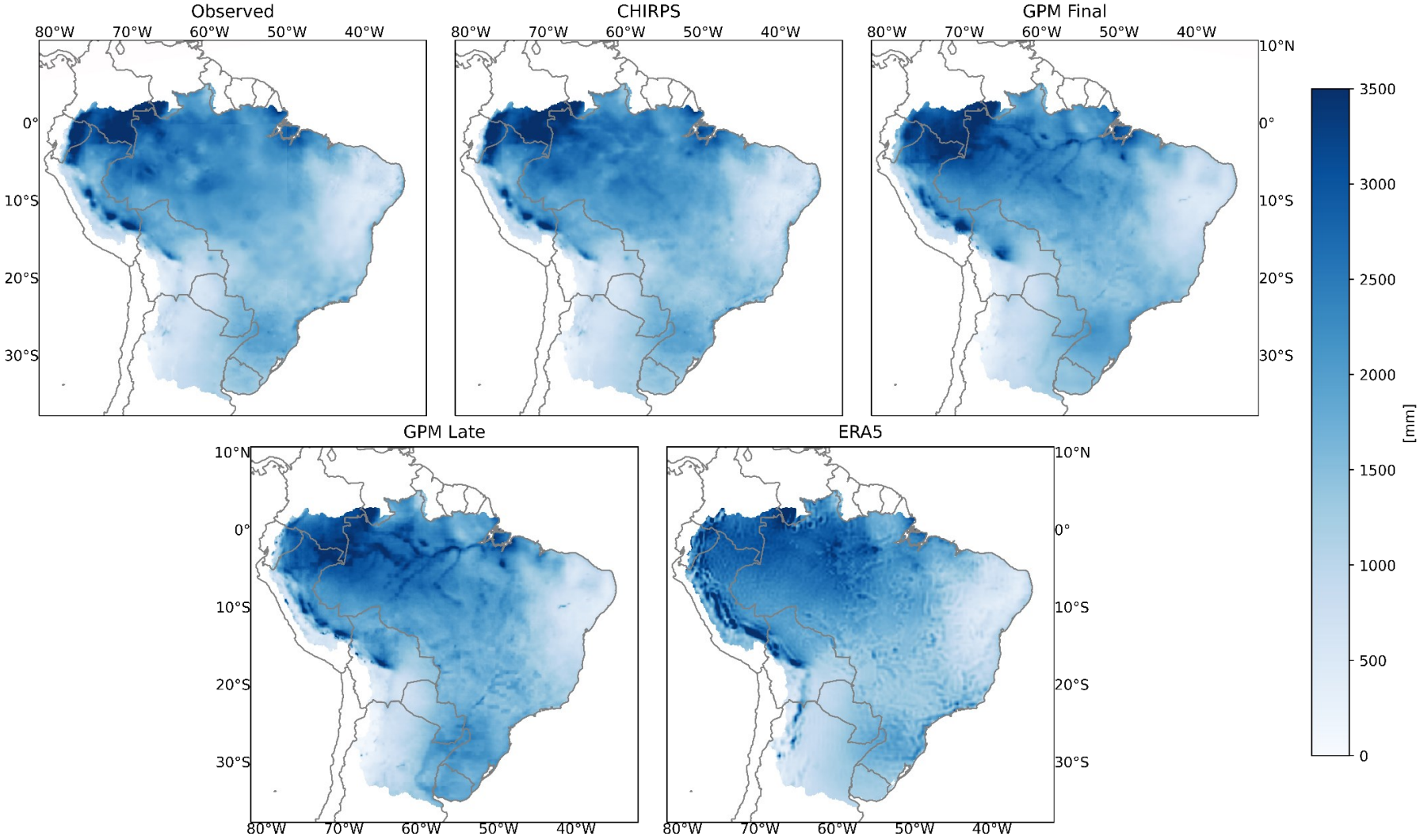


Source: Author.

## 4.2 BRAZILIAN TERRITORY

This section describes the model results according to the different precipitation forcing datasets in the entire Brazilian territory. The results are evaluated in terms of Mean Error (ME) - based on mean yearly depth runoff, Mean Relative Error - (MRE) - based on mean yearly depth runoff, Kling-Gupta efficiency (KGE), ads its components: Linear Correlation (r), Flow Variability Error (Alpha), and Bias (Beta).

The analyses utilized the whole observed discharge dataset built in the last section. However, station number 30055000 showed a large ME, which was compromising the overall statistics. In this sense, the statistics calculation does not include this gauge for this/next sections. The total number of analyzed stations is 767.

### 4.2.1 Mean Error (ME)

As the first overview of results over the Brazilian territory, the ME is explored related to each precipitation dataset. Table 5 shows the measures of central tendency. In this sense, the ERA5 dataset showed the best results, which respectively presents mean and median (Q 50%) equals 96.78 mm and 95.02 mm. However, as expected, the statistics for the Observed run also indicate a low error in average (100.74 mm) and in its median (105.13 mm). Additionally, it was expected a better performance for the CHIRPS dataset, since it combines sources of satellite and bias correction. However, the mean ME for the running is 145.29 mm, and the median of 153.86 mm. The GPM products presented the highest error, the results indicate an important improvement related to the Final version in comparison with the Late dataset, indicating how fundamental the bias correction is for the area.

Table 5 - Brazilian territory - ME.

| Dataset | Mean [mm] | S. D. [mm] | Min. [mm] | Q 25% [mm] | Q 50% [mm] | Q75% [mm] | Max. [mm] |
|---|---|---|---|---|---|---|---|
| Observed | 100.74 | 159.80 | -611.19 | 11.30 | 105.13 | 192.88 | 719.04 |
| CHIRPS | 145.29 | 162.48 | -492.60 | 45.14 | 153.86 | 243.93 | 718.16 |
| GPM Final | 192.49 | 152.86 | -489.82 | 97.82 | 203.46 | 285.14 | 640.08 |
| GPM Late | 214.38 | 196.72 | -633.41 | 92.50 | 215.93 | 348.01 | 719.31 |
| ERA5 | 96.78 | 182.96 | -820.73 | -3.99 | 95.02 | 206.15 | 652.08 |

In this sense, Figure 10 presents the variability of the results centered on zero error. The Q 25% for ERA5 (-3.99 mm) confirms the model's accuracy when forced by the dataset.

In contrast to GPM Final that presents a Q 25% close to the ERA 5 median. However, the smallest Interquartile Range is provided by the Observed dataset (181.58 mm).

Figure 10 - Brazilian territory - ME.

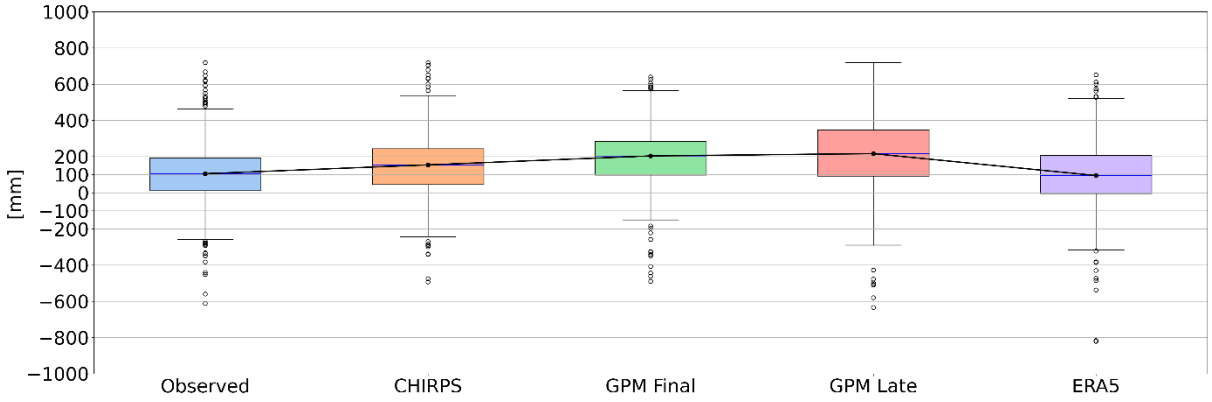


Source: Author.

Additionally, the same pattern of a positive bias is presented for the five different simulations. Thus, it stresses the importance of a better understanding related to the water balance in the Brazilian territory – further analysis about the evapotranspiration forcing is taken in Section 4.5.

Besides, Figure 11 shows the ME spatial distribution over the Brazilian territory, comparing the precipitation datasets. The improvement between the GPM Final version and GPM Late is more visible in the south. In a general overview, all the datasets are overestimating the discharge in the north of the country. For the observed dataset, some punctual issues rise, mainly a result of local interpolation problems - lack of rainfall gauges.

Figure 11 - Map Brazilian territory - ME.

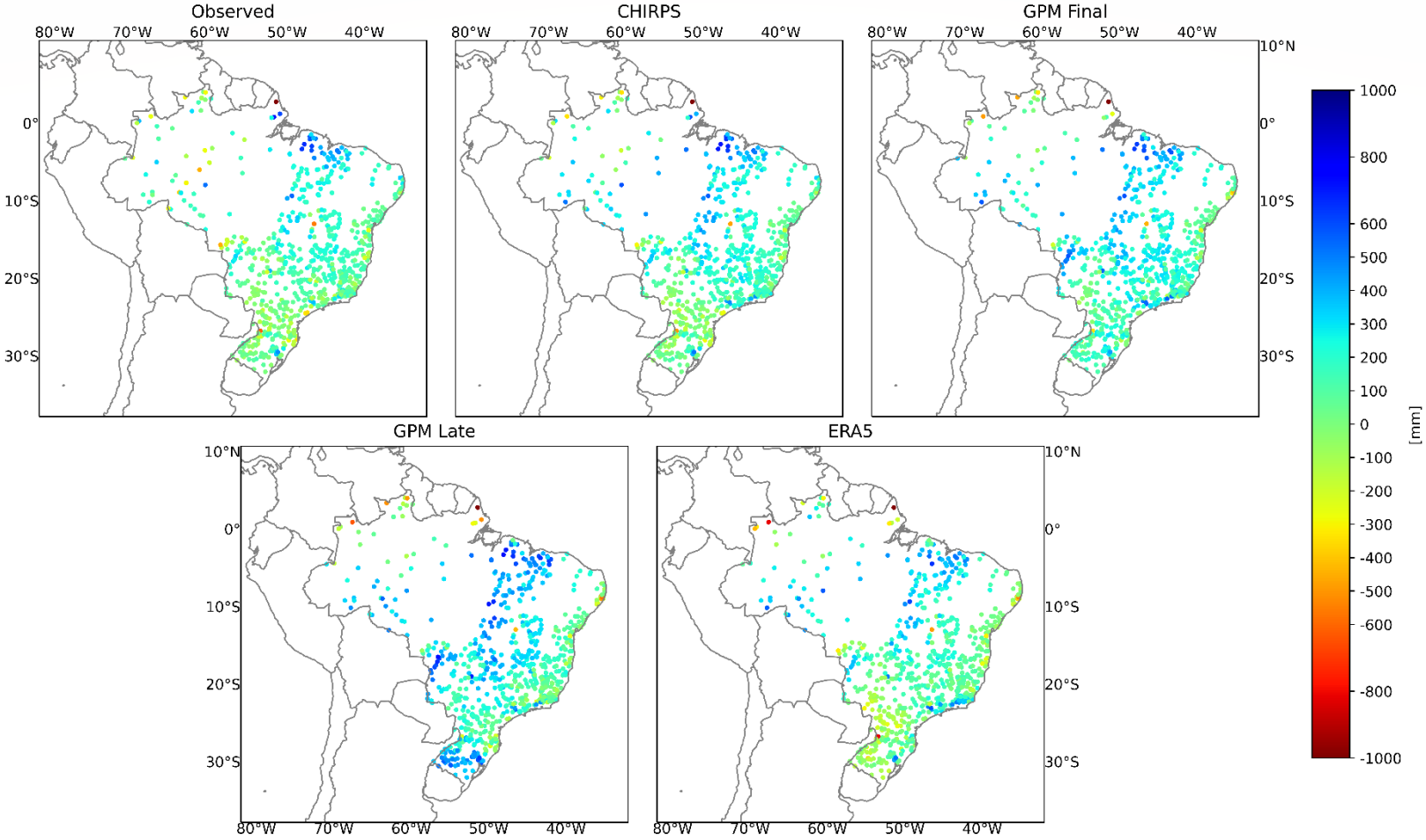


Source: Author.

### 4.2.2 Mean Relative Error (MRE)

Table 6 summarizes the Mean Relative Error (MRE) in the terms of the ratio between the simulated and observed runoff depth. It is an important measurement since the model deals with a large range of river discharge amounts. As a result of being a ratio indicator, the values themselves might assume extreme results. Thus, it makes sense to analyze the Q 50% (median) as the main indicator.

As observed in the ME analyzes. ERA5 and Observed runs show the best accuracy. Concerning these datasets, the median assumes a value close to 25%: 26.49% for ERA5 and 23.66% for Observed. However, the Q 25% shows an error close to 0% for both datasets: 1.73% (Observed) and -0.92% (ERA5).

Table 6 - Brazilian territory - MRE.

| Dataset | Mean [%] | S.D. [%] | Min. [%] | Q 25% [%] | Q 50% [%] | Q75% [%] | Max.[%] |
|---|---|---|---|---|---|---|---|
| Observed | 83.80 | 241.65 | -66.48 | 1.73 | 26.49 | 71.49 | 4748.92 |
| CHIRPS | 96.66 | 220.04 | -54.20 | 7.26 | 40.16 | 95.63 | 3662.67 |
| GPM Final | 117.05 | 255.80 | -65.07 | 18.46 | 49.37 | 104.31 | 3715.32 |
| GPM Late | 126.49 | 276.64 | -92.71 | 18.47 | 51.44 | 116.00 | 3309.81 |
| ERA5 | 69.95 | 196.98 | -87.14 | -0.92 | 23.66 | 68.35 | 3320.25 |

Also, Figure 12 shows a comparison of the different datasets according to MRE group intervals. The group (-20%:20%) is considered the focus since it represents the stations with the best model results.

Figure 12 - Brazilian territory - MRE.

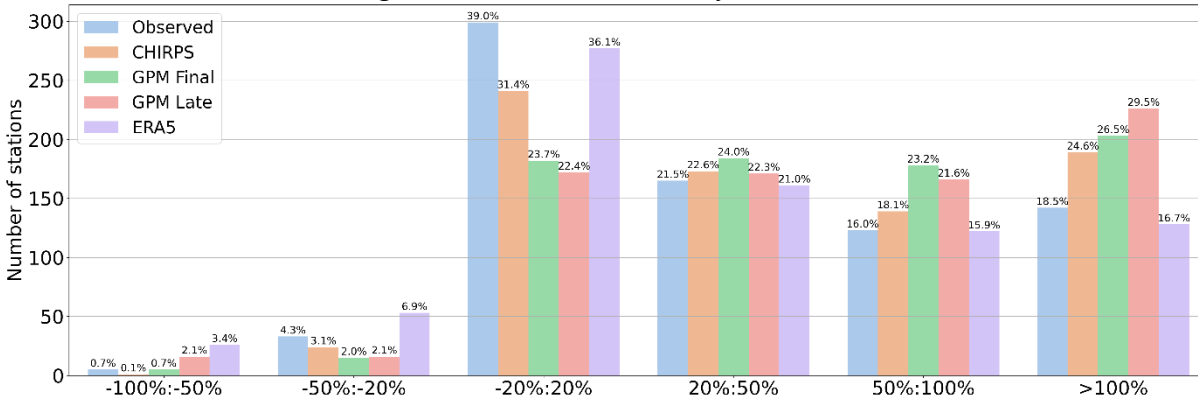


Source: Author.

The same pattern in Figure 11 is observed in Figure 13. The satellite products (CHIRPS and GPM Final/Late) tend to overestimate (113.40% on average) more the MRE than the Observed and ERA5 products.

Figure 13 - Map Brazilian territory - MRE.

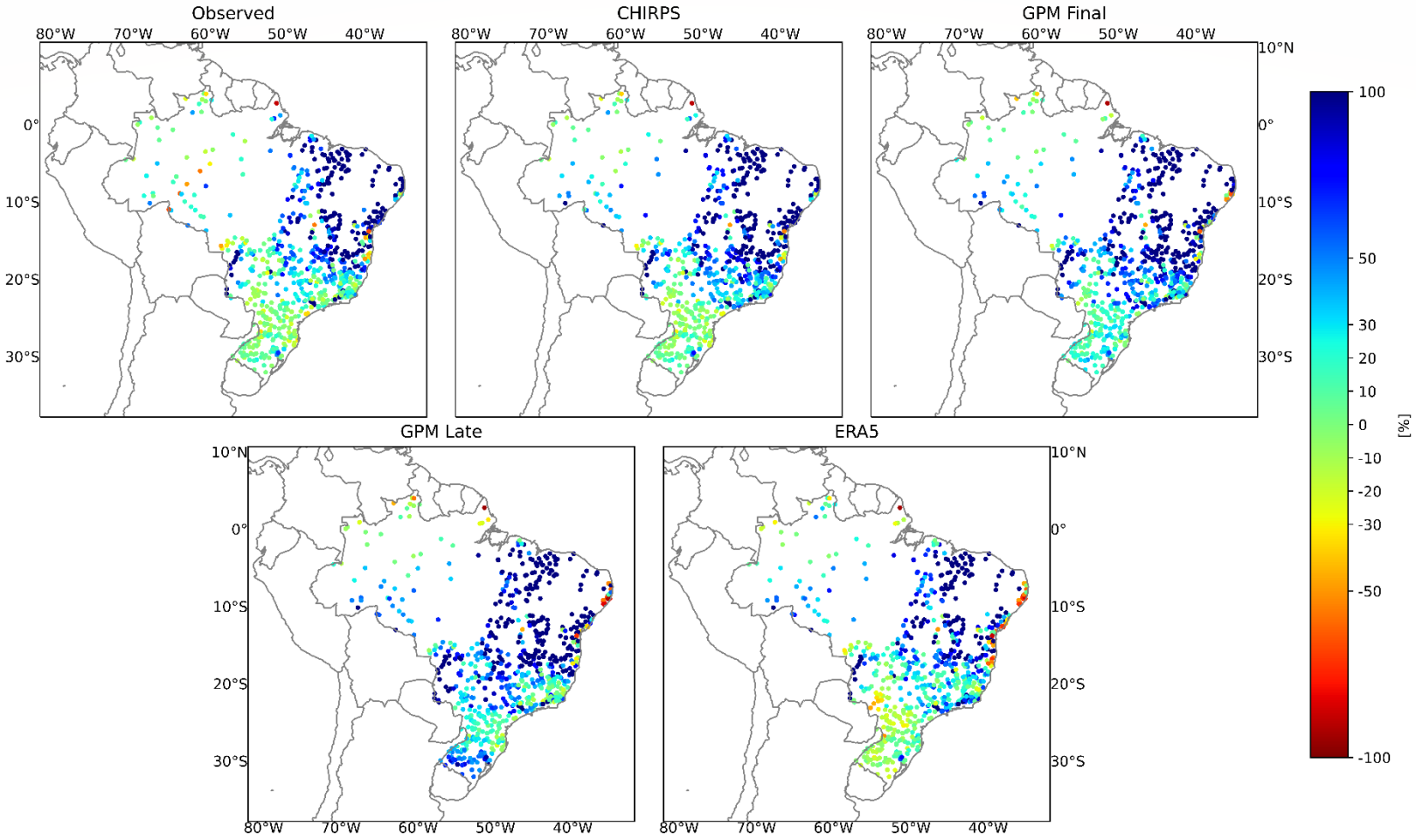


Source: Author.

### 4.2.3 Kling-Gupta Efficiency - KGE

The Kling-Gupta efficiency was grouped in different ranges: < 0.00; 0.00:0.25; 0.25:0.50; 0.50:0.75; 0.75:1.00. Figure 14 shows the station's frequency grouped by KGE intervals and precipitation datasets. The interval < 0.00 is not shown in the plot to make the visualization easier, but Figure 15 shows its locations. The station's frequencies for each simulation in this interval are Observed (63.2%), CHIRPS (66.0%), GPM Final (68.8%), GPM Late (75.9%), ERA5 (62.8%). The model results would be satisfactory for a KGE threshold of 0.50, thus, the focus interval groups are 0.50:0.75, and 0.75:1.00.

With regards to the interval of 0.50:0.75, CHIRPS (17.1%) and the Observed (17.7%) dataset presents the highest station frequency. While only 8.6% of the stations in the ERA5 run show a KGE in this range. For the last two analyzed error measurements (ME and MRE), ERA5 had provided better accuracy than CHIRPS. It suggests that ERA5 has a better performance in terms of water balance, but not for the hydrograph shape. In this sense, the interval 0.75:1.00 computes a small frequency for all the simulations. However, the same pattern happens.

For the next three sections, further analysis is conducted to investigate each component of the KGE (Linear Correlation [r], Flow Variability Error [Alpha], and Bias [Beta]). It is therefore expected fitter linear correlation results for the CHIRPS and Observed datasets than for ERA5. Although ERA5 would perform better for the Bias coefficient than CHIRPS.

Figure 15 indicates a good improvement for the GPM Final when compared to GPM Late. It stresses the importance of observation correction conducted by the GPM Final algorithm in the South of Brazil. Nevertheless, there is still a large difference between satellite/observation-corrected products (GPM Final and CHIRPS).

Figure 14 - Brazilian territory - KGE.

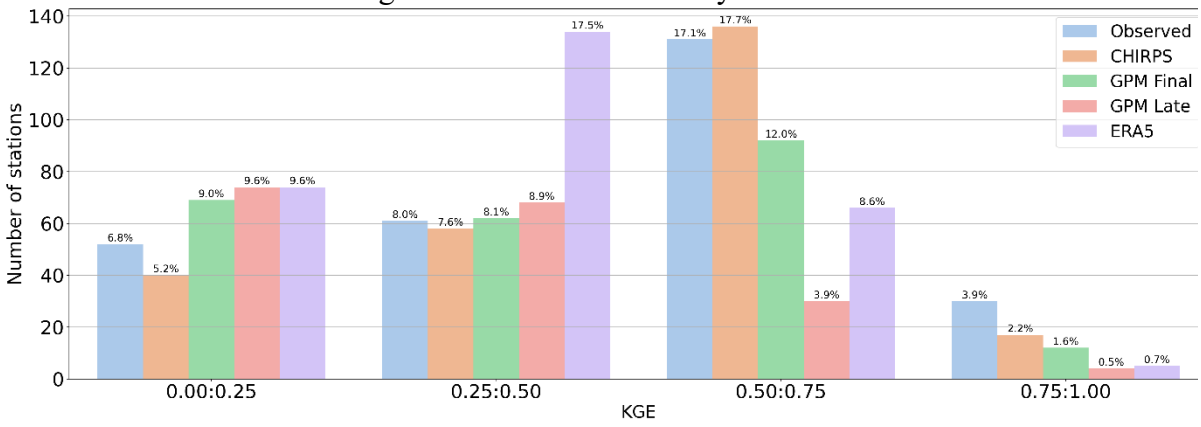


Source: Author.

Figure 15 - Map Brazilian territory - KGE.

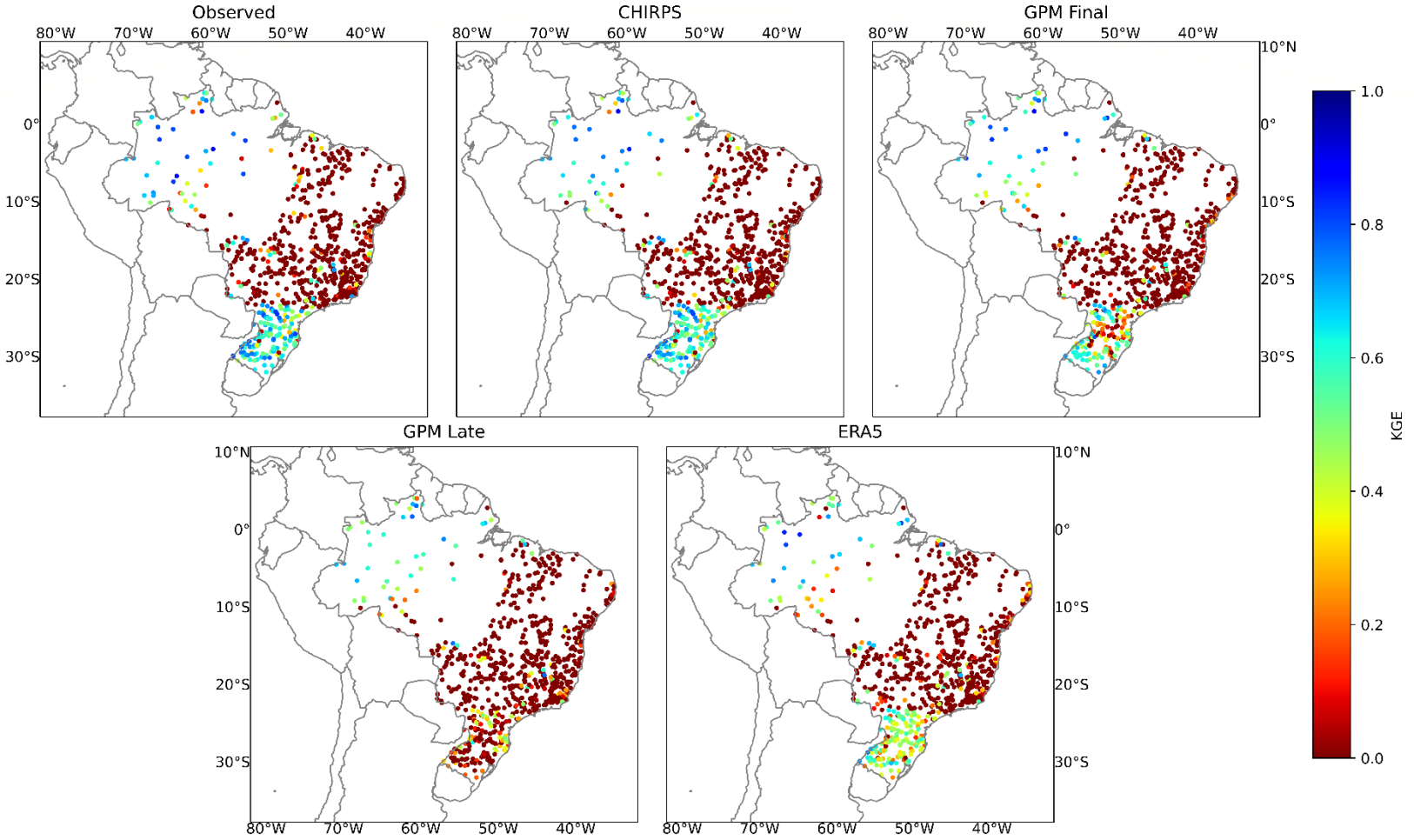


Source: Author

*4.2.3.1Linear Correlation (r)*

The Linear Correlation (r) is the first analyzed KGE component. Table 7 shows the calculated statistics for the r coefficient. The model efficiency is analyzed in terms of the median. The Observed dataset provided the highest median (0.78). Besides, the satellite/observation-corrected products (CHIRPS and GPM Final) showed a similar accuracy, respectively, 0.73 and 0.74. As expected when analyzing the KGE results, ERA5 provided the worse results with a medium equals to 0.65, and the same pattern for the mean (0.62). It demonstrates why the product presented low values of KGE, even though it performs well for ME and MRE.

Table 7 - Brazilian territory - Linear Correlation (r)

| **Dataset** | Mean | Standard Deviation | Minimum | Q 25% | Q 50% | Q75% | Maximum |
|---|---|---|---|---|---|---|---|
| Observed | 0.73 | 0.16 | -0.14 | 0.68 | 0.78 | 0.83 | 0.95 |
| CHIRPS | 0.69 | 0.16 | -0.30 | 0.64 | 0.73 | 0.80 | 0.94 |
| GPM Final | 0.71 | 0.16 | -0.15 | 0.66 | 0.74 | 0.81 | 0.93 |
| GPM Late | 0.63 | 0.17 | -0.25 | 0.57 | 0.67 | 0.74 | 0.94 |
| ERA5 | 0.62 | 0.18 | -0.28 | 0.53 | 0.65 | 0.75 | 0.95 |

The following range groups were created to classify the calculated coefficients over the different datasets: < 0.00; 0.00:0.25; 0.25:0.50; 0.50:0.75; 0.75:1.00. The negatives r values are shown only in Figure 17 as it presents a low frequency. As three of the datasets provided medians close to 0.75, this value is set as the threshold for satisfactory model results. Figure 16 shows the grouped linear correlation coefficients, more than 400 stations are classified in the most upper group for the Observed dataset, followed by the satellite/observation-corrected products (CHIRPS and GPM Final), which approximately 300 stations are presented.

Figure 16 - Brazilian territory - Linear Correlation (r).

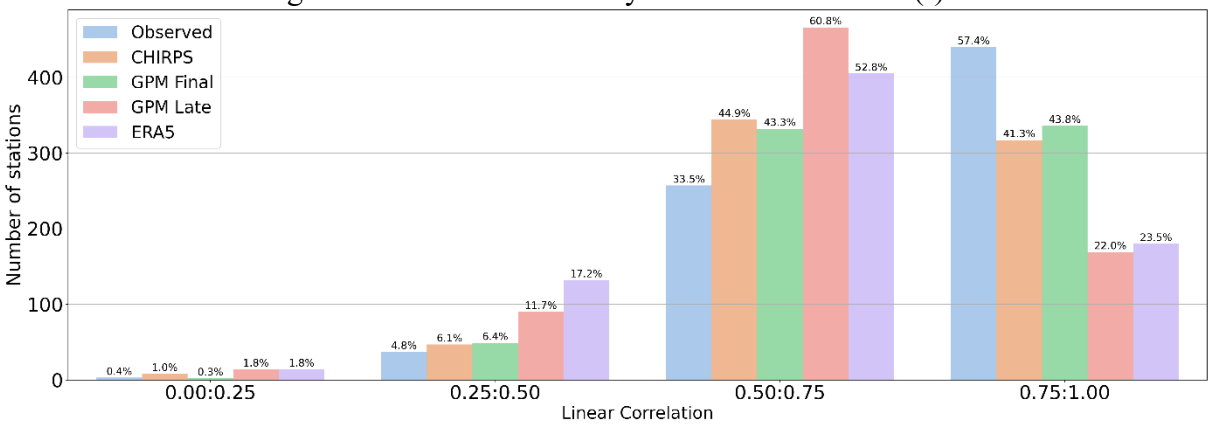


Source: Author.

Figure 17 shows the spatial distribution of the linear correlation over the Brazilian territory. Despite the high values for ME and MRE in the north region, the r values identify a high linear correlation between observed and simulated discharges.

Figure 17 - Map Brazilian territory - Linear Correlation (r).

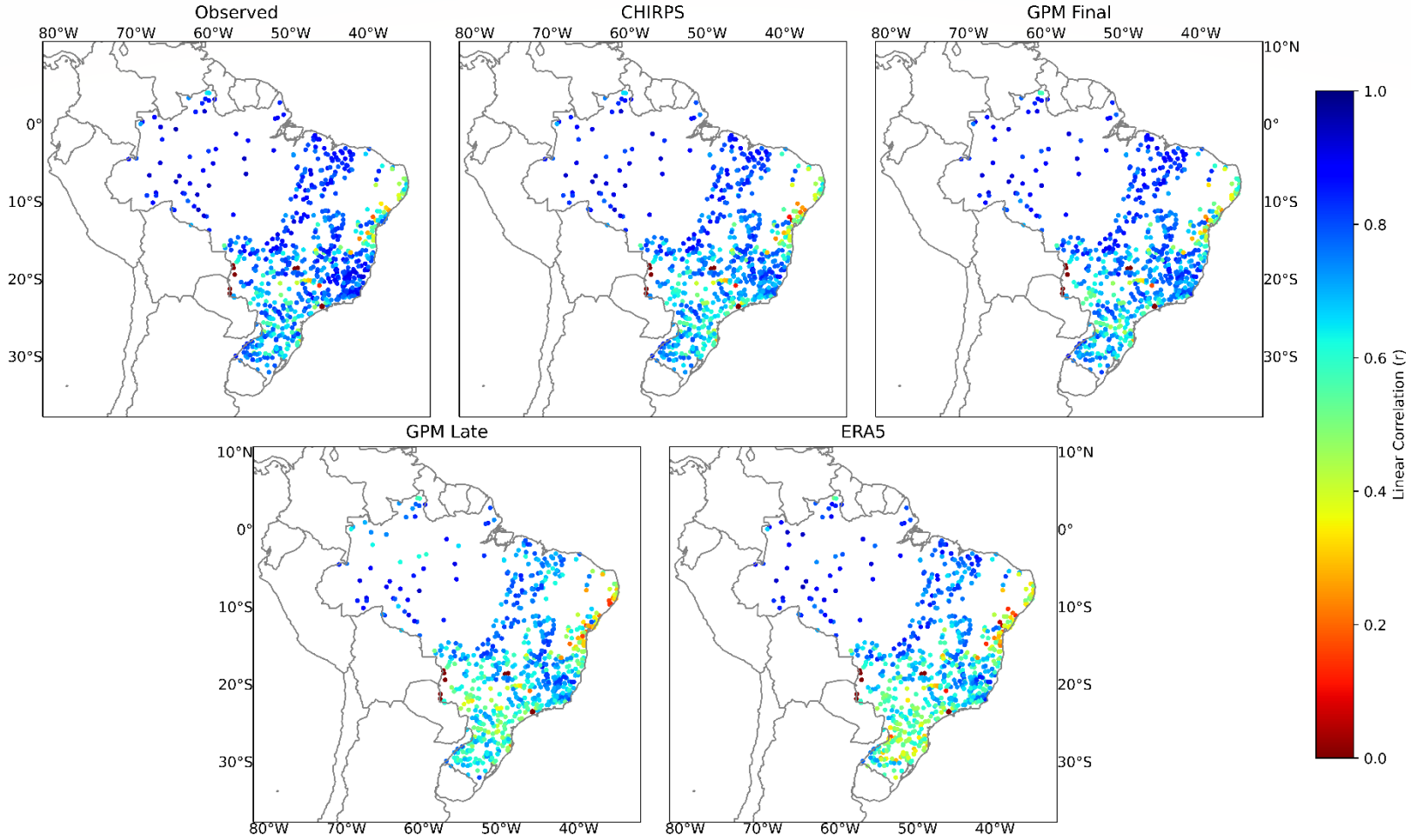


Source: Author.

*4.2.3.2Flow Variability Error (Alpha)*

Table 8 shows the statistics calculated from the Flow Variability Error (Alpha) over the precipitation products. As the statistics presented sparse maximum values (a good result would be centered on one), the median is again utilized to evaluate the model performance concerning the variability. Therefore, the calculated medians for the datasets do not show a significant difference between them. Additionally, the Observed, CHIRPS, and ERA presents approximately the same mean (~3). Thus, the KGE is mainly defined by the Linear Correlation (r) and the Bias (Beta).

Table 8 - Brazilian territory - Flow Variability (Alpha).

| **Dataset** | Mean | Standard Deviation | Minimum | Q 25% | Q 50% | Q75% | Maximum |
|---|---|---|---|---|---|---|---|
| Observed | 3.04 | 3.13 | 0.28 | 1.31 | 2.33 | 3.28 | 26.80 |
| CHIRPS | 3.03 | 3.01 | 0.29 | 1.32 | 2.35 | 3.29 | 25.90 |
| GPM Final | 3.45 | 3.55 | 0.41 | 1.59 | 2.56 | 3.68 | 32.44 |
| GPM Late | 3.61 | 3.94 | 0.26 | 1.82 | 2.50 | 3.61 | 37.15 |
| ERA5 | 2.97 | 3.35 | 0.22 | 1.22 | 2.18 | 3.19 | 30.45 |

As shown in the statistics, there are large maximum values for the calculated Alpha. The following range groups were created to classify the calculated ratios over the different datasets: 0.00:0.50; 0.50:1.50; 1.50:2.00; 2.00:3.00; 3.00:4.00; >4.00. In this sense, the model efficiency according to the precipitation datasets is evaluated in the range group centered on one (0.50:1.50). In this range, the station frequency is almost the same for Observed, CHIRPS, and ERA5 (Figure 18).

Figure 18 - Brazilian territory - Flow Variability Error (Alpha).

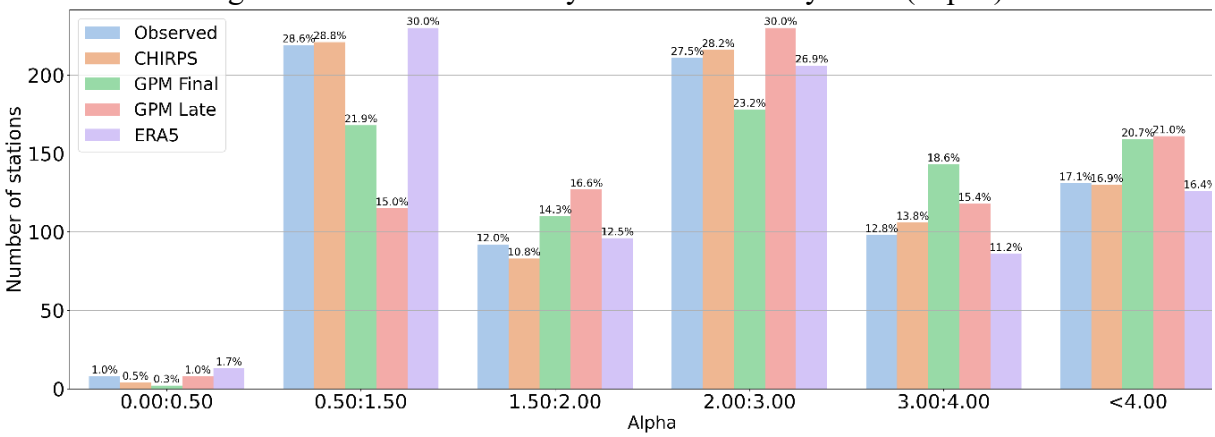


Source: Author.

Figure 19 shows almost the same pattern as the ME and MRE indicators. But in this case, the CHIRPS dataset shows results close to the Observed and ERA5 datasets.

Figure 19 - Map Brazilian territory - Flow Variability Error (Alpha).

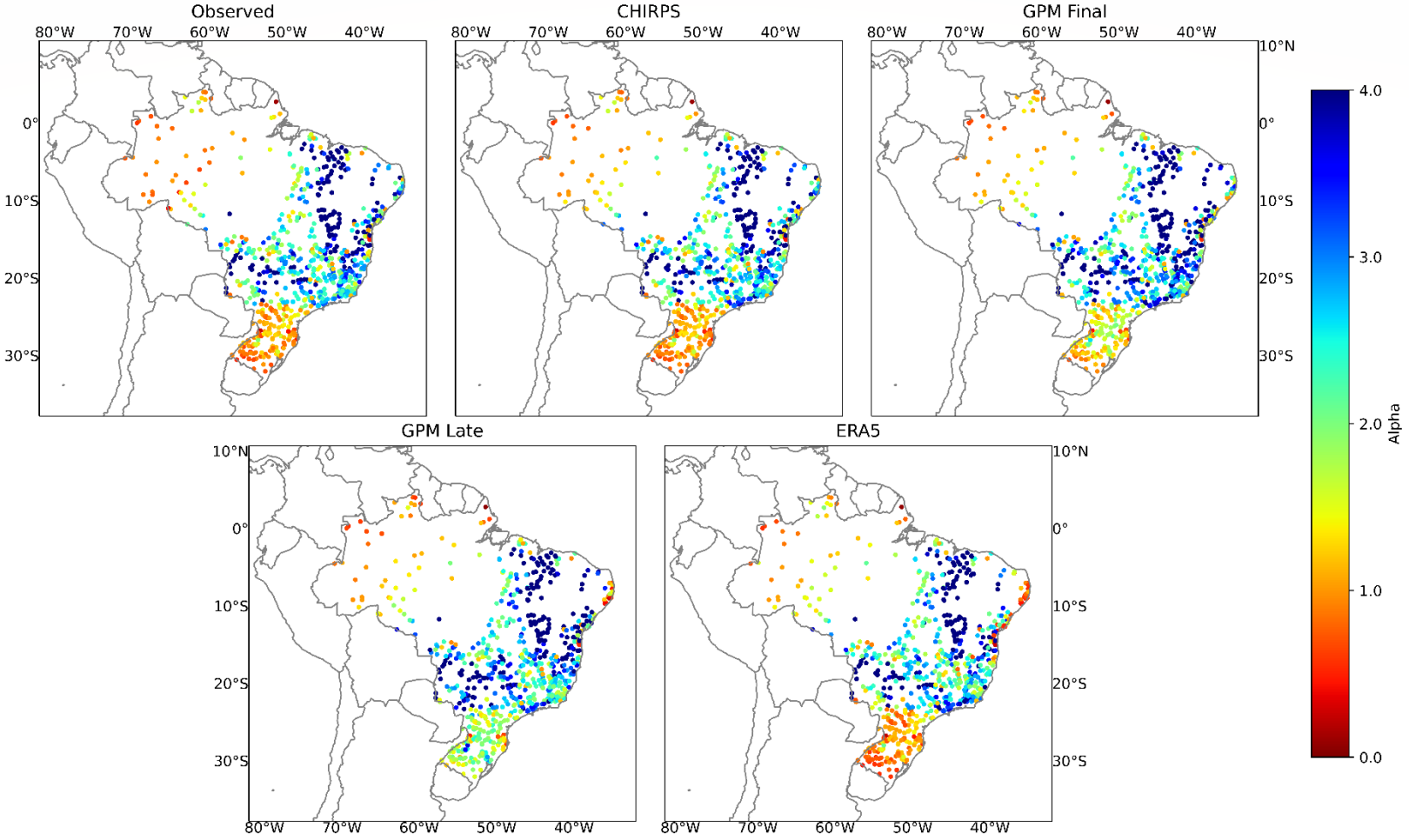


Source: Author.

*4.2.3.3Bias (Beta)*

Table 9 shows the Bias (Beta) statistics. The MRE (section 4.2.2) has the same interpretation as the Bias, but the MRE is presented in percentage and the Bias as a ratio. The median is used as the main efficiency measurement. ERA5 and Observed datasets show the best results for the median, 1.26 and 1.24 respectively. While CHIRPS presented a median equals to 1.40.

Table 9 - Brazilian territory -Bias (Beta).

| **Dataset** | Mean | Standard Deviation | Minimum | Q 25% | Q 50% | Q75% | Maximum |
|---|---|---|---|---|---|---|---|
| Observed | 1.84 | 2.42 | 0.34 | 1.02 | 1.26 | 1.72 | 48.46 |
| CHIRPS | 1.97 | 2.20 | 0.46 | 1.07 | 1.40 | 1.96 | 37.61 |
| GPM Final | 2.17 | 2.56 | 0.35 | 1.19 | 1.49 | 2.04 | 38.18 |
| GPM Late | 2.27 | 2.77 | 0.07 | 1.18 | 1.51 | 2.16 | 34.12 |
| ERA5 | 1.70 | 1.97 | 0.13 | 0.99 | 1.24 | 1.69 | 34.19 |

Utilizing the same group range as the Flow Variability Error (Alpha), the model efficiency is also considered reasonable in the range centered on one (0.50:1.50). The results are illustrated in Figure 20. Among the KGE components, Bias shows the best results. Observed and ERA5 datasets show a frequency of almost 500 stations (~64%), while CHIRPS presents more than 400 stations (56.6%). The GPM products do not show a large difference between the two datasets.

Figure 20 - Brazilian territory -Bias (Beta).

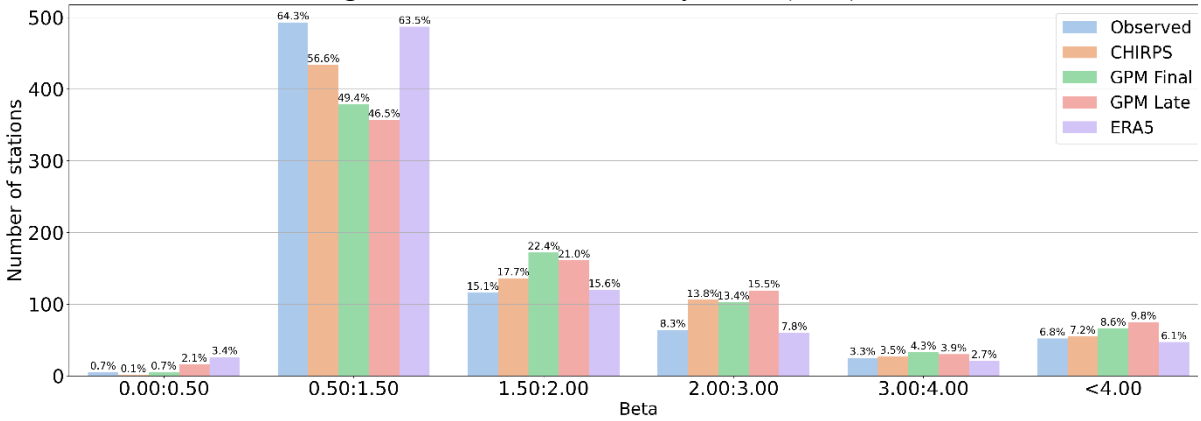


Source: Author.

Figure 21 reaffirms the MRE (section 4.1.2) comparison, in which the satellite/observation-corrected products (CHIRPS and GPM Final) tend to present a higher BIAS than the Observed and ERA5 datasets.

Figure 21 - Map Brazilian territory -Bias (Beta).

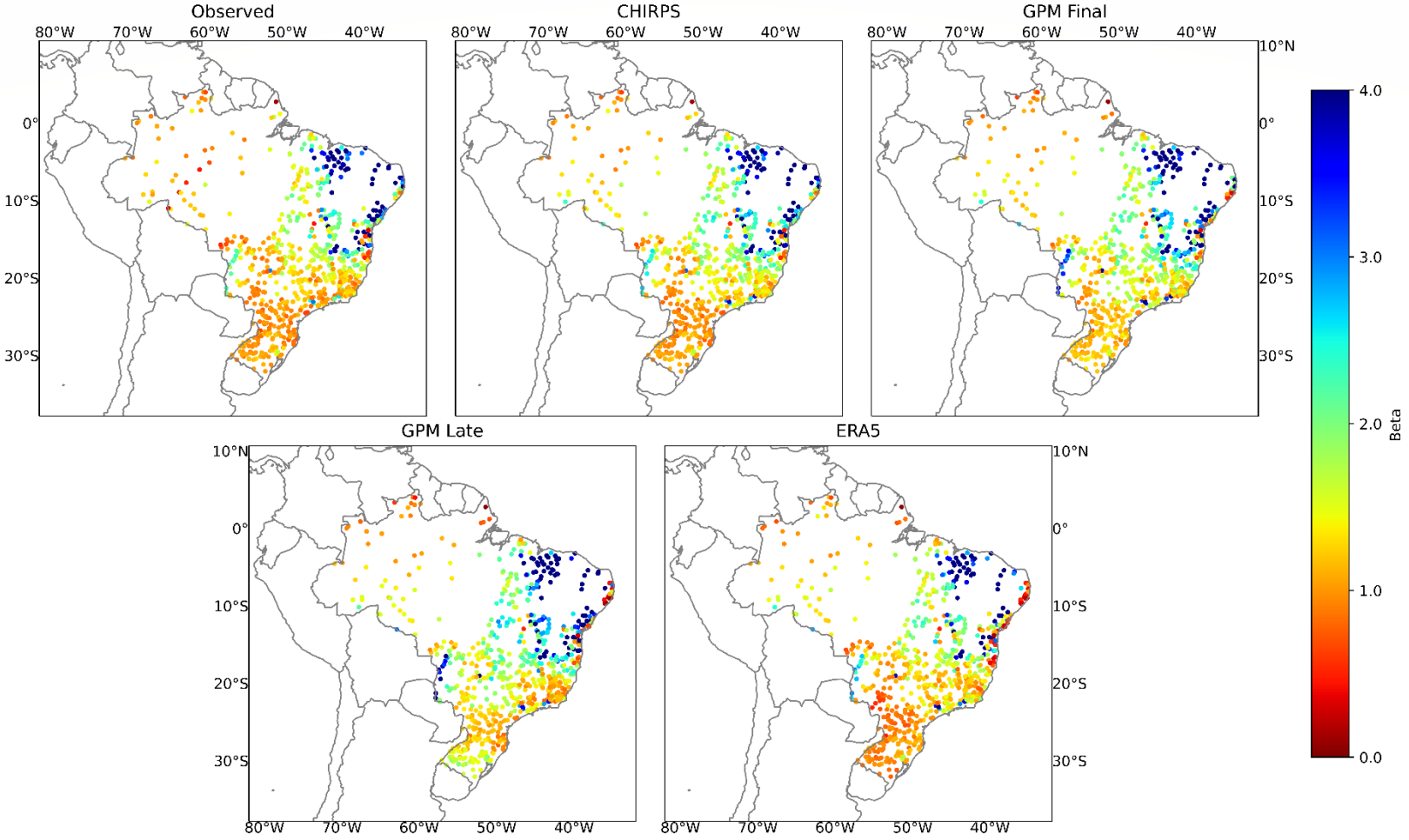


Source: Author.

## 4.3 HYDRO-REGIONS

This section describes the model evaluation analysis grouped by the Brazilian Hydro-Regions (introduced in section 3.2) for the different precipitation products. Hence, the model evaluation over the entire Brazilian territory had indicated a large variability in the calculated model efficiency indicators. Thus, this section aims to cluster the discharge gauges according to the physical characteristics of their basins/drainage areas. Figure 22 summarizes the Mean Error (ME). Each plot (row) describes a precipitation dataset, while the box plots (columns) refer to a specific Hydro Region numbered from #1 to #12 (indicated in section 3.2).

Since section 4.2.1 determined that ERA5 and the Observed runs had shown the best accuracy for the ME indicator, it is relevant to understand the error pattern across the regions for both simulations. Concerning the Observed dataset, the region Uruguai (#12) gives the best median result (16.02 mm). However, CHIRPS provides a better median result (15.63 mm) for the region. Although ERA5 showed a small ME median for the region, it is the only negative value (-50.80 mm). Therefore, it indicates that the ERA5 simulated discharge values are lower than the observed ones. In respect of the region Amazônica (#1), the boxplots indicate a sparse error for most of the datasets, which is expected due to the large discharges in the region - the relative error (covered in section 4.3.1.2) would be more meaningful in this case. In this sense, ERA5 provided the smallest Interquartile Range (250.24 mm) among the simulations for region #1.

In contrast to the region Amazônica (#1), the Hydro-Regions Parnaíba (#9) and São Francisco (#10) provide the small Interquartile Ranges over all the combinations (5 precipitation datasets x 12 Hydro-Regions). For instance, region #9 Interquartile Range presents an averaged value over the precipitation datasets equals to 82.47 mm, while region #10 gives 79.23 mm. However, the ME median is approximately 200 mm or larger for both regions across all the simulations - which indicates a systematic calibration problem in the model for these areas.

Finally, the analyses covered in this section, and the KGE coefficient spatial distribution (Figure 15) suggest that further evaluation of the precipitation products should be investigated in the following Hydro Regions: Amazônica (#1), Atlântico Sul (#6), and Uruguai (#12). Since the model had shown the best accuracy in these regions.

Figure 22 - Hydro Regions -ME.

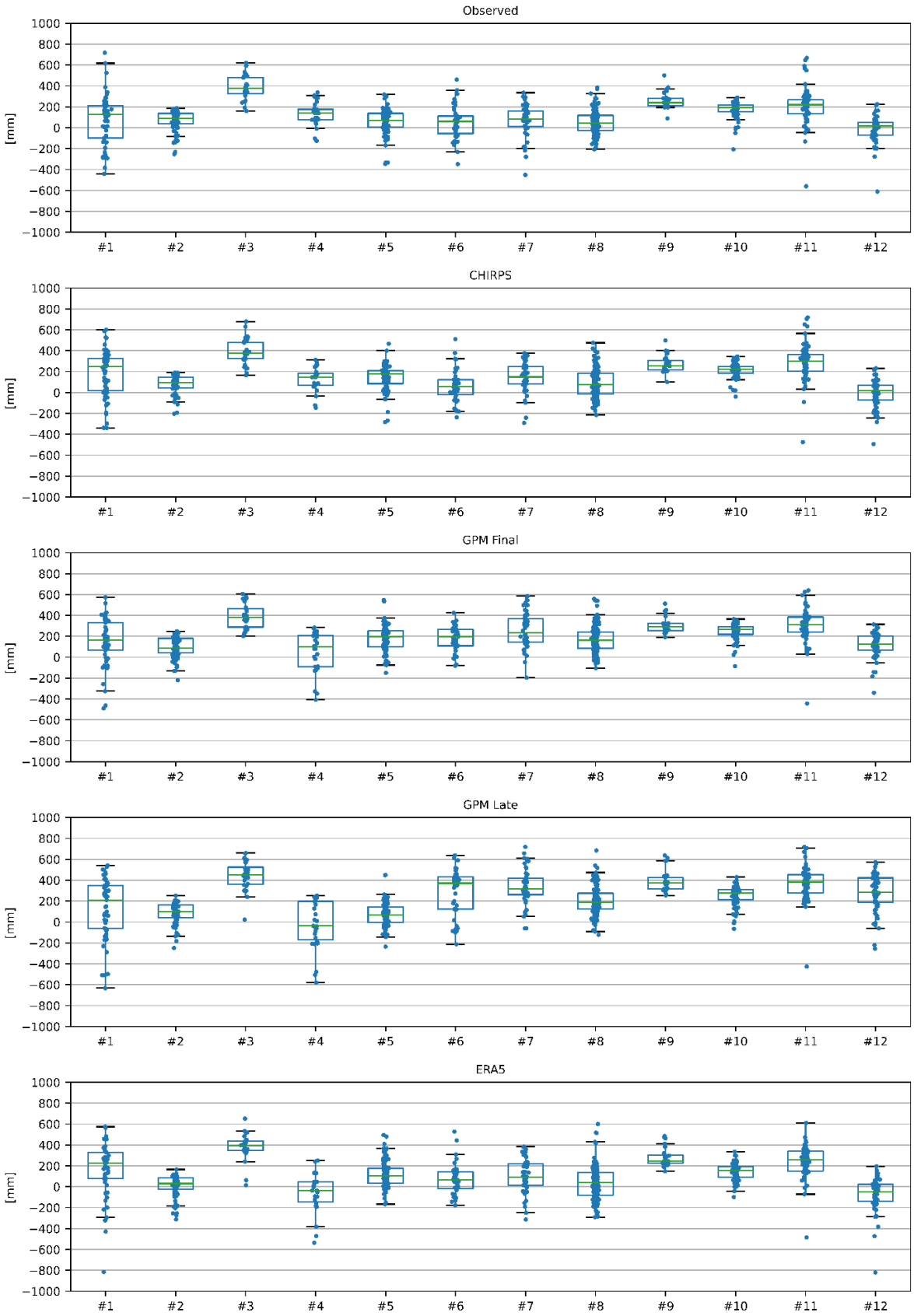


Source: Author.

### 4.3.1 Hydro Region Amazônica (#1)

This section evaluates the models results according to the different datasets for the Hydro Region Amazônica (#1). The statistical analyses over the Hydro Regio Amazônica investigated 53 discharge gauges, corresponding to 6.91% of the total analyzed stations. For these gauges, the yearly mean observed depth runoff in the region is 1015.11 mm for the studied period (2000-2020).

*4.3.1.1Mean Error (ME)*

With this in view, Table 10 describes the statistics for the Mean Error (ME). Again, the statistics might be influenced by the extremal minimum and maximal values, thus the median provides the best measurement for the indicator. Therefore, the Observed dataset gives the best results in the region, since it presents a median ME equals to 128.27 mm. However, it is relevant to notice that the run provided the largest maximum value among all the simulation, additionally, it gives the only outlier for the maximum threshold. As presented in Section 3.5.1, the Amazon Basin shows the lowest spatial coverage of rainfall gauges. Thus, the high variability showed in the discharge results, might be correlated to local interpolation issues in the precipitation grid.

Table 10 - Hydro-Region Amazônica - ME.

| Dataset | n | Mean [mm] | S. D. [mm] | Min. [mm] | Q 25% [mm] | Q 50% [mm] | Q75% [mm] | Max. [mm] |
|---|---|---|---|---|---|---|---|---|
| Observed | 53 | 78.55 | 243.55 | -440.66 | -99.25 | 128.27 | 213.13 | 719.04 |
| CHIRPS | 53 | 177.61 | 228.90 | -339.72 | 19.33 | 247.49 | 323.12 | 601.32 |
| GPM Final | 53 | 145.39 | 223.48 | -489.82 | 65.30 | 162.55 | 331.99 | 572.94 |
| GPM Late | 53 | 127.84 | 287.55 | -633.41 | -59.60 | 209.20 | 350.36 | 542.33 |
| ERA5 | 53 | 154.70 | 266.40 | -816.04 | 77.30 | 224.69 | 327.54 | 574.24 |

As the region presents a low coverage of precipitation gauges, the satellite/observation-corrected products (CHIRPS and GPM Final) normally tend to show good results. But cloud contamination at rainforest such as the Amazon Forest is usually an issue for the satellite's measurements. In this sense, GPM provides a better performance in the region than CHIRPS, with median ME equals to 162.55 mm and 247.49 mm respectively (Figure 23). Concerning the GPM products (Final and Late), the observation corrections applied to the Final version plays a relevant role, hence the interquartile range decreases from 409.96 mm (GPM

Late) to 266.69 mm (GPM Final). Thus, good improvements in the results are locally expected when high-quality observed precipitation data corrects the satellite measurements. In this sense, further investigation might be conduced to understand the local forcings. Although the ME indicates some tendencies about the model sensibility to the rainfall products, the next section investigate the MAE - important indicator for the area, hence the region presents a high yearly mean observed depth runoff.

Figure 23 - Hydro-Region Amazônica- ME.

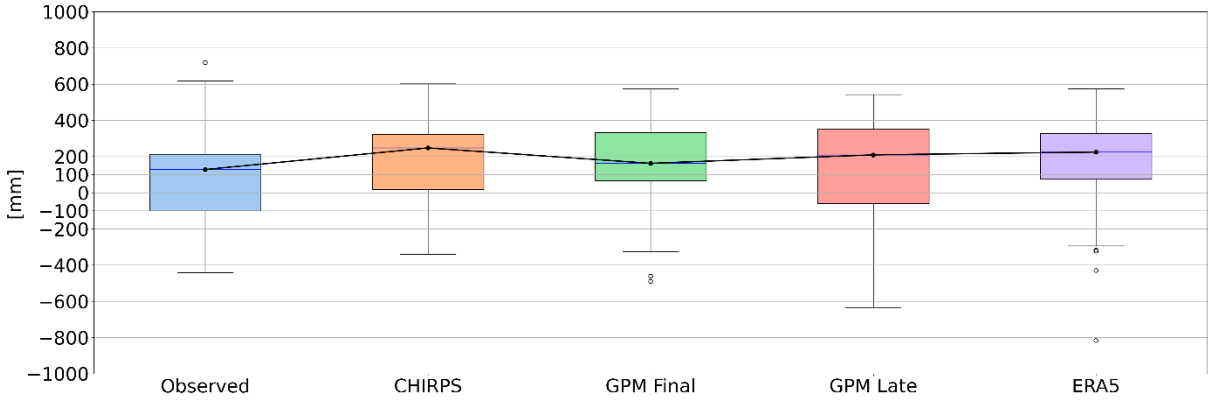


Source: Author.

Figure 24 shows the spatial distribution of ME in the region. The high variability presented in the Observed run is concentered in some sub-areas of the regions, which once again indicates local interpolation issues over precipitation grid.

Figure 24 - Map Hydro-Region Amazônica- ME.

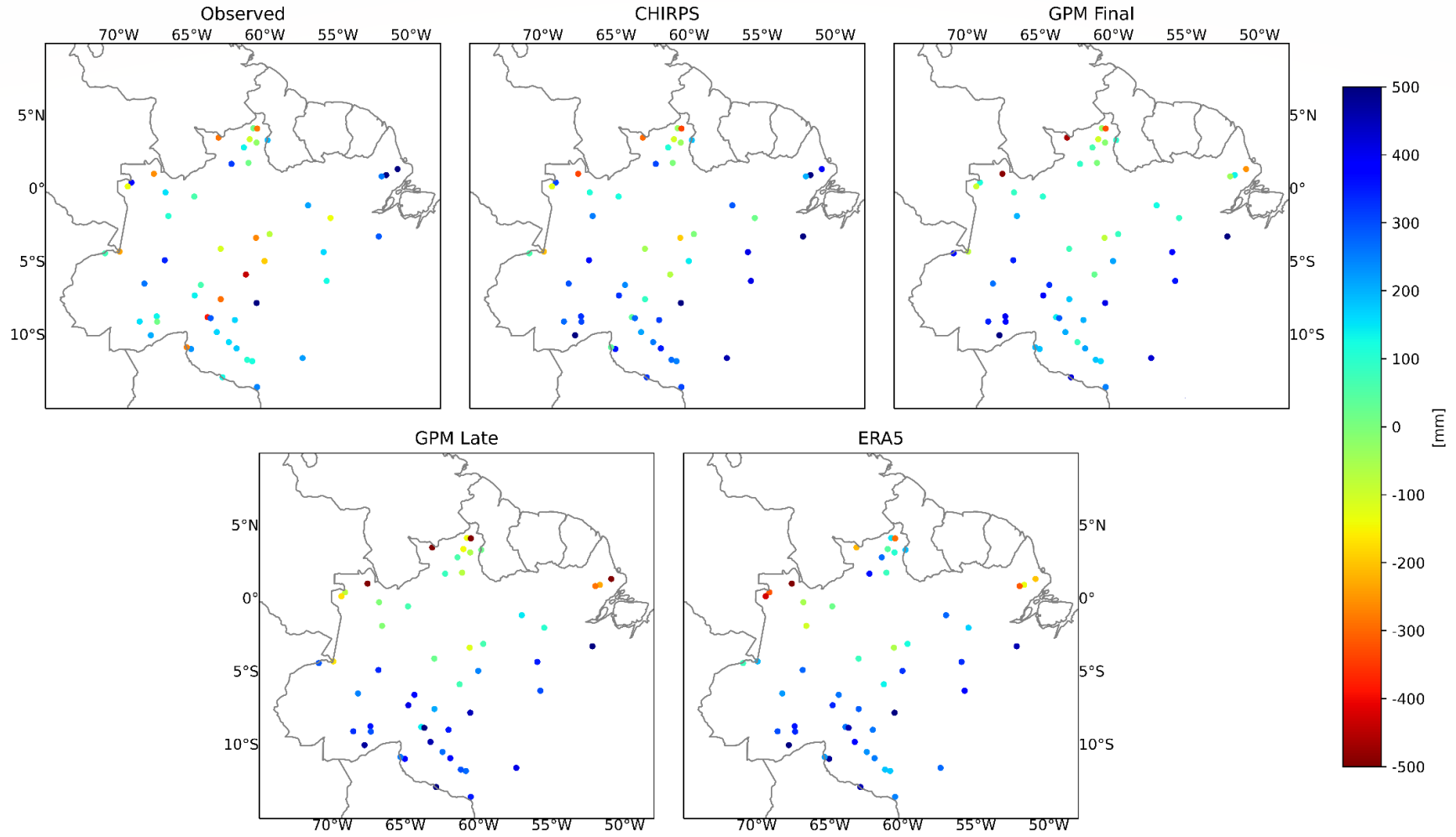


Source: Author.

*4.3.1.2Mean Relative Error (MRE)*

Table 11 presents the MRE for the region, which demonstrates the same pattern observed in the MAE indicator. The Observed run gives a median MRE equals to 14.65%. However, a minimum MRE of -65.75% for the run results, which confirms the large variability.

Table 11 - Hydro-Region Amazônica- MRE.

| **Dataset** | **n** | **Mean [%]** | **S. D. [%]** | **Min. [%]** | **Q 25% [%]** | **Q 50% [%]** | **Q75% [%]** | **Max. [%]** |
|---|---|---|---|---|---|---|---|---|
| Observed | 53 | 9.74 | 29.83 | -65.75 | -5.95 | 14.65 | 27.02 | 66.66 |
| CHIRPS | 53 | 26.24 | 34.11 | -38.27 | 1.59 | 25.75 | 43.96 | 133.63 |
| GPM Final | 53 | 24.20 | 36.97 | -39.71 | 4.35 | 19.86 | 36.71 | 171.89 |
| GPM Late | 53 | 24.47 | 42.74 | -56.54 | -4.16 | 22.85 | 48.23 | 205.33 |
| ERA5 | 53 | 28.20 | 38.80 | -33.29 | 5.50 | 27.70 | 44.91 | 187.49 |

Also, Figure 25 indicates the same pattern observed for the ME.

Figure 25 - Hydro-Region Amazônica- MRE.

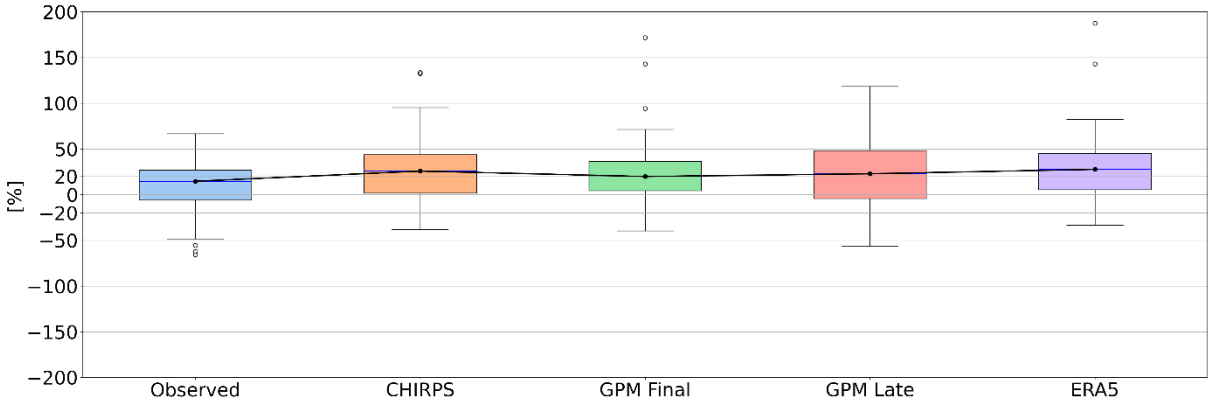


Source: Author.

While Figure 26 stress the variability presented by the Observed run.

Figure 26 - Map Hydro-Region Amazônica- MRE

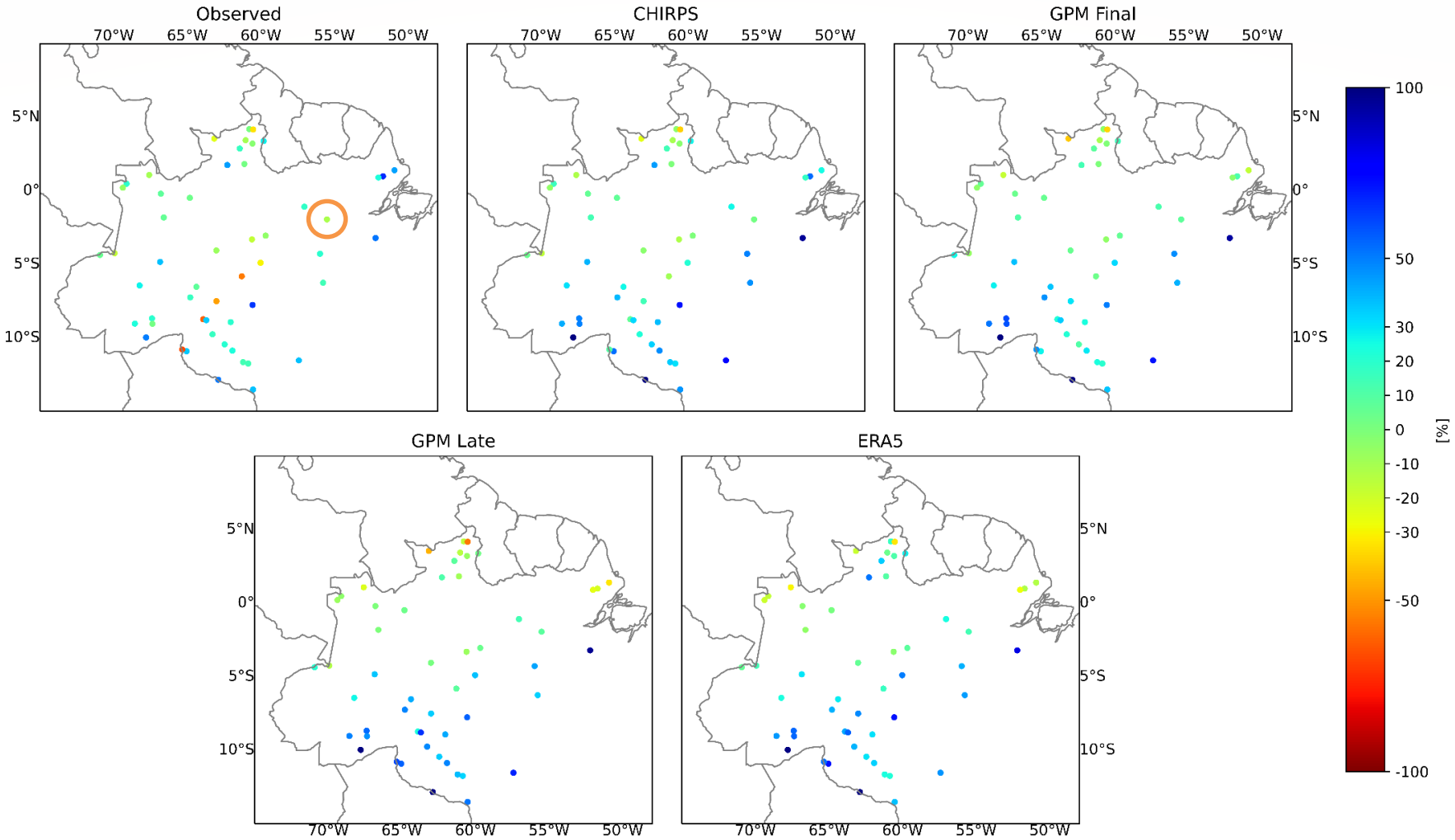


Source: Author.

*4.3.1.3Sensibility Analyze Obidos Station - 17050001*

This section focuses on the discharge results for the Obidos Station - 17050001, which is the most downstream gauge in the Amazon Basin. The station location (-1.95°, -55.18°) is pointed in Figure 26 - orange circle. The drainage area is 4,680,000 km$^2$ (~1/3 of the model area), it measures the Amazon River flow. The altitude corresponds to 7 meters. The station was chosen between the 53 gauges in the Hydro Region Amazônica because the results determine a good model accuracy for the location over all the precipitation datasets (KGE ~>= 0.50). Additionally, the Amazon River is the largest in the world - in terms of water volume (BRITANNICA, 2021), which emphasizes its importance for the hydrological process in South America.

Table 12 presents the calculated statistics for the station, while Figure 27 shows the observed and simulated daily hydrograph for the simulation periods. In this sense, the Observed grid demonstrates the best KGE (0.82). Also, it provides the best results for variability (Alpha), and Linear Correlation (r), which indicates a good agreement between the simulated and observed hydrographs - confirmed by the modeled and observed hydrographs shapes in the plot (Figure 23). However, this simulation provides a MRE larger than absolute 10%.

Table 12 - Obidos Station - 17050001.

| **Datase** | **KGE** | **Alpha** | **Beta** | **r** | **Simulated Annual Depth Runoff [mm]** | **Observed Annual Depth Runoff [mm]** | **ME [mm]** | **MRE [%]** |
|---|---|---|---|---|---|---|---|---|
| Observed | 0.82 | 0.97 | 0.89 | 0.87 | 1076.48 | 1216.34 | -139.86 | -11.50 |
| CHIRPS | 0.75 | 1.17 | 1.02 | 0.83 | 1237.63 | 1218.30 | 19.33 | 1.59 |
| GPM Final | 0.70 | 1.22 | 1.07 | 0.81 | 1307.45 | 1217.75 | 89.70 | 7.37 |
| GPM Late | 0.54 | 1.30 | 1.08 | 0.66 | 1317.60 | 1217.75 | 99.85 | 8.20 |
| ERA5 | 0.49 | 1.43 | 1.14 | 0.77 | 1388.17 | 1218.30 | 169.87 | 13.94 |

With regards to CHIRPS simulation, it gives a reasonable KGE (0.75). Additionally, the Bias (Beta) shows an excellent result (1.02), since it approximately equals 1. But, the simulated variability provides an Alpha equals to 1.17.

Next, a large improvement is observed from the GPM Late to GPM Final - the same pattern observed for the entire Hydro Region. The period from approximately 2010 to 2016 reflects this behavior. The GPM Final algorithm applied a relevant Bias correction when compared to GPM Late.

Figure 27 - Obidos Station - 17050001.

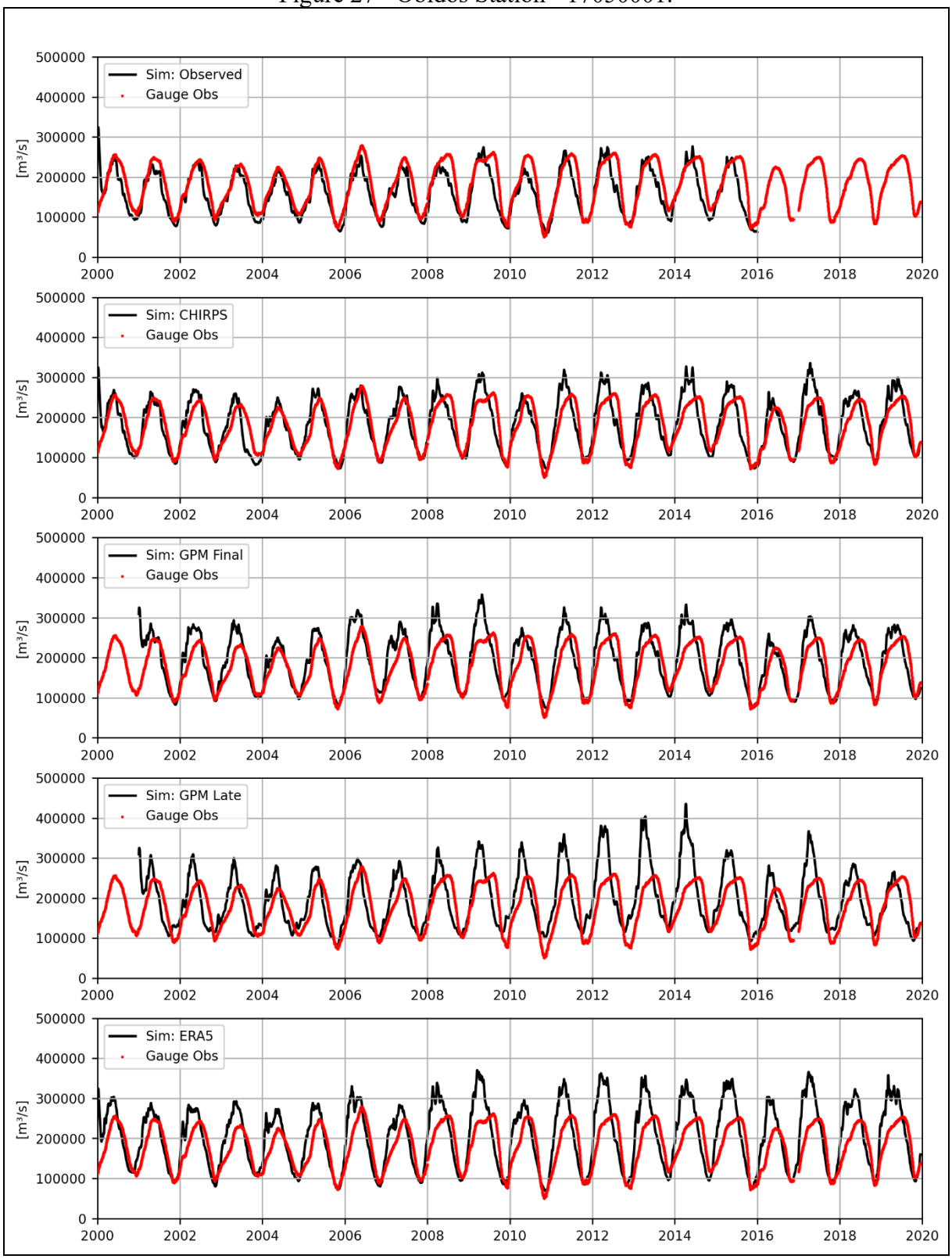


Source: Author.

### 4.3.2 Hydro Region Uruguai (#12)

This section evaluates the model results according to the different datasets for the Hydro Region Uruguai (#12). The statistical analyses over the Hydro Regio Amazônica investigated 57 discharge gauges, corresponding to 8.18 % of the total analyzed stations. For these gauges, the yearly mean observed depth runoff in the region is 935.66 mm for the studied period (2000-2020).

*4.3.2.1Mean Error (ME)*

Table 13 presents the ME calculated statistics. Likewise, in the region Amazônica #1, the Observed grid and CHIRPS provide the best results in terms of ME median in the area, 16.02 mm and 15.63 mm respectively. In opposite direction, the ERA5 presents negative ME in the region - a pattern that differs from the Brazilian Territory conclusions.

Table 13 - Hydro-Region Uruguai- ME.

| Dataset | n | Mean [mm] | S. D. [mm] | Min. [mm] | Q 25% [mm] | Q 50% [mm] | Q75% [mm] | Max. [mm] |
|---|---|---|---|---|---|---|---|---|
| Observed | 57 | -17.41 | 136.07 | -611.19 | -71.21 | 16.02 | 49.78 | 225.89 |
| CHIRPS | 57 | -9.23 | 131.11 | -492.60 | -69.57 | 15.63 | 68.45 | 231.38 |
| GPM Final | 57 | 116.65 | 122.70 | -340.58 | 65.92 | 123.07 | 201.66 | 314.49 |
| GPM Late | 57 | 276.19 | 184.88 | -255.56 | 187.60 | 286.47 | 421.90 | 573.39 |
| ERA5 | 57 | -72.93 | 162.06 | -820.73 | -137.47 | -50.80 | 23.37 | 195.42 |

Figure 28 demonstrates a large difference between the GPM Late and GPM Final related to interquartile range and median. Also, both products show a large error when compared to the others precipitation products.

Figure 28 - Hydro-Region Uruguai- ME

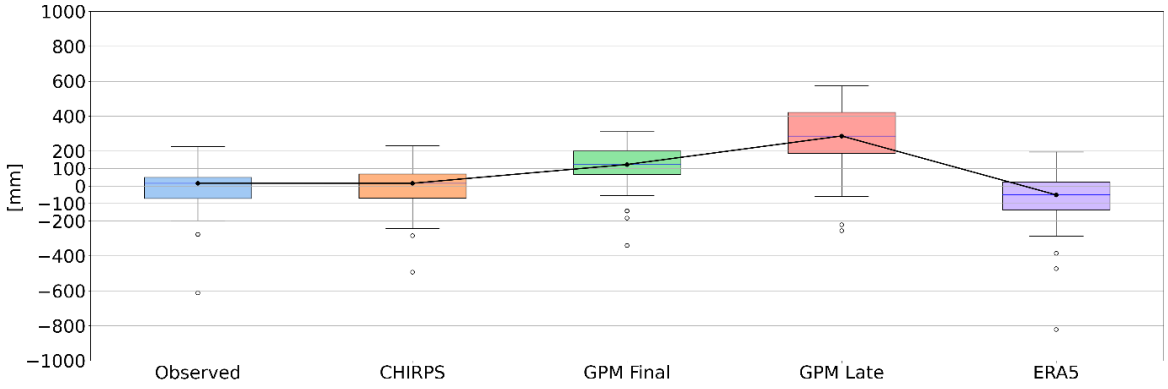


Source: Author.

Figure 29 shows the spatial distribution of the ME in the region.

Figure 29 - Map Hydro-Region Uruguai- ME.

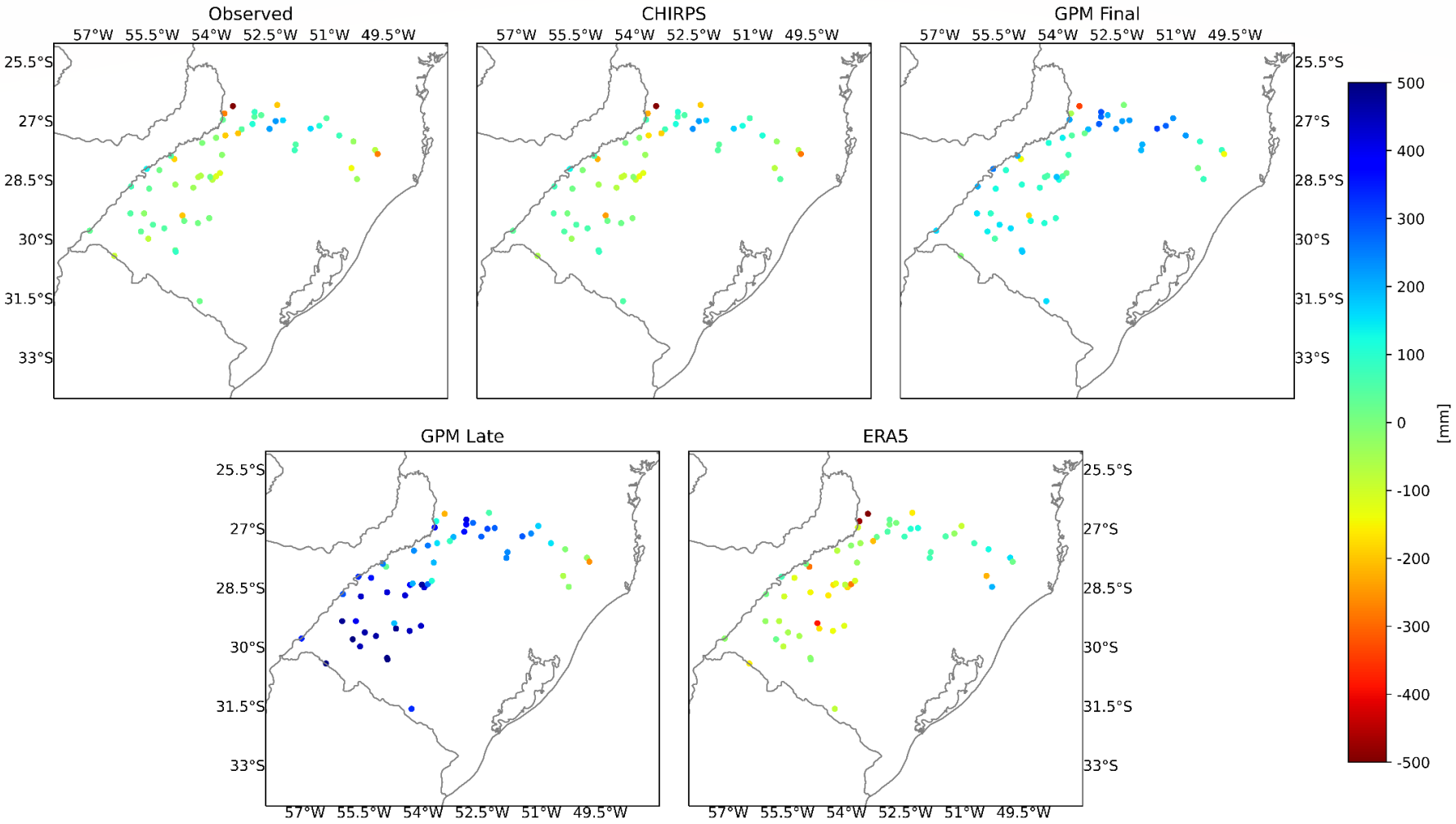


Source: Author.

*4.3.2.2Mean Relative Error (MRE)*

Table 14 shows the calculated MRE in the region. The Observed Grid and CHIRPS provide a mean of approximately 0%, which demonstrates an excellent water balance agreement between the simulated and observed values. Among the satellite/observation-corrected products (CHIRPS and GPM Final), the region follows the Brazilian Territory pattern - CHIRPS performs better than the GPM Final.

Table 14 - Hydro-Region Uruguai- MRE.

| Dataset | n | Mean [%] | S. D. [%] | Min. [%] | Q 25% [%] | Q 50% [%] | Q75% [%] | Max. [%] |
|---|---|---|---|---|---|---|---|---|
| Observed | 57 | -0.37 | 11.76 | -35.45 | -7.69 | 2.06 | 6.99 | 22.83 |
| CHIRPS | 57 | 0.53 | 12.12 | -31.08 | -7.64 | 1.73 | 8.24 | 23.4 |
| GPM Final | 57 | 14.19 | 12.87 | -21.3 | 7.61 | 13.8 | 22.61 | 39.34 |
| GPM Late | 57 | 32.94 | 24.51 | -22.55 | 19.05 | 30.92 | 45.74 | 97.54 |
| ERA5 | 57 | -6.63 | 13.55 | -51.77 | -14.72 | -7.23 | 2.94 | 20.60 |

In this sense, Figure 30 shows a small interquartile range for almost all the products, except for GPM Late, which demonstrates a notable media MRE in the region (30.92 %).

Figure 30 - Hydro-Region Uruguai- MRE.

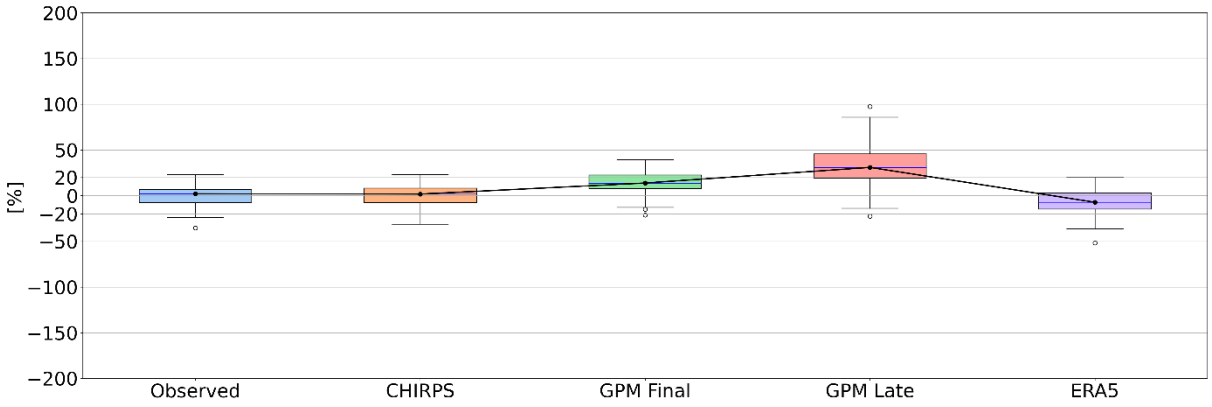


Source: Author.

Figure 31 shows the MRE spatial distribution in the region, it suggests the good agreement between the Observed, CHIRPS, and ERA5 in the region.

Figure 31 - Map Hydro-Region Uruguai- MRE.

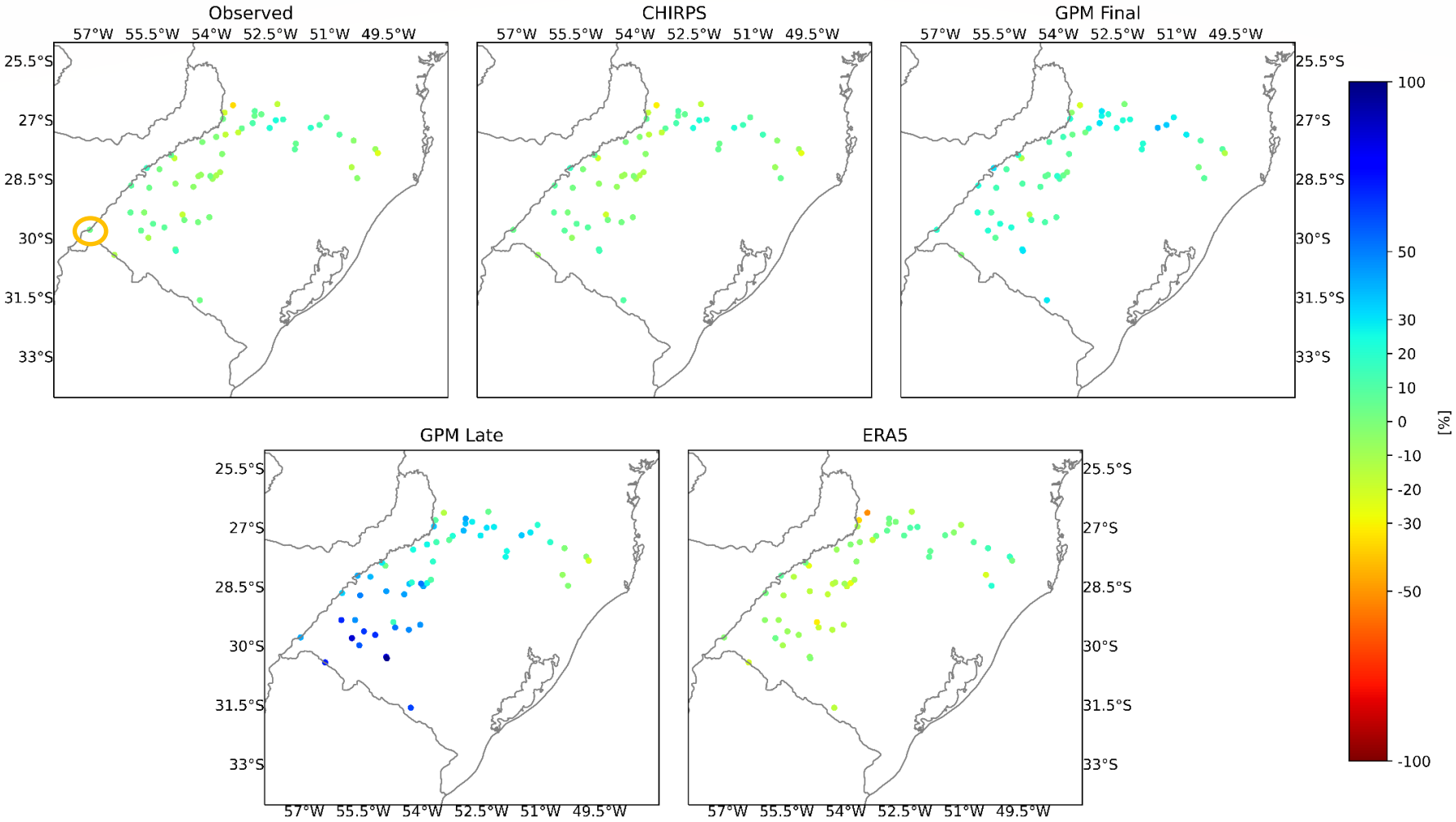

*4.3.2.3Sensibility Analyze Uruguaiana Station - 77150000*

This section focuses on the discharge results for the Uruguaiana Station - 77150000, which is the most downstream gauge in the Uruguai Basin. The station location (-29.75°, -57.09°) is pointed in Figure 31 (orange circle). The drainage area is 190,000 km$^2$, it measures the Urugaui River flow. The altitude corresponds to 38 meters. The station was chosen between the 57 gauges in the Hydro Region Uruguai because the results determine a good model accuracy for the location over almost all the precipitation datasets (KGE ~>= 0.50).

Table 15 presents the calculated efficiency coefficients for the station, while Figure 32 shows the observed and simulated daily hydrograph for the simulation periods. In this sense, the Observed grid and CHIRPS demonstrate almost the same KGE, 0.82 and 0.83, respectively. Therefore, the KGE components (Alpha, Beta, and r) values are almost the same for both datasets.

For this discharge gauge, the improvement quality from GPM Late to GPM Final is notable again. The calculated KGE for GPM Late is equal to 0.31, while GPM Final presents a much better KGE (0.73). Since GPM Late does not perform well for the Bias (Beta) and Variability (Alpha), but there is a reasonable Linear Correlation between the observed and simulated hydrograph as shown in Figure 32.

Finally, the station follows the pattern presented by its Hydro Region, which presented a better performance for the CHIRPS and Observed datasets. Also, ERA5 performs well for the specific basin, giving the only negative ME - the same pattern concluded for the region.

Table 15 - Uruguaiana Station - 17050001.

| **Datase** | **KGE** | **Alpha** | **Beta** | **r** | **Simulated Annual Depth Runoff [mm]** | **Observed Annual Depth Runoff [mm]** | **ME [mm]** | **MRE [%]** |
|---|---|---|---|---|---|---|---|---|
| Observed | 0.82 | 0.91 | 1.04 | 0.85 | 839.10 | 810.34 | 28.76 | 3.55 |
| CHIRPS | 0.83 | 0.94 | 1.04 | 0.84 | 856.42 | 820.64 | 35.78 | 4.36 |
| GPM Final | 0.73 | 1.13 | 0.73 | 0.87 | 984.60 | 821.62 | 162.98 | 19.84 |
| GPM Late | 0.31 | 1.49 | 1.42 | 0.78 | 1168.02 | 821.62 | 346.40 | 42.16 |
| ERA5 | 0.72 | 0.84 | 0.97 | 0.78 | 798.91 | 820.64 | -21.73 | -2.65 |

Figure 32 - Uruguaiana Station - 17050001.

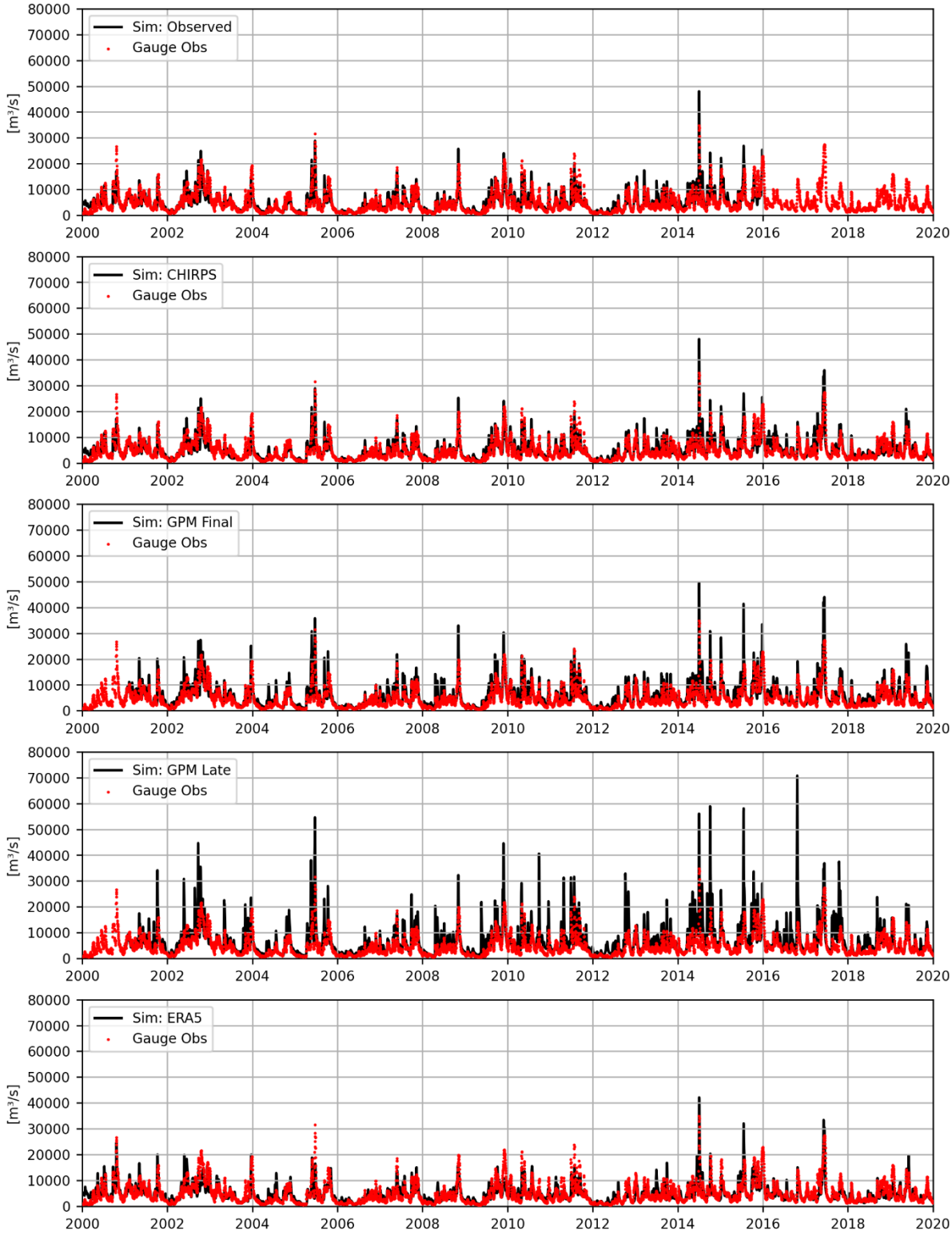


Source: Author.

### 4.3.3 Hydro Region Atlântico Sul (#6)

This section evaluates the model results according to the different datasets for the Hydro Region Atlântico Sul (#6). The statistical analyses over the Hydro Regio Atlântico Sul investigated 42 discharge gauges, corresponding to 6.30 % of the total analyzed stations. For these gauges, the yearly mean observed depth runoff in the region is 818.66 mm for the studied period (2000-2020).

*4.3.3.1Mean Error (ME)*

Table 16 presents the ME calculated statistics. The Hydro Regions Uruguai (#12) and Atlântico Sul (#6) are neighbor regions. Thus, it is expected similar error pattern for both regions. Thus, the Observed Grid and CHIRPS still give the best results related to the median MEA, 60.38 mm and 54.80 mm respectively. However, ERA5 also presents close performance.

Table 16 - Hydro-Region Uruguai- ME.

| Dataset | n | Mean [mm] | S. D. [mm] | Min. [mm] | Q 25% [mm] | Q 50% [mm] | Q75% [mm] | Max. [mm] |
|---|---|---|---|---|---|---|---|---|
| Observed | 42 | 49.59 | 161.35 | -348.24 | -55.30 | 60.38 | 111.82 | 462.44 |
| CHIRPS | 42 | 63.92 | 154.57 | -236.22 | -20.31 | 54.80 | 122.75 | 512.15 |
| GPM Final | 42 | 177.90 | 119.06 | -81.95 | 109.25 | 195.52 | 265.46 | 425.99 |
| GPM Late | 42 | 278.27 | 230.70 | -213.37 | 121.86 | 370.84 | 433.64 | 638.21 |
| ERA5 | 42 | 69.75 | 147.11 | -178.85 | -17.85 | 66.87 | 140.83 | 527.19 |

Figure 33 stress the large interquartile range for the GPM Late (647.01 mm).

Figure 33 - Hydro-Region Atlântico Sul- ME.

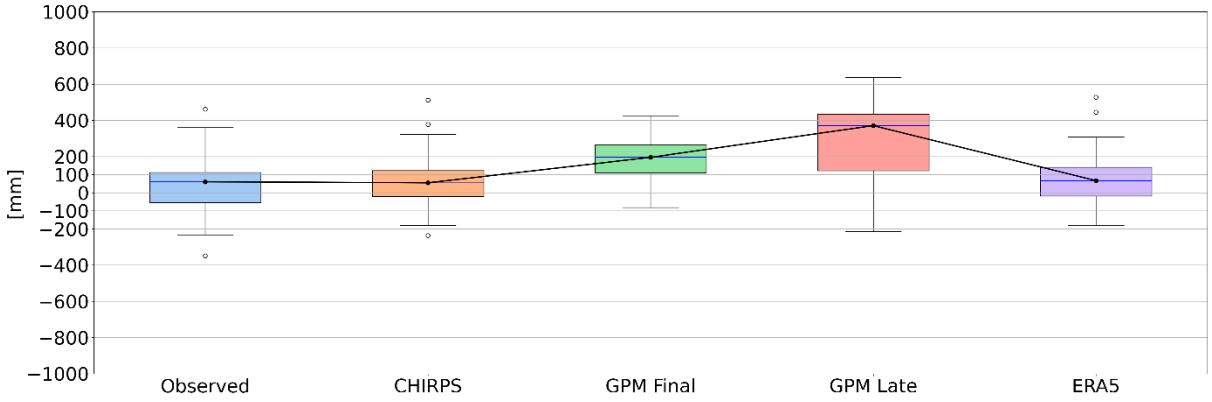


Source: Author.

Figure 34 shows the ME spatial distribution

Figure 34 - Map Hydro-Region Atlântico Sul- ME.

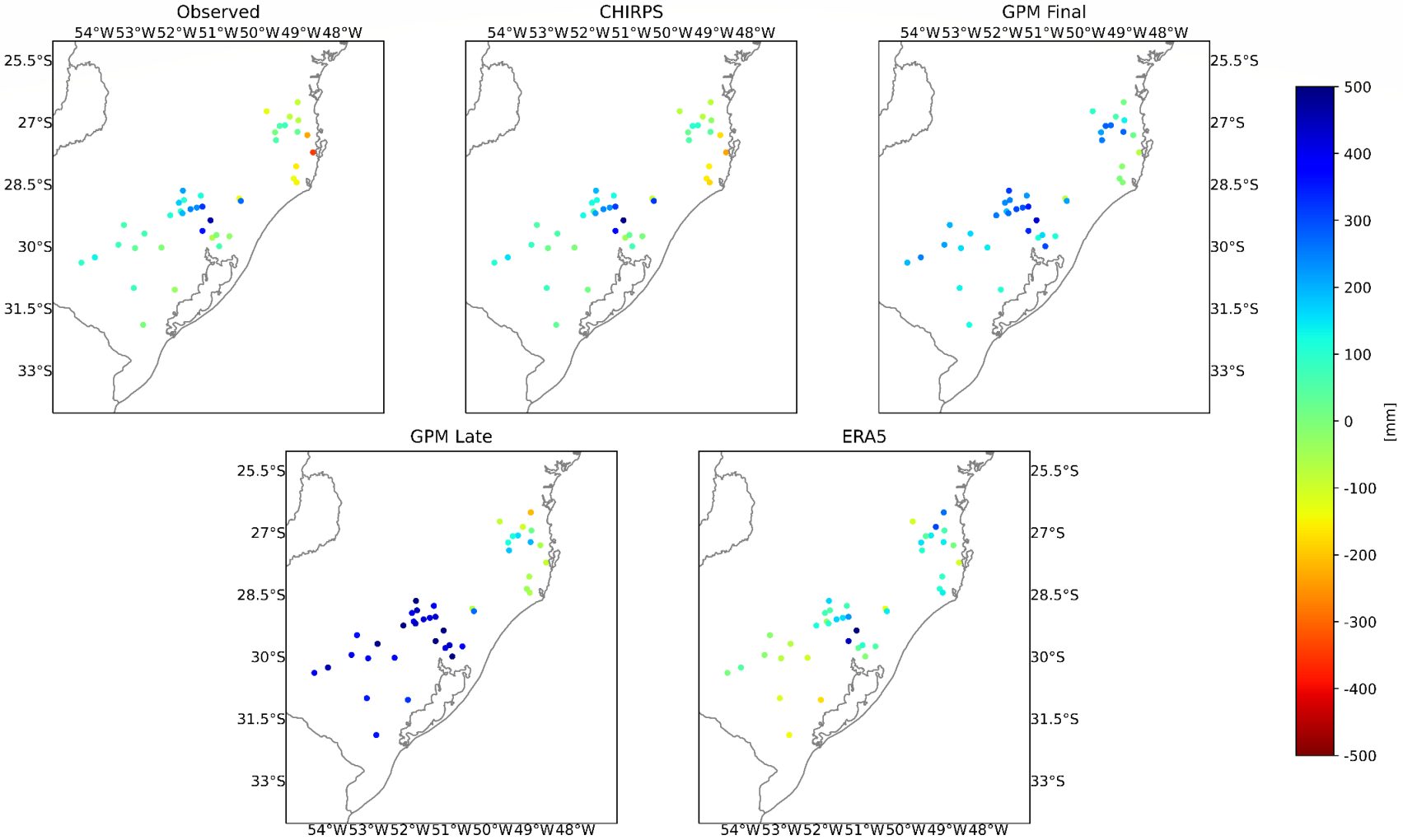


Source: Author.

*4.3.3.2Mean Relative Error (MRE)*

Table 17 shows the MRE statistics. Differently than the Hydro Region Uruguai (#12), the Observed grid and CHIRPS do not provide mean MRE close to 0%, they give a mean MRE close to 10%. However, both datasets provide the best results related to the median MRE: 7.90% (Observed) and 6.75% (CHIRPS).

Table 17 - Hydro-Region Uruguai- MRE.

| Dataset | n | Mean [%] | S. D. [%] | Min. [%] | Q 25% [%] | Q 50% [%] | Q75% [%] | Max. [%] |
|---|---|---|---|---|---|---|---|---|
| Observed | 42 | 7.77 | 19.89 | -32.63 | -6.13 | 7.90 | 15.45 | 66.26 |
| CHIRPS | 42 | 9.47 | 20.01 | -23.16 | -2.55 | 6.75 | 15.45 | 76.13 |
| GPM Final | 42 | 24.07 | 17.02 | -7.4 | 12.49 | 24.61 | 38.19 | 63.47 |
| GPM Late | 42 | 37.35 | 31.07 | -20.96 | 16.555 | 44.81 | 54.67 | 105.16 |
| ERA5 | 42 | 9.10 | 19.76 | -24.8 | -2.675 | 8.23 | 19.19 | 78.36 |

Figure 35 shows the same pattern concluded for the Hydro Region Uruguai (#12) for the GPM products, which shows improvement from GPM Late to GPM Final, but not enough to perform well as the Observed grid and CHIRPS.

Figure 35 - Hydro-Region Atlântico Sul- MRE.

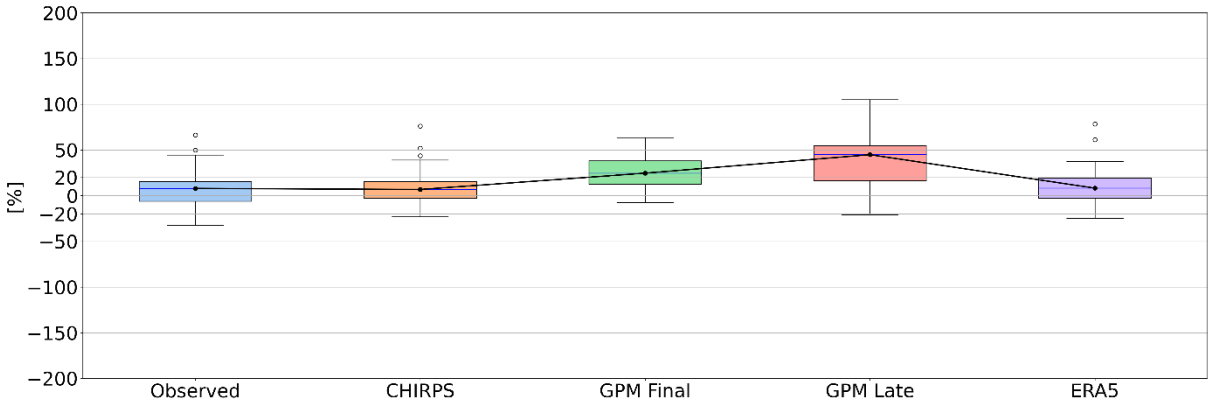


Source: Author.

Figure 36 shows the MRE spatial distribution

Figure 36 - Map Hydro-Region Atlântico Sul- MRE.

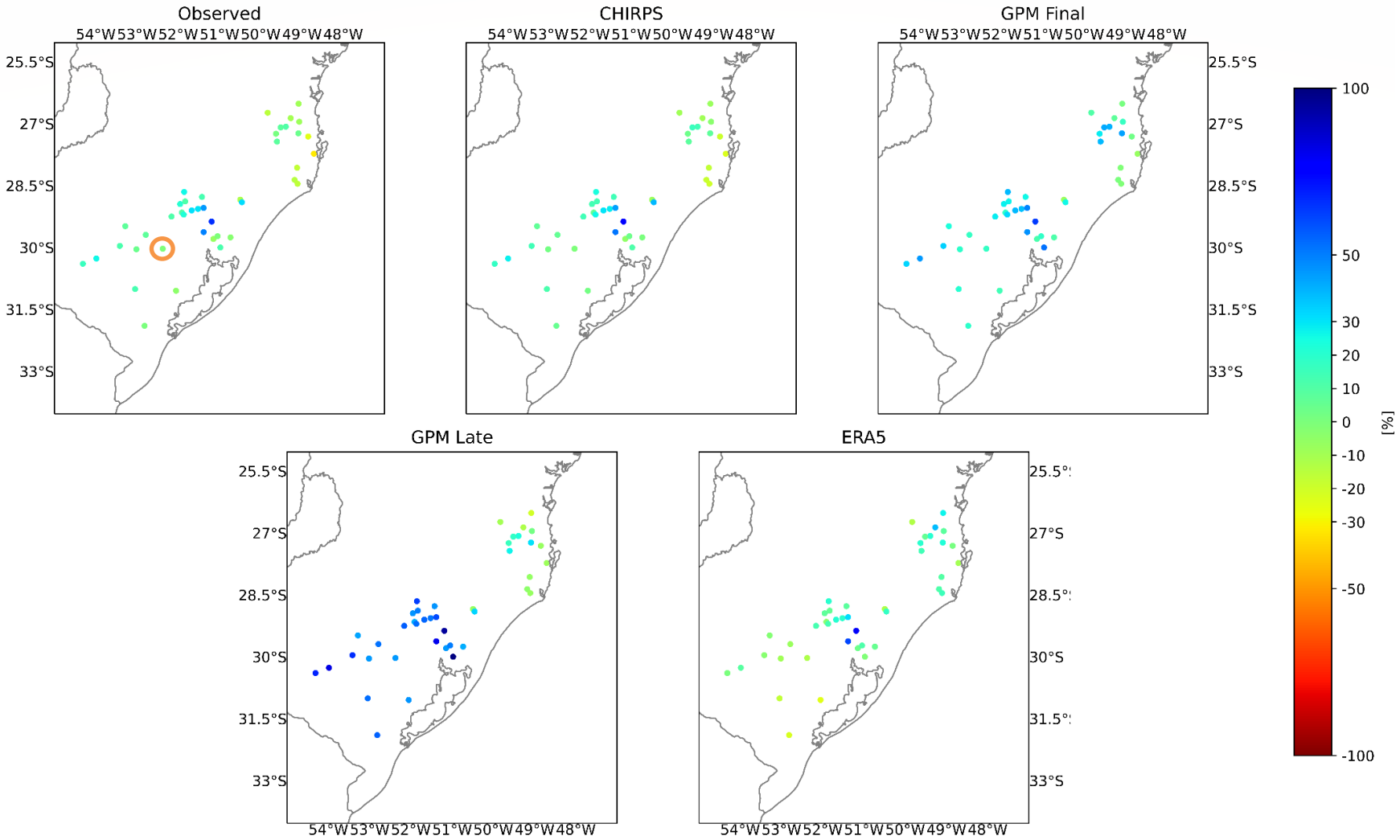


Source: Author.

*4.3.3.3Sensibility Analyze Pardo Station - 85900000*

This section focuses on the discharge results for the Pardo Station - 85900000. The station location (-29.99°, -52.37°) is pointed in Figure 36- (orange circle). The drainage area is 38,700 km$^2$, it measures the Jacua River flow. The altitude corresponds to 2 meters. The station was chosen between the 42 gauges in the Hydro Atlantic South because the results determine a good model accuracy for the location over almost all the precipitation datasets (KGE ~>= 0.50). Additionally, it presents the smallest drainage area between the 3 analyzed basins - further investigation through different drainage areas on the basin analyses scale. Table 18 shows the calculated model efficiency indicators, while Figure 37 presents the observed and simulated hydrographs.

Once again, the Observed grid and CHIRPS provide the best KGE results, 0.78 and 0.77, respectively. Also, both simulations give excellent results in terms of Variability (Alpha) and Bias (beta), values close to 1. The Linear Correlation (r) is similar for the datasets, but the Obitos Station (Section 4.3.1.3) and Uruguaiana Station (Section 4.3.2.3) lightly provide higher r coefficients, since they present larger areas.

The GPM products provide the worse KGE between the different simulations. For instance, GPM Late gives a negative KGE, mainly a result of high simulated variability as shown in Figure 37. Also, the ERA5 provides negative MRE such as in the Uruguaiana Station (Section 4.3.2.3).

Table 18 - Pardo Station - 85900000.

| **Datase** | **KGE** | **Alpha** | **Beta** | **r** | **Simulated Annual Depth Runoff [mm]** | **Observed Annual Depth Runoff [mm]** | **ME [mm]** | **MRE [%]** |
|---|---|---|---|---|---|---|---|---|
| Observed | 0.78 | 0.96 | 0.99 | 0.79 | 808.32 | 814.15 | -5.83 | -0.72 |
| CHIRPS | 0.77 | 0.97 | 1.00 | 0.77 | 819.01 | 822.47 | -3.46 | -0.42 |
| GPM Final | 0.61 | 1.23 | 1.17 | 0.74 | 969.95 | 826.19 | 143.76 | 17.40 |
| GPM Late | -0.11 | 1.95 | 1.45 | 0.62 | 1195.44 | 826.19 | 369.25 | 44.69 |
| ERA5 | 0.63 | 0.84 | 0.88 | 0.69 | 722.73 | 822.47 | -99.74 | -12.13 |

Figure 37 - Pardo Station - 85900000.

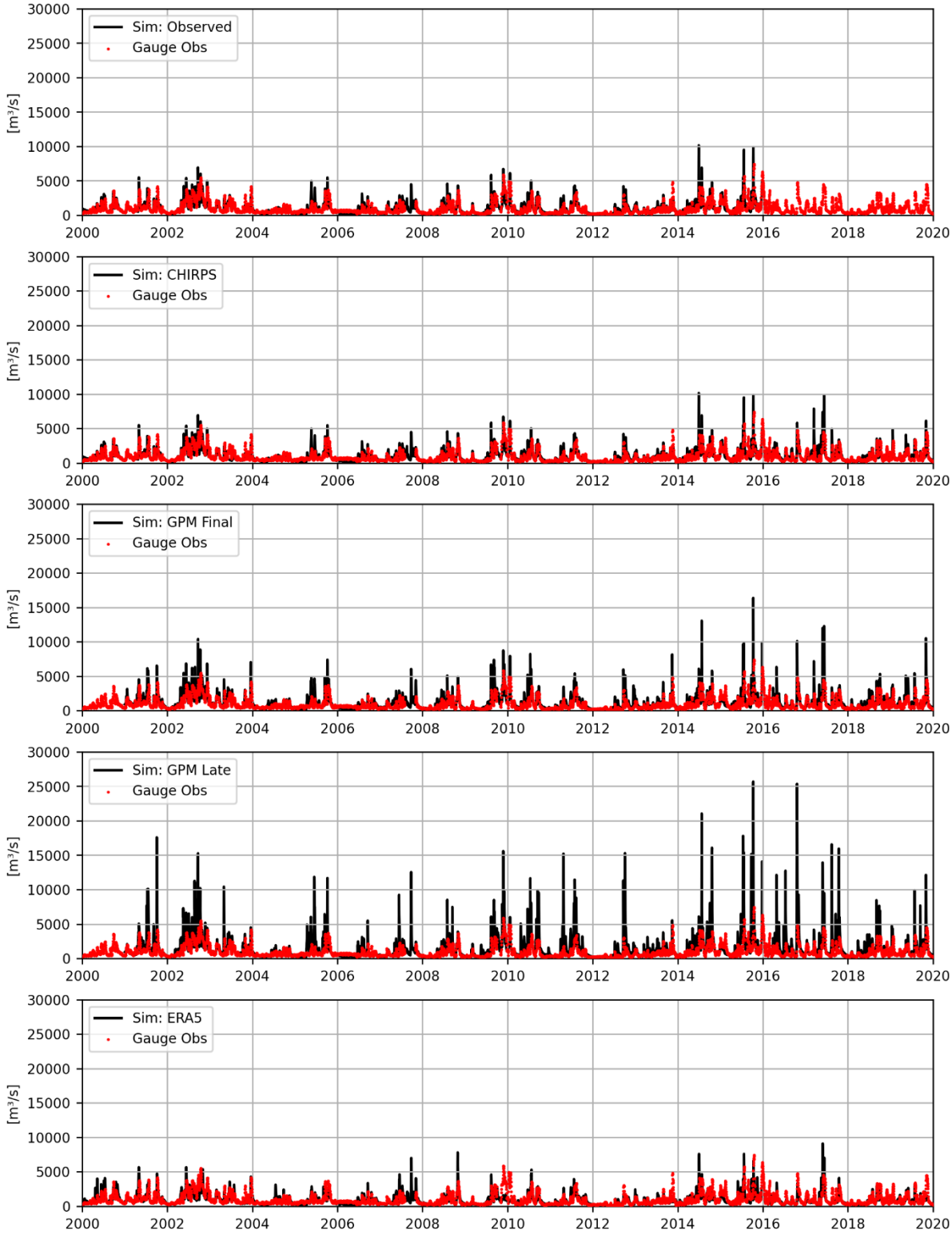


Source: Author.

## 4.4 RESULTS SUMMARY

This section summarizes and discusses the calculated model efficiency coefficients for each simulation and studied spatial coverage (country, region, and basin-scale). Figure 38 shows the ME and MRE (medians), while Figure 39 presents the KGE and its components (medians).

*Mean Error (ME) and Mean Relative Error (MRE)*

Firstly, the model results for the different precipitation datasets were evaluated in the entire Brazilian territory. The calculated median ME are 105.13 mm (Observed), 153.86 mm (CHIRPS), 203.46 mm (GPM Final), 215.93 mm (GPM Late), and 95.02 mm (ERA5). With this in view, all the simulations present a positive deviation from the observed runoff, although the Observed grid and ERA5 presented the lowest biases.

Additionally, the calculated median MRE determines that the Observed grid (26.49%) and the ERA5 (23.66%) dataset provide a lower level of biases when compared to the others simulations, which present values close to 40% and 50%. In terms of water balance, the Observed grid and ERA5 are the most accurate precipitation datasets.

With regards to the downscaling analysis, the MRE seems more appropriate to compare the different Hydro-Regions, hence they present large variation in the matter of observed mean yearly depth runoff. Thus, in the southern regions (Uruguai and Atlântico Sul), the CHIRPS and ERA5 show results close to zero error, which demonstrates the ability of both datasets to reproduce almost the same bias as the Observed simulation. However, the same does not occur with the Hydro-Region Amazônica, where all the simulations give MRE larger than 10%, even for the observed dataset. Although the GPM Final provides the closest results to the Observed simulation – differently to the southern regions.

On the basin scale, once again the MRE seems more appropriate. In this sense, almost all the combinations (precipitation datasets x basins) show satisfactory results. Except for GPM products that present high biases – the same pattern for the regional-scale. Therefore, the smallest analyzed basin (Pardo - 38,700 $km^2$) shows the best results over all the simulations, which indicates the ability of CHIRPS and Observed grid to deal with different areas. Figure 38 presents the ME and MRE summary (medians) for the simulations and spatial coverage analysis.

Figure 38 - ME and MRE summary

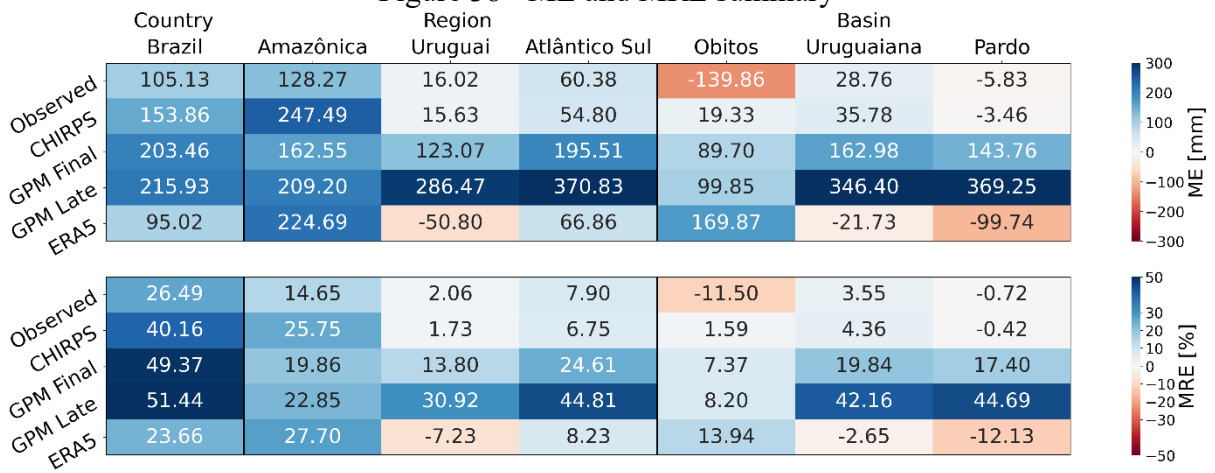


*Kling-Gupta Efficiency (KGE) and components*

Secondly, the KGE and its components were computed for the country and basin scale. On the basin scale, all the precipitation products present good performance for the different basins, except for GPM Late. Therefore, it demonstrates the capacity of the precipitation products to generate discharge through the model in different basin areas (Obidos – 4,680,000 km$^2$, Uruguaiana – 190,000 km$^2$, and Pardo – 38,700 km$^2$).

The calculated linear correlation (r) demonstrates that all the precipitation products can represent the hydrographs dynamics. Although the Observed, CHIRPS, and GPM Final present the high values. Also, there is a tendency for better results in the larger basins. Besides, the variability error (Alpha) presents large values for all the simulations on the country scale. However for the selected basins, the simulations Observed grid, CHIRPS, and GPM Final show better results. It is important to stress that the results for the Observed grid are close to one over the chosen catchments. Finally, the bias term (Beta) has the same interpretation as the MRE.

Figure 39 presents the KGE and components summary (medians) for the simulations over the country and basin scale.

Figure 39 - KGE and components summary

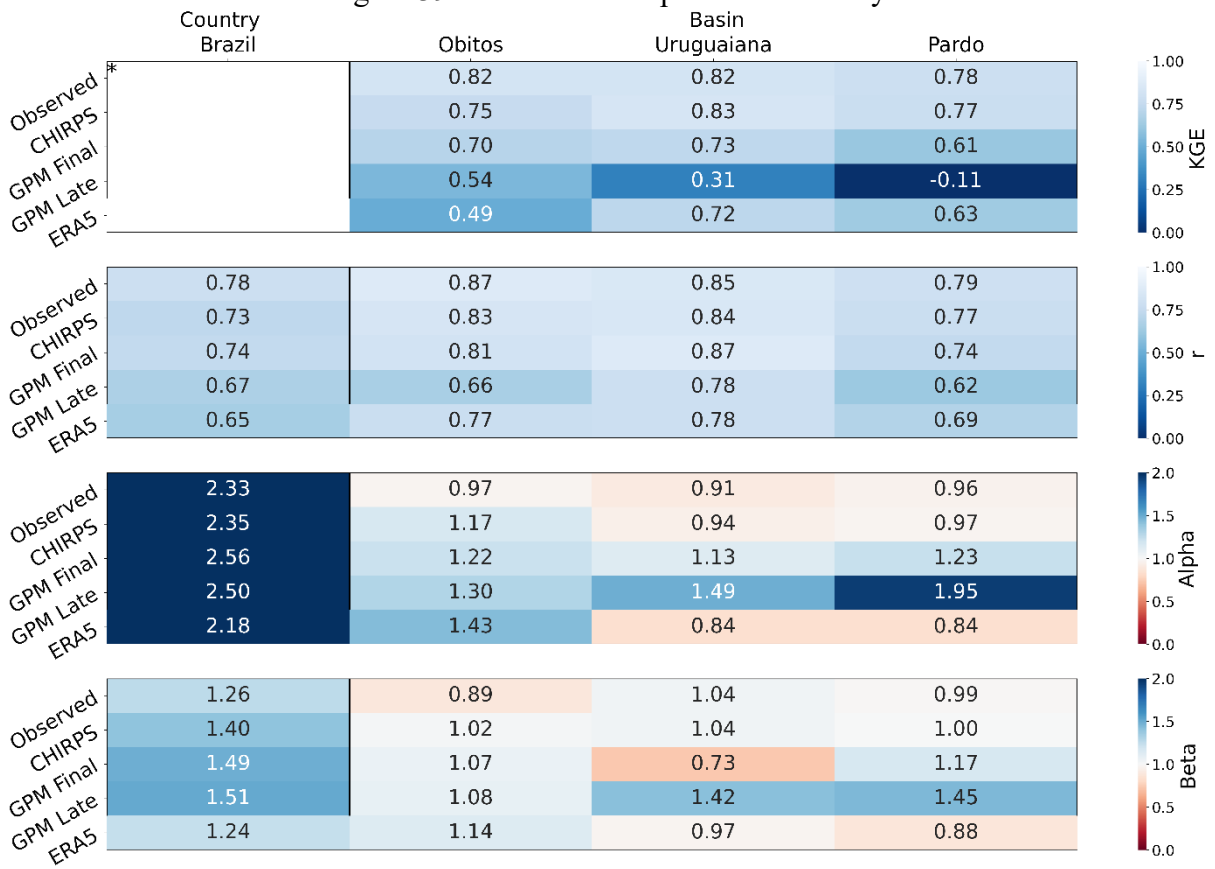


* Where means that no KGE was calculated in the country scale, once the several negative values would affect the final statistics.

## 4.5 EVAPOTRANSPIRATION ANALYSIS

This section describes an additional investigation motivated by the positive bias obtained from the five different simulations (section 4.2.1). Section 3.6 describes how each one of the studied datasets methodologies estimate the Evapotranspiation values over the grids. The studied datasets are the Observed grid and TerraClimate datasets (used as forcings in the simulations) and the MODIS Potential Evapotranspiration (only utilized in terms of comparison).

In this sense, the mean yearly evapotranspiration was calculated for the period from Jan/2000 to Jan/2016 (Observed grid time coverage) over the entire model area. The original grids were interpolated to 0.1° resolution (GHM grid). Figure 41 shows the calculated averages. From visual inspection, the MODIS Potential Evapotranspiration provides notable higher values in the entire grid when compared to the others. Additionally, the Observed grid gives higher mean evapotranspiration values over the model area when compared to TerraClimate.

Finally, a correction factor was calculated (diving one grid by another) to quantify the difference in terms of mean yearly evapotranspiration from the MODIS Evapotranspiration compared to the others two datasets (MODIS/TerraClim and MODIS/Observed). Figure 40 shows the density for each calculated factor. Both datasets converge to a factor approximately equals to 1.6 (60% higher) for the highest density.

Figure 40 - Correction Factors.

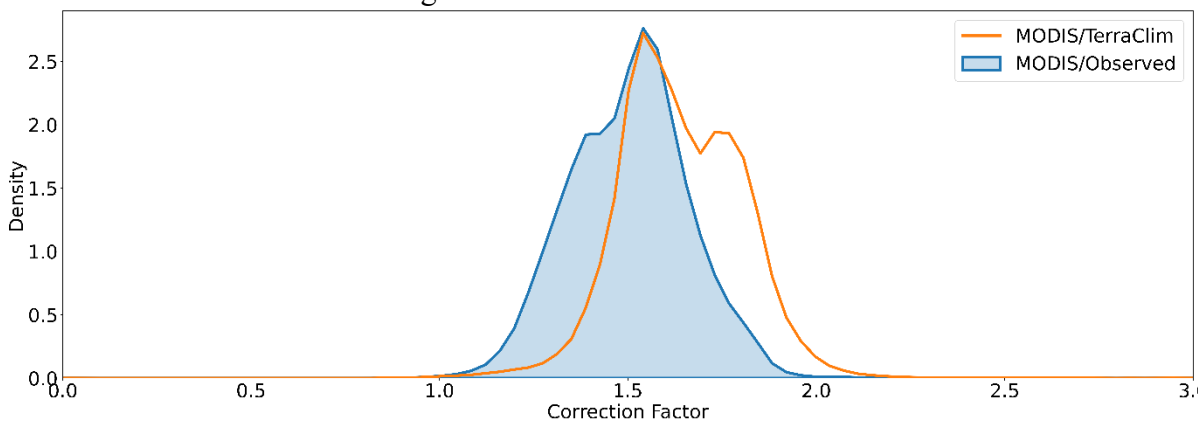


Source: Author.

Figure 42 presents the spatial distribution of the calculated factor for both datasets.

Figure 41 - Map Mean Yearly Evapotranspiration.

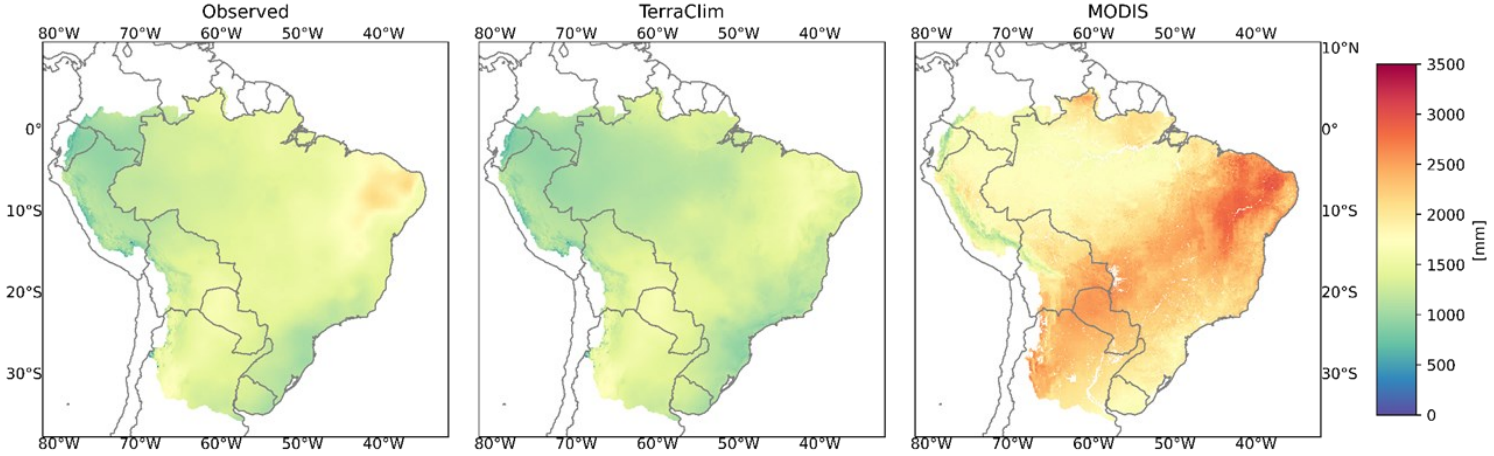


Figure 42 - Map Correction Factor.

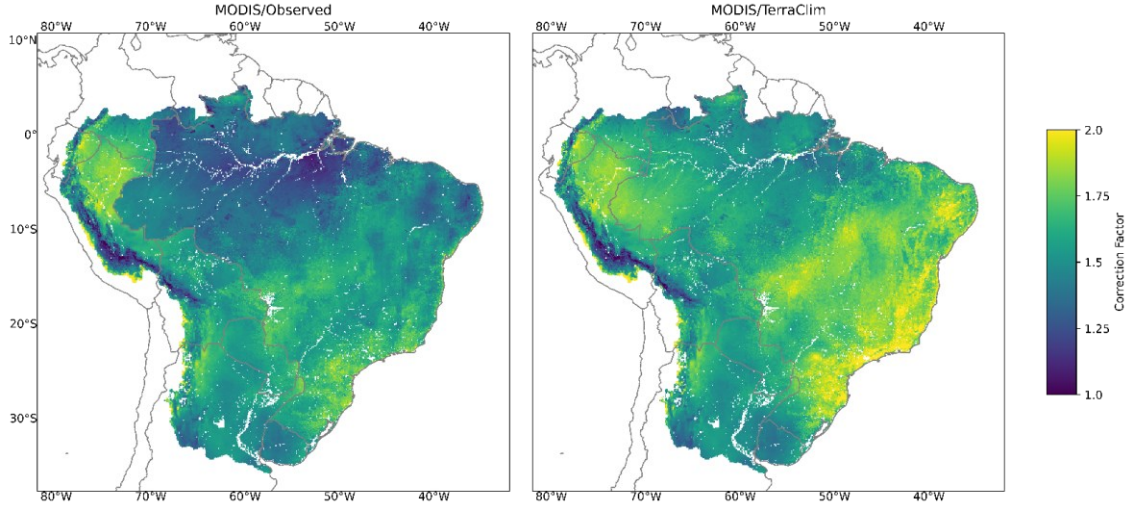


Source: Author.

As described in Section 2.1.1.1.2, the impact of Evapotranspiration on the water balance is not as great as for precipitation, but it presents a significant role in the spatial and temporal runoff process. Also, Section 3.6.2 alerted that a grass cover reference for the Evapotranspiration calculation might yield biases on the process estimation. The mean positive difference of 60% calculated between the evapotranspiration products indicates that further analysis should happen to better understand the evapotranspiration participation on the simulated water balance – which might explain the positive ME for all the studied simulations (Section 4.2.1).

Thus, the more specific approach utilized by MODIS Evapotranspiration to calculate the surface resistance ($r_s$) and aerodynamics resistance ($r_a$) seems to be more appropriate for the Brazilian territory conditions, despite the grass generalization (explained in Section 3.6.1). Hember, Coops, and Spittlehouse (2017) have studied the spatial and temporal variability of Potential Evapotranspiration across the North American Forets. The variation of the surface resistance ($r_s$) and aerodynamics resistance ($r_a$) from the grass reference cover to a well-coupled canopy significantly alters the process estimation along the latitudes.

Finally, mainly in the center of Brazilian territory (Hydro-Regions #11, #8, and #10). Many species have deep root systems, Ferreira *et al.* (2007) observed water depletion by plants down to 10 m depth, which allows transpiration to be maintained even during the dry months (the dry season, May to August) as reported by Oliveira et al. (2005). Section 2.1.3 showed the importance of the root zone model component on the Actual Evapotranspiration. So, an increased $L_{max}$ would affect the water balance in the region by modifications on the model parameters – physically justified.

# 5 CONCLUSIONS

This study successfully evaluated the ability of individual global-scale precipitation datasets to reproduce river discharges simulated by the DHI Global Hydrological Model in the Brazilian territory. The five investigated precipitation products are Observed grid (XAVIER, KING, and SCALON, 2016), CHIRPS (FUNK *et al.*, 2015), GPM Final (NASA, 2021), GPM Late (NASA, 2021), and ERA5 (ECMWF, 2021). Thus, the simulated discharges were compared to the observation of 769 stations in the Brazilian territory.

For the entire country extension, the calculated median ME are 105.13 mm (Observed), 153.86 mm (CHIRPS), 203.46 mm (GPM Final), 215.93 mm (GPM Late), and 95.02 mm (ERA5). With this in view, all the simulations present a positive deviation from the observed runoff, although the Observed grid and ERA5 presented the lowest biases.

Additionally, the calculated median MRE determines that the Observed grid (26.49%) and the ERA5 (23.66%) dataset provide a lower level of biases when compared to the other simulations, which present values close to 40% and 50%. Then, among the four global-scale analyzed products, ERA5 is the most accurate one to represent the water balance in the Brazilian territory. While the Observed grid is a reasonable reference to compare results from other datasets. However, the positive pattern of the error over all the simulations suggests that further investigation might be conducted on the secondary importance model forcing: evapotranspiration.

Parallelly, the precipitation analysis indicated that the ERA5 mean yearly precipitation over the Brazilian territory is the lowest one (1,386.82 mm/year) - reaching a difference of -10.58% when compared to GPM Late, followed by the Observed grid (1,408.58 mm/year). Additionally, the ERA5 dataset presents lower precipitation in eight of the twelve Brazilian Hydro-Regions when compared to the Observed dataset. Thus, it clarifies the relationship between the precipitation quantity and the smallest ME and MRE found for both runs among the simulations.

With regards to the downscaling analysis, the water balance error pattern is variable over the Brazilian Hydro-Regions – as expected for a country with a continental scale. In the southern regions (Atlântico Sul [#6] and Uruguai [#12]), CHIRPS performs better than GPM Final among the satellite/observation-corrected datasets. Since both GPM products overestimate the rainfall amount in the area. However, in the Hydro-Region Amazônica (#1), GPM presents good performance, even slightly better than CHIRPS. In this sense, in a rainforest

as the Amazon, the satellite/observation-corrected products (CHIRPS and GPM Final) tend to show measurement issues related to cloud contamination. However, they play an important role as the region presents a lack of precipitation gauges.

In terms of KGE, the CHIRPS and Observed datasets present the highest station frequency for the range (0.50:0.75) - approximately 140 stations (~17% of total). While only 8.6% of the stations in the ERA5 run show KGE in this range. It affirms that ERA5 has the best performance in terms of water balance, but not for the hydrograph shape representation.

Among all the analyzed model efficiency coefficients, the Linear Correlation (r) showed the best results – it suggests that the model and some of the precipitation products present enough ability to represent the hydrographs dynamics in the country scale. Therefore, more than 400 stations showed a linear correlation factor larger than 0.75 for the Observed grid, while approximately 300 are presented in the range for the satellite/observation-corrected products (CHIRPS and GPM Final). As expected, ERA5 provided the worse results with a median of 0.65. It demonstrates why the product presented low values of KGE, even though it performs well in terms of water quantity (ME and MRE).

Differently from the Linear Correlation (r) investigation, the model and all the studied precipitation datasets showed not satisfactory results for the flow variability error (Alpha) in terms of the Brazilian territory. Thus, the Observed, CHIRPS, and ERA5 present approximately the same mean (~3). Thus, the KGE is mainly defined by the Linear Correlation (r) and the Bias (Beta) – which has the same interpretation as the MRE.

For the selected basins, there is not a significant difference when comparing the precipitation datasets for water balance performance, except for the GPM products. Once more, the GPM products demonstrate significant issues to force the model. Also, there is a tendency for better hydrographs dynamics representation in larger basins – as expected, since small basins are more sensible.

Finally, the study showed different conclusions for each simulation/precipitation product by downscaling the geographical investigation. In this sense, the usability of the different rainfall products depends on the final application of the model and focus area. For the next studies, researchers can explore additional precipitation datasets or combinations of them. Also, the evapotranspiration analyses stress the necessity to better understand the process on the country scale, hence it would strongly affect the simulated discharges.

# REFERENCES


ABATZOGLOU, J. T. *et al.* TerraClimate, a high-resolution global dataset of monthly climate and climatic water balance from 1958-2015. **Scientific Data**, v. 5, n. 1, p. 170191, 9 jan. 2018.

ALLEN, R. G. *et al.* Crop evapotranspiration: guidelines for computing crop water requirements. In: FOOD AND AGRICULTURE ORGANIZATION OF THE UNITED NATIONS (Ed.). . **5-AGWA-8**. FAO irrigation and drainage paper. Rome: FAO - Food and Agriculture Organization of the United Nations, 1998. p. 300.

ANA. **As Regiões Hidrográficas**. Available at: <https://www.gov.br/ana/pt-br/assuntos/gestao-das-aguas/panorama-das-aguas/regioes-hidrograficas/as-regioes-hidrograficas>. Accessed: 22 abr. 2021a.

ANA. **National Water Agency (ANA)**. Available at: <https://www.gov.br/ana/en/national_water_agency>. Accessed: 23 abr. 2021b.

BECK, H. E. *et al.* Global-scale evaluation of 22 precipitation datasets using gauge observations and hydrological modeling. **Hydrology and Earth System Sciences**, v. 21, n. 12, p. 6201-6217, 8 dez. 2017.

BEHRANGI, A. *et al.* Hydrologic evaluation of satellite precipitation products over a mid-size basin. **Journal of Hydrology**, v. 397, n. 3, p. 225-237, 3 fev. 2011.

BELETE, M. *et al.* Evaluation of satellite rainfall products for modeling water yield over the source region of Blue Nile Basin. **Science of The Total Environment**, v. 708, p. 134834, 15 mar. 2020.

BEVEN, K. **Rainfall-Runoff Modelling: The Primer**. 2. ed. [s.l.] John Wiley & Sons, 2011.

BOHNENSTENGEL, S. I.; SCHLÜNZEN, K. H.; BEYRICH, F. Representativity of in situ precipitation measurements - A case study for the LITFASS area in North-Eastern Germany. **Journal of Hydrology**, v. 400, n. 3, p. 387-395, 11 abr. 2011.

BRITANNICA. **"Amazon River." Encyclopedia Britannica**. Available at: <https://www.britannica.com/place/Amazon-River>. Accessed: 6 maio. 2021.

CHEN, J. *et al.* Basin-Scale River Runoff Estimation From GRACE Gravity Satellites, Climate Models, and In Situ Observations: A Case Study in the Amazon Basin. **Water Resources Research**, v. 56, n. 10, p. e2020WR028032, 2020.

CHO, J. *et al.* Effect of Spatial Distribution of Rainfall on Temporal and Spatial Uncertainty of SWAT Output. **Transactions of the ASABE**, v. 52, 1 set. 2009.

COHIDRO. **Water Resources and Irrigation Development Company of Sergipe State (COHIDRO)**. Available at: <https://cohidro.se.gov.br/>. Accessed: 23 abr. 2021.

COLE, R. A. J.; JOHNSTON, H. T.; ROBINSON, D. J. The use of flow duration curves as a data quality tool. **Hydrological Sciences Journal**, v. 48, n. 6, p. 939-951, 1 dez. 2003.

COLLISCHONN, B.; COLLISCHONN, W.; TUCCI, C. E. M. Daily hydrological modeling in the Amazon basin using TRMM rainfall estimates. **Journal of Hydrology**, v. 360, n. 1, p. 207-216, 15 out. 2008.

CONSTRUFAM. **Hidrometria - Construfam - Telemetria , Hidrologia, Hidrometria, Medição de Vazão**. Available at: <http://construfam.com.br/hidrometria>. Accessed: 23 abr. 2021.

CPRM. **Geological Survey of Brazil (CPRM)**. Available at: <http://www.cprm.gov.br/>. Accessed: 23 abr. 2021.

DAEE-SP. **Water and Energy Department of the São Paulo State (DAEE-SP)**. Available at: <http://www.daee.sp.gov.br/site/>. Accessed: 23 abr. 2021.

DAVIE, T.; QUINN, N. W. **Fundamentals of Hydrology**. 3. ed. [s.l.] Routledge, 2019.

DAVID, Paula Cunha. **ANÁLISE DO DESEMPENHO DE MODELOS HIDROLÓGICOS CONCEITUAIS EM 508 BACIAS HIDROGRÁFICAS BRASILEIRAS**. 2020. 110 f. Dissertação (Mestrado) - Curso de Programa de Pós-Graduação em Engenharia Ambiental, Universidade Federal de Santa Catarina - UFSC, Florianópolis, 2020.

DHI. **MIKE 1D: DHI Simulation Engine for 1D river and urban modelling - Reference Manual**. [s.l.] DHI, 2017.

DHI. **Solving the toughest water challenges through applied research and innovation**. Available at: <https://research.dhigroup.com/>. Accessed: 6 maio. 2021.

DÖLL, P. *et al.* Modelling Freshwater Resources at the Global Scale: Challenges and Prospects. **Surveys in Geophysics**, v. 37, n. 2, p. 195-221, 1 mar. 2016.

ECMWF. **ERA5: data documentation**. Available at: <https://onlinelibrary.wiley.com/doi/abs/10.1002/qj.3803>. Accessed: 23 abr. 2021.

EPAGRI. **Agricultural Research and Rural Extension Company of Santa Catarina (EPAGRI)**. Available at: <https://www.epagri.sc.gov.br/>. Accessed: 23 abr. 2021.

FUNK, C. *et al.* The climate hazards infrared precipitation with stations—a new environmental record for monitoring extremes. **Scientific Data**, v. 2, n. 1, p. 150066, 8 dez. 2015.

GUIMBERTEAU, M. *et al.* Discharge simulation in the sub-basins of the Amazon using ORCHIDEE forced by new datasets. **Hydrology and Earth System Sciences**, v. 16, n. 3, p. 911-935, 22 mar. 2012.

GUPTA, H. V. *et al.* Decomposition of the mean squared error and NSE performance criteria: Implications for improving hydrological modelling. **Journal of Hydrology**, v. 377, n. 1, p. 80-91, 20 out. 2009.

HUFFMAN, G. J. *et al.* The TRMM Multisatellite Precipitation Analysis (TMPA): Quasi-Global, Multiyear, Combined-Sensor Precipitation Estimates at Fine Scales. **Journal of Hydrometeorology**, v. 8, n. 1, p. 38-55, 1 fev. 2007.

HYBAM. **Data SO-HYBAM  Amazon bazin water resources observation service**. Available at: <https://hybam.obs-mip.fr/data/>. Accessed: 22 abr. 2021.

IAT. **Paraná Water Institute (IAT)**. Available at: <http://www.iat.pr.gov.br/>. Accessed: 23 abr. 2021.

IGAM. **Water Management Institute of Minas Gerais (IGAM)**. Available at: <http://www.igam.mg.gov.br/>. Accessed: 23 abr. 2021.

INAMHI. **National Meteorology and Hydrology Institute (INAMHI)**. Available at: <http://www.serviciometeorologico.gob.ec/>.

IRD. **French Institute of Research for Development (IRD)**. Available at: <https://en.ird.fr/>. Accessed: 23 abr. 2021.

JAMESON, A. R.; KOSTINSKI, A. B. Spurious power-law relations among rainfall and radar parameters. **Quarterly Journal of the Royal Meteorological Society**, v. 128, n. 584, p. 2045-2058, 2002.

KIRCHNER, J. W. Catchments as simple dynamical systems: Catchment characterization, rainfall-runoff modeling, and doing hydrology backward. **Water Resources Research**, v. 45, n. 2, 2009.

KRAUSE, P.; BOYLE, D. P.; BÄSE, F. Comparison of different efficiency criteria for hydrological model assessment. **Advances in Geosciences**, v. 5, p. 89-97, 16 dez. 2005.

LAMMERS, Taikan Oki; HANASAKI, Naota; KIM, Hyungjun. FIRST RESULTS FROM INTERCOMPARISON OF SURFACE WATER AVAILABILITY MODULES. 2008.

LEHNER, B.; GRILL, G. Global river hydrography and network routing: baseline data and new approaches to study the world's large river systems. **Hydrological Processes**, v. 27, n. 15, p. 2171-2186, 2013.

MASKEY, S.; GUINOT, V.; PRICE, R. K. Treatment of precipitation uncertainty in rainfall-runoff modelling: a fuzzy set approach. **Advances in Water Resources**, v. 27, n. 9, p. 889-898, 1 set. 2004.

MONTEITH, J. L. Evaporation and environment. **Symposia of the Society for Experimental Biology**, v. 19, p. 205-234, 1965.

MOTOVILOV, Y. G. *et al.* Validation of a distributed hydrological model against spatial observations. **Agricultural and Forest Meteorology**, v. 98-99, p. 257-277, 31 dez. 1999.

MUSIE, M.; SEN, S.; SRIVASTAVA, P. Comparison and evaluation of gridded precipitation datasets for streamflow simulation in data scarce watersheds of Ethiopia. **Journal of Hydrology**, v. 579, p. 124168, 1 dez. 2019.

NASA. **National Aeronautics and Space Administration (NASA): Global Precipitation Measurement Mission**. Available at: <https://gpm.nasa.gov/resources/faq>. Accessed: 23 abr. 2021.

NIELSEN, S. A.; HANSEN, E. NUMERICAL SIMULATION OF THE RAINFALL-RUNOFF PROCESS ON A DAILY BASIS. **Hydrology Research**, v. 4, n. 3, p. 171-190, 1 jun. 1973.

NTSG, N. T. S. G. **MODIS Global Evapotranspiration Project (MOD16)**. Available at: <http://ntsg.umt.edu/project/modis/mod16.php>. Accessed: 6 maio. 2021.

OREGGIONI WEIBERLEN, F.; BÁEZ BENÍTEZ, J. Assessment of satellite-based precipitation estimates over Paraguay. **Acta Geophysica**, v. 66, n. 3, p. 369-379, 1 jun. 2018.

PAIVA, R. C. D. DE *et al.* Large-scale hydrologic and hydrodynamic modeling of the Amazon River basin. **Water Resources Research**, v. 49, n. 3, p. 1226-1243, 2013.

SAPIANO, M. R. P.; ARKIN, P. A. An Intercomparison and Validation of High-Resolution Satellite Precipitation Estimates with 3-Hourly Gauge Data. **Journal of Hydrometeorology**, v. 10, n. 1, p. 149-166, 1 fev. 2009.

SCHILLING, W.; FUCHS, L. Errors in Stormwater Modeling—A Quantitative Assessment. **Journal of Hydraulic Engineering**, v. 112, n. 2, p. 111-123, 1 fev. 1986.

SENAMHI-BO. **National Meteorology and Hydrology Service (SENAMHI)**. Available at: <http://senamhi.gob.bo/index.php/inicio>. Accessed: 23 abr. 2021.

SENAMHI-PE. **Servicio Nacional de Meteorología e Hidrología del Perú (SENAMHI)**. Available at: <https://www.gob.pe/>. Accessed: 23 abr. 2021.

SOOD, A.; SMAKHTIN, V. Global hydrological models: a review. **Hydrological Sciences Journal**, v. 60, n. 4, p. 549-565, 3 abr. 2015.

SIQUEIRA, V. A. *et al.* Toward continental hydrologic–hydrodynamic modeling in South America, Hydrol. **Earth Syst. Sci.**, v. 22, p. 4815–4842, 2018.

UNDUCHE, F. *et al.* Evaluation of four hydrological models for operational flood forecasting in a Canadian Prairie watershed. **Hydrological Sciences Journal**, v. 63, n. 8, p. 1133-1149, 11 jun. 2018.

WATSON, R. T. *et al.* **Climate change 1995 :** [s.l.] Cambridge University Press, for the Intergovernmental Panel on Climate Change, 1996.

XAVIER, A. C.; KING, C. W.; SCANLON, B. R. Daily gridded meteorological variables in Brazil (1980-2013). **International Journal of Climatology**, v. 36, n. 6, p. 2644-2659, 2016.

XAVIER, A. C.; KING, C. W.; SCANLON, B. R. **An update of Xavier, King and Scanlon (2016) daily precipitation gridded data set for the Brazil**. . In: XVIII SIMPÓSIO BRASILEIRO DE SENSORIAMENTO REMOTO - SBSR. Santos SP: Anais do XVIII Simpósio Brasileiro de Sensoriamento Remoto - SBSR, 2017Available at: <http://careyking.com/wp-content/uploads/2017/08/Xavier-et-al-2017-SBSR-Update-of-Brazil-precipitation-gridded-data-set.pdf>

ZHU, H. *et al.* Using SWAT to simulate streamflow in Huifa River basin with ground and Fengyun precipitation data. **IWA Publishing**, v. 17, n. 5, p. 834- 844., 2015.

# APPENDIX A - NAM PARAMETERS

NAM Parameter: Umax [mm]

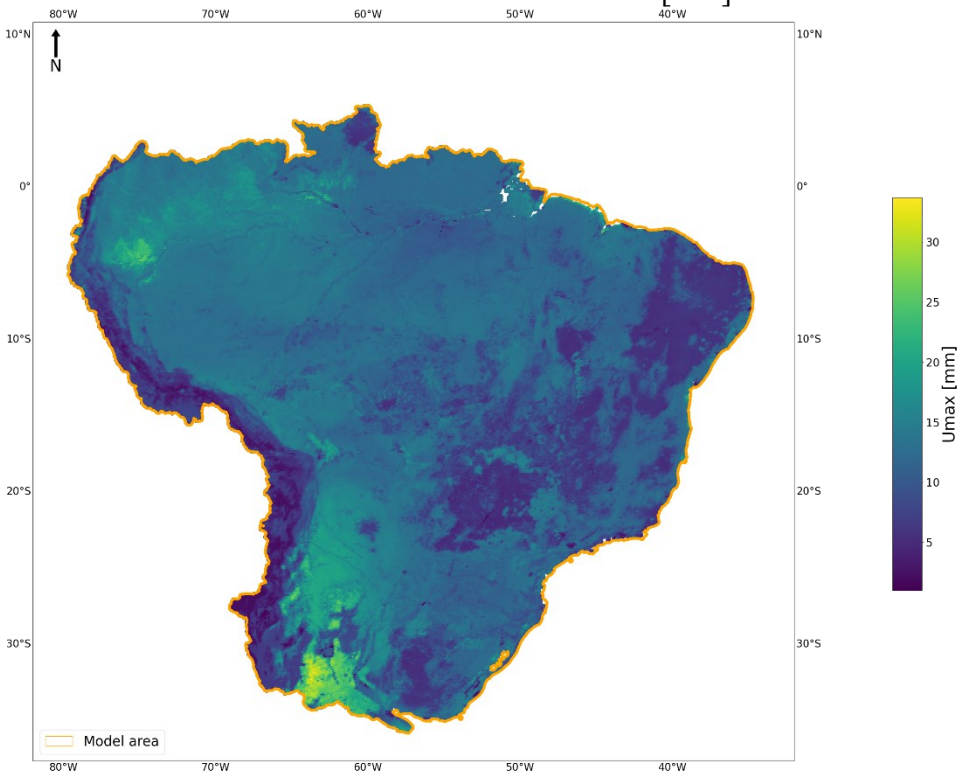


Source: Author.

NAM Parameter: Lmax [mm]

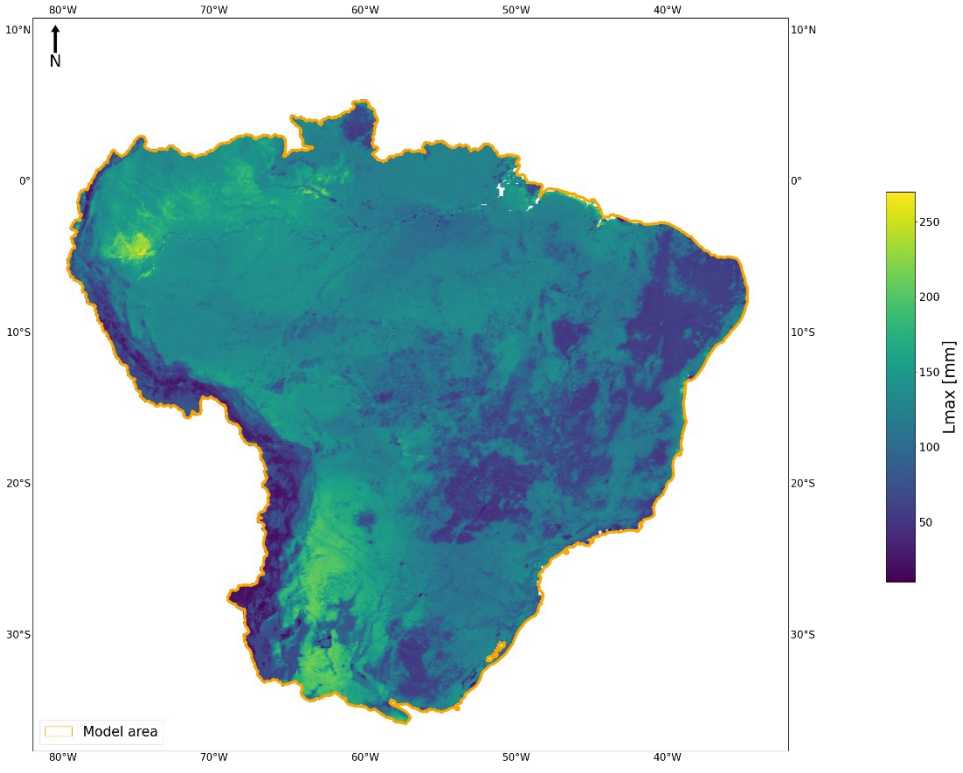


Source: Author.

NAM Parameter: CQOF

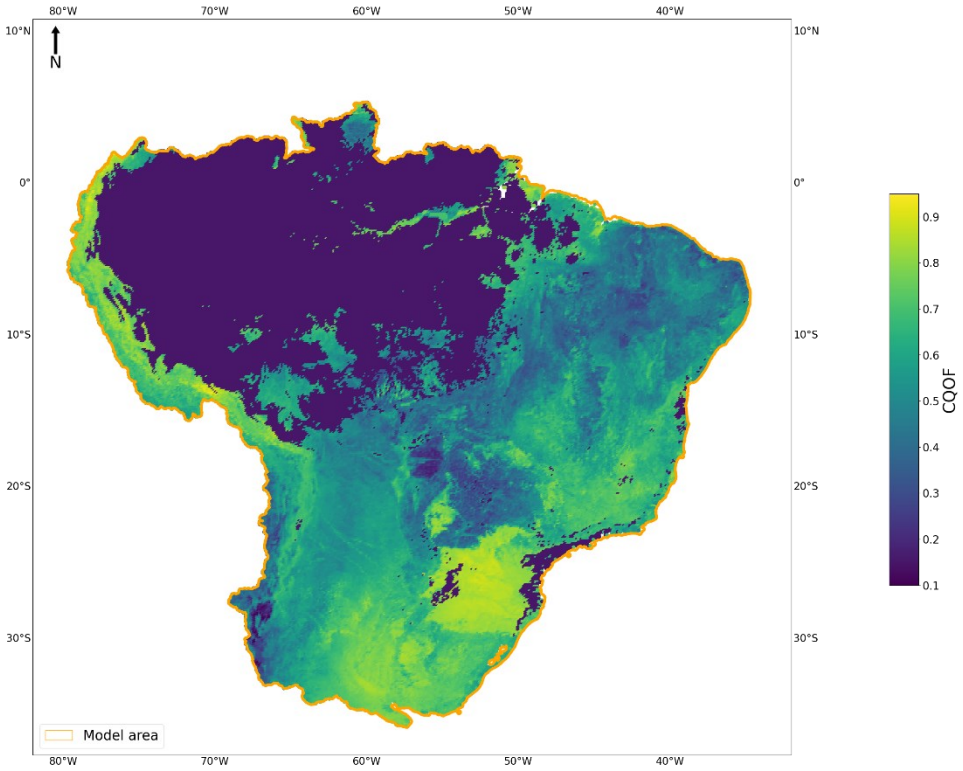


Source: Author.

NAM Parameter: CKIF [hours]

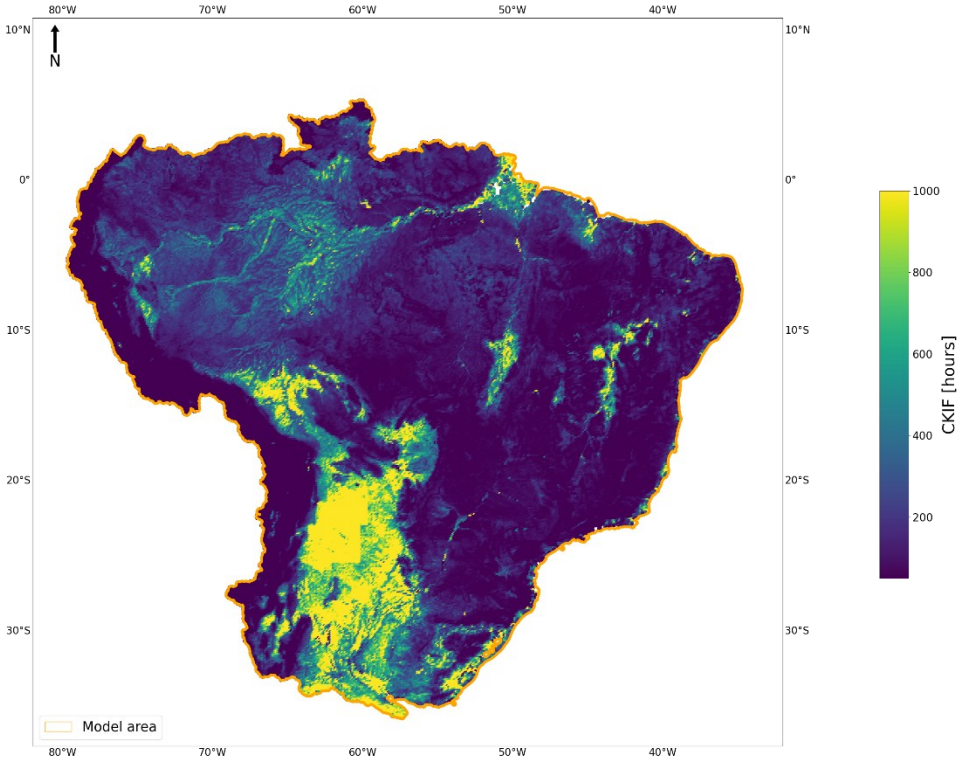


Source: Author.

NAM Parameter: CKOF 1,2 [hours]

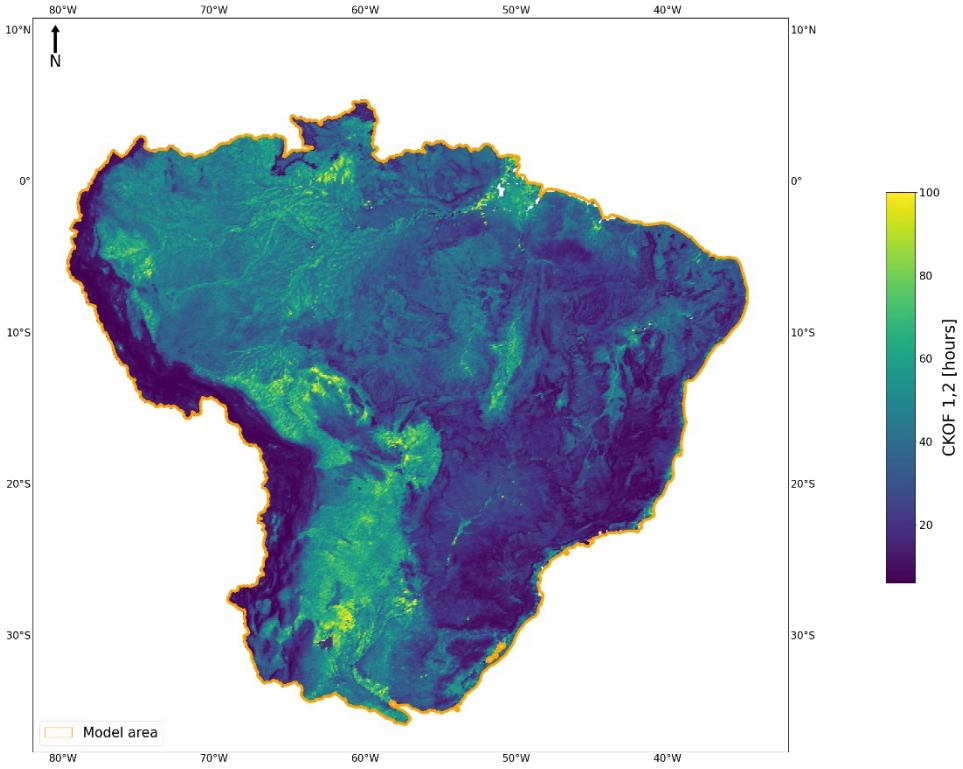


Source: Author.

NAM Parameter: TOF

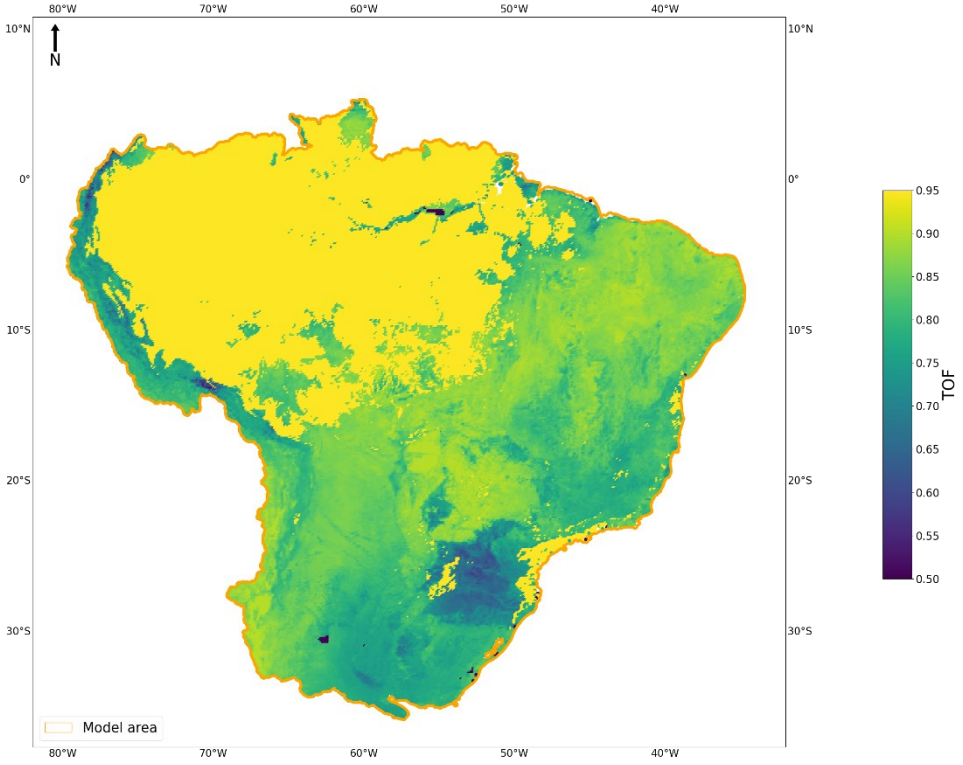


Source: Author.

NAM Parameter: TIF

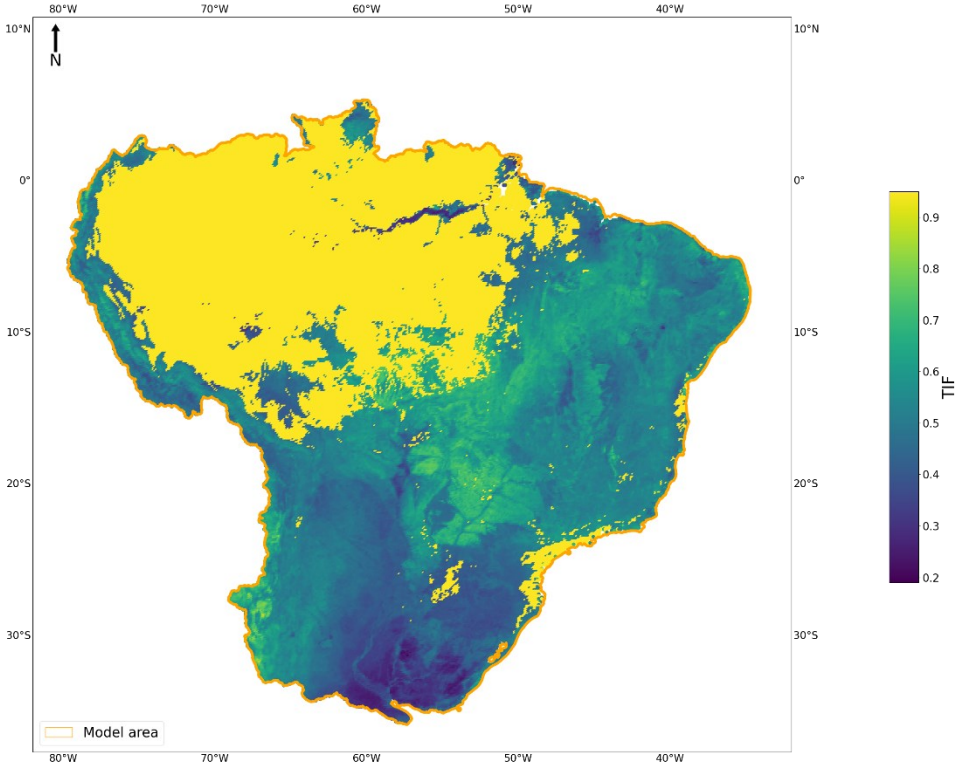


Source: Author.

NAM Parameter: TG

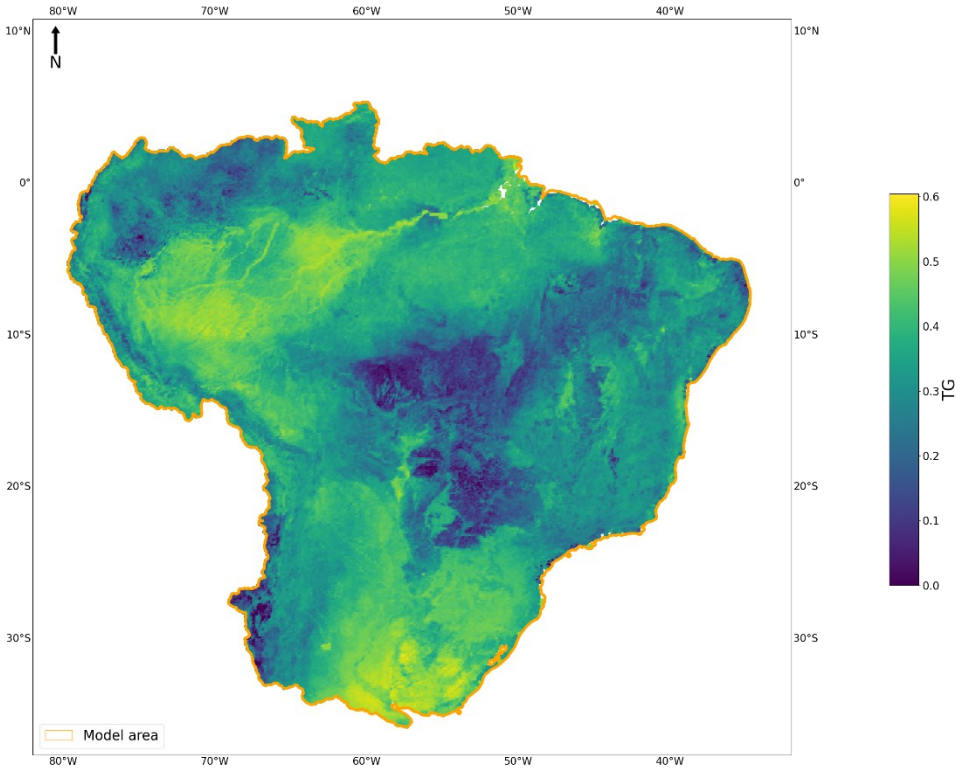


Source: Author.

NAM Parameter: CK$_{BF}$

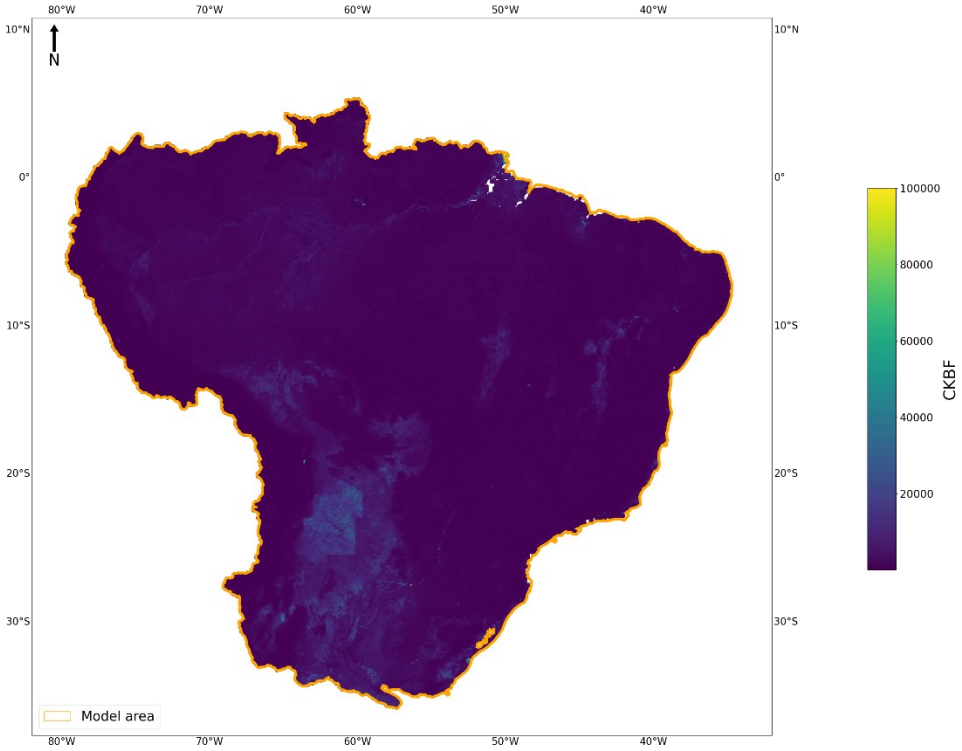


Source: Author.

NAM Parameter: CQlow (fixed value=0)

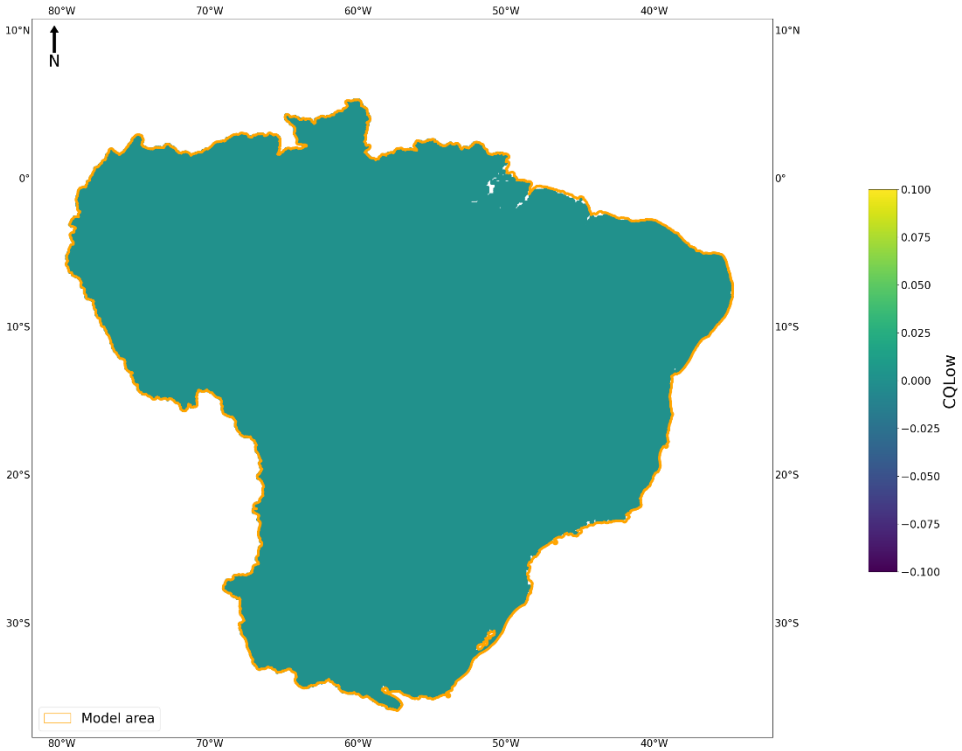


Source: Author.

NAM Parameter: CKlow (fixed value=1000)

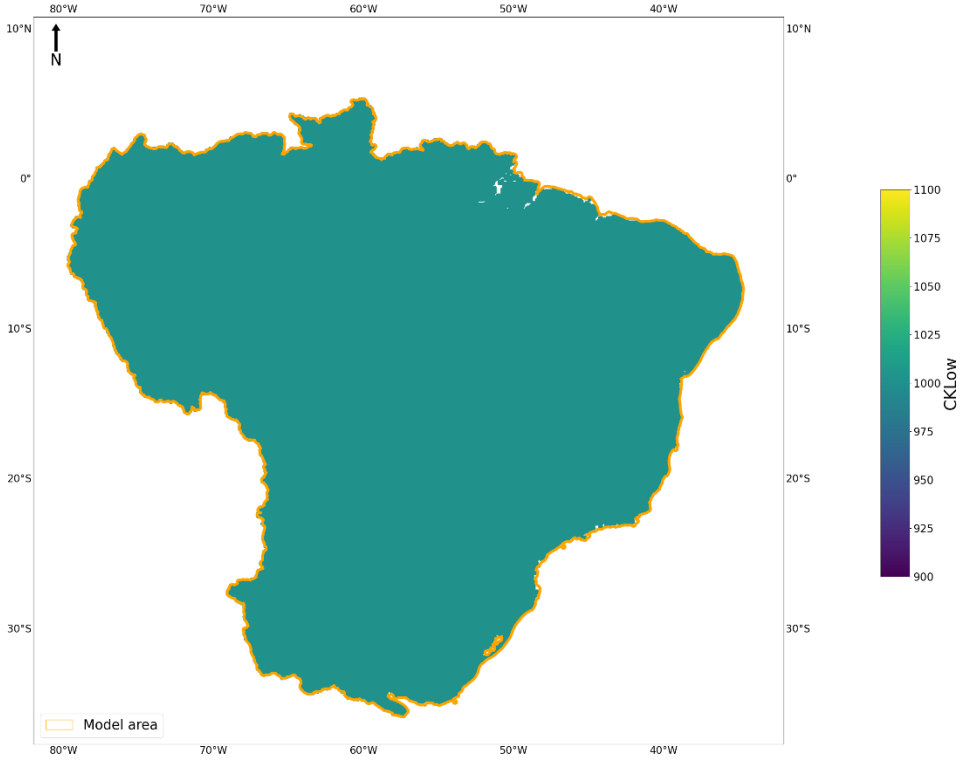


Source: Author.